Coordinated Energy Management in a Network of Microgrids

COORDINATED ENERGY MANAGEMENT IN A NETWORK OF MICROGRIDS

BY

MOHSEN RAFIEE, M.Sc

A THESIS

SUBMITTED TO THE DEPARTMENT OF ELECTRICAL & COMPUTER ENGINEERING

AND THE SCHOOL OF GRADUATE STUDIES

OF MCMASTER UNIVERSITY

IN PARTIAL FULFILMENT OF THE REQUIREMENTS

FOR THE DEGREE OF

DOCTOR OF PHILOSOPHY

Doctor of Philosophy (2018) McMaster University
(Electrical & Computer Engineering) Hamilton, Ontario, Canada

TITLE:	Coordinated Energy Management in a Network of Microgrids
AUTHOR:	Mohsen Rafiee M.Sc./B.Sc. (Electrical and Computer Engineering) K.N Toosi University of Technology/University of Tehran, Tehran, Iran
SUPERVISOR:	Dr. Shahin Sirouspour
NUMBER OF PAGES:	xv, 136

This thesis is dedicated to Shahla and Reza

Abstract

This thesis is concerned with the problem of coordinated energy management in a network of grid-connected microgrids. In particular, the research investigates methods for optimal coordinated control of storage units and sharing of electricity costs among the microgrids. New multi-objective optimization models are proposed for efficient integration of the microgrids local energy storage and renewable energy resources into the power grid. In these models, individual microgrids can exchange power locally with each other as well as with the utility grid. Components of the objective function are the electricity costs of the individual microgrids over a rolling window of time, e.g, a 24-hour prediction horizon. A pricing regime is introduced in which differences in the local and grid buy and sell time-of-use rates of electricity incentivize local inter-microgrid exchanges of power over power exchange with the grid. Optimization problems are formulated and solved on a rolling horizon basis to allow for on-line management of energy resources, using up-to-date forecast of microgrid electricity demand, renewable generation, and electricity rates.

In Chapter 4, a novel formulation of a multiple-objective constrained optimization is presented for solving the microgrids energy management problem under the proposed electricity pricing regime using the concept of compromise programming. This approach minimizes l_1 or l_2 distances of the microgrids cost vector to a utopia point

in the solution space. Components of the utopia point are defined as the minimum cost achievable by the corresponding microgrid when it always uses the favourable local buy/sell rates. The proposed optimization models are in the form of convex linear/quadratic programs without any binary or integer variables for l_1/ l_2 norms, respectively. In Chapter 5, the multiple-objective optimization is converted to a single-objective optimization by adding up the costs of the individual microgrids. An equivalent linear program free of binary/integer variables is derived from the original nonlinear optimization model, which can be effectively solved using existing solvers. The total cost saving and computational complexity are significantly improved in this method compared to the compromise programming technique in Chapter 4. In Chapter 6, the multi-objective optimization is formulated as a lexicographic program, to allow for preferential treatment of groups of microgrids based on pre-assigned priorities. This, for example, allows for giving greater incentives to microgrids that bring lager storage and renewable energy capacity into the network. Finally, in Chapter 7, the optimization model is extended to enable dispatch of reactive power in addition to real power. Simulation results with real data demonstrate that the proposed coordinated energy management strategies can yield substantial cost savings, in some cases in excess of 70 %, for the microgrids in the network compared to a case in which they manage their resources individually. Moreover, the solution to the convex binary/integer free optimization models can be obtained in real-time for a fairly large network, making the proposed models suitable for on-line energy management.

Acknowledgements

Foremost, I would like to express my sincere appreciation to my supervisor, Dr. Shahin Sirouspour, for his patience, encouragement, faith, and support during my studies towards Ph.D. at McMaster University. I am truly grateful for working under his supervision.

I would like to thank my supervisory committee, which included, at various times, Dr. Prashant Mhaskar, Dr. Mehdi Narimani, and Dr. Nigel Schofield, for providing advice when needed, and helping me keep my progress towards the completion of my doctoral studies on track.

I would like to record my warmest gratitude to my family since their love and endless support have made it possible for me to excel in my studies.

My kind regards to my fellow colleagues in the Telerobotics, Haptics and Computational Vision Laboratory, who I have had the pleasure of working with. Special thanks to my friends and lab mates, Dr. Adhi Ravichandran, Raheleh Khodabakhsh, Mohammad Jafarinasab, Eric Dyer, Huawei Zhu and Muzamil Rashid for their intellectual supports and suggestions. Also, Cheryl Gies, the graduate assistant, has been invaluable with her help and wisdom in dealing with the everyday life as a graduate student. I thank all of them.

Contents

List of Figures

Chapter 1

Introduction

In Marnay *et al.* (2015), microgrids are defined "... electricity distribution systems containing loads and distributed energy resources, (such as distributed generators, storage devices, or controllable loads) that can be operated in a controlled, coordinated way either while connected to the main power network or while islanded." Microgrids, enabled by advancements in the field of power electronics, can help realize a truly distributed concept of the power system. The power grid of the future will be an interconnected network of microgrids exchanging energy with each other. Distributed renewable energy sources and energy storage systems will be key components of the grid. Microgrids will help better integrate these resources into the grid with the aim of improving resiliency, reducing cost, and increasing penetration of renewable energy. Intelligent management of the storage and renewable energy capacity within the gird will be critical for successful implementation of this distributed generation model.

In recent years, interest has grown in creating technology solutions that can help transform the electric power grid from its current mostly centralized top-to-bottom model of operation to a more interactive distributed model. Energy losses in long-distance transmission, unreliability and security vulnerabilities of the centralized operation, and heavy reliance on polluting sources of energy are among some of the concerns that have given rise to substantial research in the area of smart grid. In this context, microgrids have emerged as an effective vehicle for enabling a bottom-up transition to a distributed grid operation model. Microgrids can help integrate distributed energy storage capacity and renewable power into the grid, increasing its efficiency and resilience to natural and man-caused disruptive events. They can facilitate electrification of the transportation sector, which will have significant positive economical and environmental consequences.

Energy storage devices and renewable sources of power are also becoming more prevalent in the electricity grid. This is in large part due to a recognition by many of the stakeholders of the need for transition to a distributed grid operation model with more reliance on clean renewable energy. Distributed generation backed-up by distributed energy storage can increase penetration of renewable energy, reduce transmission losses, and enhance resiliency of the grid. Aside from its obvious environmental advantages, a distributed generation system can yield other significant socio-economical benefits. It is not hard to envision a future grid in which small-scale consumers can trade electricity among each other and with the grid. By participating in such an open energy market, microgrid operators can lower their electricity cost and help the grid reduce its dependence on conventional generation.

As microgrid energy systems become more prevalent, they create new opportunities for aggregation of resources and demand side management across multiple microgrids. Coordination of energy management among microgrids in a network can help them better utilize and share available storage and renewable energy resources. The present work focuses on solving the energy management problem for a network of grid-connected microgrids. Networks of microgrids with integrated energy management intelligence can help in the transition of the conventional power system into a distributed operation model.

1.1 Problem Statement

This thesis focuses on the problem of energy storage management for a network of microgrids connected to a utility grid. For the purpose of this work, a microgrid is defined as a small electricity consumer, e.g, a residential home, that is potentially equipped with an energy storage device and renewable sources such as wind and solar energy. The term nanogrid may also be used to describe what is considered as a microgrid here.

A notable application of the proposed storage control method is in a residential community where individual units may be equipped with renewable energy sources and energy storage devices. More broadly, the method could be used for control of distributed renewable energy and energy storage assets available in a group of institutional, commercial, and industrial customers of a utility. In this work, it is assumed that a number of microgrids (NoG) enter into a partnership to share their storage and renewable energy resources, and the grid operator agrees to treat them as a single customer. A typical configuration of such network is shown in Fig. 1.1. It should be noted that no particular power distribution topology is assumed or required here. For example in the case of a residential community, existing local power infrastructure would be sufficient for the implementation of our resource sharing strategy. Only a

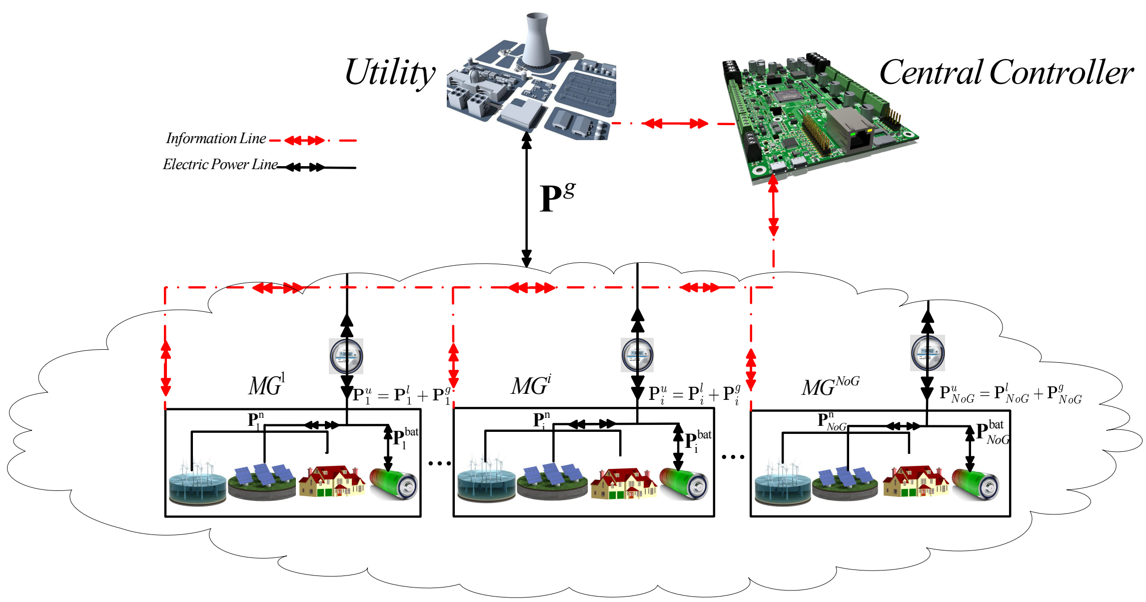

Figure 1.1: Multiple microgrids participating in a coordinated control scheme to share their storage and renewable energy resources.

communication infrastructure such as a secure Internet-based protocol is required for the communication of measurements and control commands. A centralized controller which would be owned and operated by the partnership, controls the storage devices in the individual units, and also calculates their electricity costs using the optimization framework proposed in the thesis. In this structure, the central controller acts as a high-level decision-maker, and calculates the optimal values of the powers for each unit. The battery charge/discharge commands would be sent to the local battery power convertors controllers for execution.

A unique problem arising in the network configuration is the attribution of the source/destination of the power each microgrid consumes or generates at the meter, where is coupled to the grid. This attribution problem has a trivial solution in the case of a single grid-connected microgrid, i.e., buying and selling power transactions are solely with the grid. In multi-microgrid scenarios, however, there is no unique

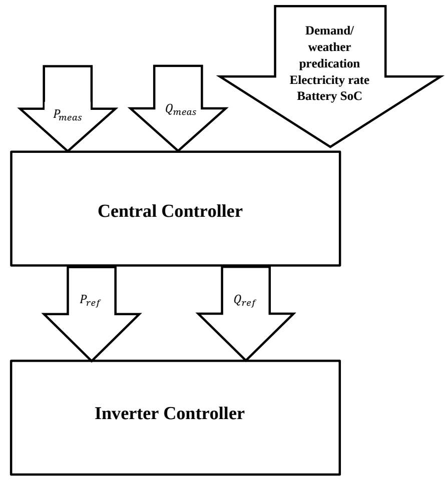

Figure 1.2: hierarchy control levels in the proposed energy management system for a network of microgrids

solution to the problem as buying and selling transactions can occur with the utility grid, other microgrids in the network, or both.

Also, in coordinating energy management in a multi-microgrid system, there are situations in which preferential treatment of microgrids based on some predefined criteria may be desirable. For instance, microgrids with a larger investment in energy storage and/or renewable energy capacity may be given a priority in the allocation of benefits as an incentive for their participation in the coordinated energy management scheme.

1.2 Proposed Solutions

In the proposed operation model, the microgrids in the network may be equipped with solar/wind generation and energy storage units. They have the option to trade energy with other local microgrids in the network or the utility grid. According to the hierarchy control scheme depicted in Fig. 1.2, a central controller in the network solves a pre-specified optimization problem to make high-level decisions about the battery charging/discharging power of each individual unit. These commands are then sent to the low-level controllers of the corresponding power convertors. As shown in Fig. 1.1, each microgrid net power $\mathbf{P}_i^u, i = 1, 2, \cdots, NoG$ is metered. The actual control variables are the battery powers denoted by $\mathbf{P}_i^{\text{bat}}$. Note that the microgrid net power is decomposed to a local $\mathbf{P}_i^l$, and a grid $\mathbf{P}_i^g$ component. These are virtual accounting variables representing local and grid power transactions. They would be determined by the solution to the optimization problem and are used to calculate the share of electricity cost for each microgrid. In this sense, local and grid power transactions are completely transparent to the individual units as they are merely virtual decompositions of their respective net power, $\mathbf{P}_i^u$.

Typically in the case of a single grid-connected microgrid, the grid electricity rates would depend on time of the day and the direction of the power flow; these are denoted by the vectors $\mathbf{c}^{bg}$ and $\mathbf{c}^{sg}$, representing buy and selling prices, respectively. Elements of these vectors correspond to different times during the day. In the multiple-microgrid configuration of Fig. 1.1, the prices would be applicable to the net power of all microgrids participating in the coordinated control scheme, $\mathbf{P}^{\text{g}}$. This can be simply computed by adding up the metered powers of the individual microgrids, $\mathbf{P}_i^u$. Note that while the figure shows only one feeder line for the network, in practice, multiple feeder lines may serve the network, and this would not affect the problem formulation.

In this thesis, the electricity rates for the local exchange of power among microgrids are represented by the vectors $\mathbf{c}^{bl}$ and $\mathbf{c}^{sl}$, for buying and selling respectively. Furthermore, it is assumed that $\mathbf{c}^{bg} \succ \mathbf{c}^{bl} \succeq \mathbf{c}^{sl} \succ \mathbf{c}^{sg}$. It is reasonable to assume that the price of buying, grid or local, is always higher or at least equal to the corresponding price of selling. The difference between the two rates can be considered as an overhead infrastructure and power loss cost for the grid and the local network operators. While the grid prices are usually set by the utility operator, the local prices would be agreed upon by the microgrids participating in the local exchange scheme. The local buy and sell prices would be within the gap in utility buy/sell rates to encourage local power transactions and to reduce reliance on the grid power for the network. By agreeing to sell locally at a lower rate and to buy locally at a higher rate than the grid, the microgrids can mutually benefit from participating in the local energy market as opposed to directly interacting with the grid on an individual basis. The simulation results later in the thesis will indeed demonstrate that the participating microgrids would substantially reduce their electricity cost under such rate regime, compared to a case where they individually interact with the grid. While the problem formulation and simulations are based on the above rate assumption, if desired, alternative pricing scenarios can also be easily accommodated with slight changes in the problem formulation. Therefore, this assumption is not limiting the applications of the proposed methods.

The energy management algorithm operates centrally, making high-level decisions for the average flow of powers in and out of the storage devices over the scheduling control time steps, usually in the order of minutes. The decisions are then sent to the low-level controllers of the power converters for the storage systems as reference power commands. Solar/wind generation, if available, are assumed to be controlled locally for maximum power, e.g, using maximum power point tracking algorithm for the control of solar converter. The energy management algorithm also calculates the local and grid components of each microgrid power. This is all achieved by formulating and solving a multi-objective optimization problem over a rolling control window, using up-to-date predictions of the demand and renewable power in each microgrid. Only the first/few steps of the control decisions are actually implemented before rolling the window forward and re-solving the problem.

The optimization model is formulated on a rolling horizon basis to take advantage of latest forecasts of the demand and renewable generation, and to respond to changing electricity rates and grid requirements as they arise. The objective to minimize for each microgrid is the net cost of electricity, i.e., buying minus selling, and any applicable peak demand cost. Four different formulations of the problem will be presented, which are briefly described below. It should be noted that problem of demand and generation forecast is beyond the scope of the current thesis. This data is assumed to be available for use in the energy management algorithms.

1.2.1 Multi-Objective Optimization Based on Compromise Programming

Using the concept of compromise programming Vira and Haimes (1983), a multi-objective optimization model is formulated as a constrained minimization of the distance of the cost vector from a predefined *utopia point*. The elements of the utopia point vector are the minimum cost achieved by each microgrid, assuming they could always benefit from the local buy/sell prices. The proposed optimization problem is convex and free of binary/integer variables. Two special cases of l_1 and l_2 distances from the utopia point are considered that result in constrained linear and quadratic optimizations, respectively.

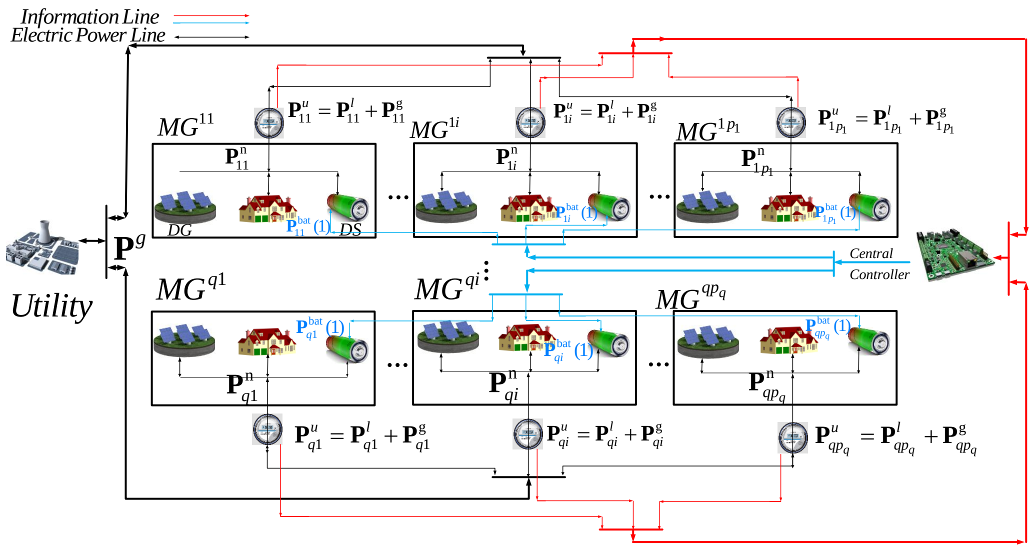

Figure 1.3: A network of grid-connected microgrids in the priority-based scheme; microgrids in one row have the same priority; each microgrid may have its own local storage and renewable power.

1.2.2 Minimizing Sum of the Costs

The multi-objective problem is converted to a conventional convex constrained optimization through a scalarization technique, namely the sum of the costs method Koski and Silvennoinen (1987). The resulting objective is essentially the total electricity cost incurred by the network of microgrids. Sharing constraints are also introduced to regularize the problem, i.e., to ensure a unique solution can be found that is fair and equitable for all participating microgrids. The resulting optimization is a convex linear program free of binary/integer variables.

1.2.3 Priority-based Multi-Objective Optimization

The network policy with respect to transactions of power plays a critical role in convincing microgrids with potentially conflicting goals to join the network. A multi-objective optimization formulation using the concept of lexicographic programming is introduced in this thesis that allows for preferential treatment of the microgrids based on their priority group. This feature can be used to provide a higher incentive to microgrid units with larger renewable and storage capacity for their participation in the network. The rationale is that the units with bigger investments in the resources should reap higher benefits from their participation. The concept of lexicographic programming Migdalas *et al.* (2013) is applied to the multi-objective optimization formulation of the energy management problem to account for microgrid priorities in the conversion of the optimization formulation. Fig. 1.3 depicts a generic configuration for a network with $NoG = p_1 + p_2 + \cdots + p_q$ grid-connected microgrids. Here q is the number of priority levels in the network, and microgrids in each row have the same priority. The priorities can be assigned based on diverse factors such as the microgrid storage and renewable energy capacity, the size of the microgrid, and any other mutually agreed upon metric among the microgrids in the network. Bidirectional power flows of the microgrids are metered at the points of their coupling to the grid.

1.2.4 Management of Reactive Power

The first three contributions of this thesis focus on management of real power in the microgrids in a network. The energy management formulations are further generalized to accommodate transactions of reactive power among the microgrids and the grid.

The objective function and constraints in the optimization are revised to account for reactive power exchange. The resulting optimization problem is of quadratically constrained linear/quadratic program form.

1.3 Summary of Contributions

In summary, the main contributions of this thesis are:

- Introducing a concept of operation for sharing renewable energy and storage capacity in a network of microgrids through coordinated control of the storage units and virtual decomposition of the microgrids metered power to local and the grid components. This framework would encourage local power transactions and can help substantially reduce the electricity cost of the microgrids, compared to the case where microgrids individually exchange power with the grid using its buy/sell rates.

- Developing four distinct multi-objective optimization formulations for on-line computation of storage charge/discharge activities and local and grid components of microgrid power transactions. These are:

  - a formulation that would minimize l_1/ l_2 distances between the actual costs vector and an ideal vector.

  - a formulation that would minimize the total cost of the electricity for the microgrids in the network.

  - a formulation that can prioritize the participating microgrids based on their attribution to predefined priority groups.

  - a generalized formulation for optimal dispatch of real and reactive power that can be used for any network regardless of the type of loads or distance between participants.

The key features of the proposed solutions are:

- The proposed grid/local rate scheme incentivizes local exchange of power over that with the utility grid. This would eventually reduce the need for centralized power generation in the grid.

- The resulting optimization formulations are convex linear/quadratic program free of binary/integer variables. This would guarantee that a globally optimal solution can be obtained in real-time for on-line control for a relatively large network of microgrids.

- the proposed methods can be implemented over existing power distribution networks, with addition of a data communication infrastructure.

- A novel utilization of aggregated energy storage in the network ensures the longest possible uninterrupted operation in the event of islanding.

- In the scenarios considered in the thesis, the proposed network energy management scheme substantially reduce the individual microgrid electricity costs, in some cases in excess of 70 %. This is when the cost is compared to that from optimally managed individually microgrids with the same local energy storage and renewable generation capacity.

1.3.1 Organization of the Thesis

The rest of the thesis is organized as follows. In Chapter 2, a survey of the literature pertinent to the core topics of the thesis is presented. A generic multi-objective optimization problem and different scalarization and non-scalarization techniques for solving such problem are briefly reviewed in Chapter 3. In Chapter 4, a nonlinear multi-objective optimization formulation of the energy management problem in multi-microgrid network is presented. Using the concept of compromise programming, linear/quadratic programming counterparts of the original problem are then developed that avoid binary/integer variables and can be solved in substantially shorter times, making them suitable for real-time implementation. In Chapter 5, the multi-objective optimization problem is converted to a conventional linear program with the goal of minimizing the total electricity cost of the microgrids. In Chapter 6, a new formulation of the multi-objective optimization is produced that would allow for preferential treatment of microgrids based on their priority assignment. In Chapter 7, the problem formulation is extended for optimal dispatch of real and reactive power in a network regardless of the type of loads or distance between participants. The thesis is concluded in Chapter 8 where some possible directions for future research are also discussed.

1.4 Related Publications

The following publications have resulted from the research conducted in this thesis:

- M. Rafiee Sandgani and S. Sirouspour, " Energy Management in a Network of Grid-Connected Microgrids/Nanogrids Using Compromise Programming," in

IEEE Transactions on Smart Grid, September 2016; DOI: 10.1109/TSG.2016.2608281.

- M. R. Sandgani and S. Sirouspour, "Coordinated Optimal Dispatch of Energy Storage in a Network of Grid-Connected Microgrids," in IEEE Transactions on Sustainable Energy, vol. 8, no. 3, pp. 1166-1176, July 2017; DOI: 10.1109/TSTE.2017.2664666.

- M. Rafiee Sandgani and S. Sirouspour, "Priority-based Microgrid Energy Management in a Network Environment," in IEEE Transactions on Sustainable Energy, November 2017; DOI: 10.1109/TSG.2016.2608281.

- M. Rafiee Sandgani; S. Sirouspour, "Optimal Dispatch of Real and Reactive Power in a Network of Grid-connected Microgrids," to be submitted to the IEEE Transactions on Smart Grid.

Chapter 2

Literature Survey

In Chapter 1, the problems addressed in this thesis were introduced along with brief descriptions of the solutions and contributions to the literature. This chapter presents a survey of the literature related to the thesis topic.

2.1 Basics of Microgrid Operation

A typical microgrid integrates elements of power generation with load and storage capacity. Microgrids may be at residential, commercial, industrial or institutional scales. A microgrid usually operates in either grid-connected or islanded mode. In multi-microgrid configurations, there is the possibility of semi-islanded operation as well. In the grid-connected mode, a microgrid either draws or supplies power from or to the utility grid, depending on the generation and its local load. A microgrid can isolate itself from the grid whenever a power quality event occurs. The main goal of a grid-connected microgrid is to supply real and reactive powers under high power quality injection constraints. In islanded mode, distributed generation units are required to supply regulated power under controllable voltage and frequency while sharing the loads among themselves. Variations in voltage and frequency can become more pronounced when microgrid switches over to islanded mode. In grid-connected mode, the voltage and frequency are enforced by the grid. In island mode, the power balance between generation and demand must be maintained and the bus frequency and voltage must be controlled. This may require temporary shedding of loads if sufficient power cannot be supplied. A smooth transition between these two modes is required for maintaining a reliable supply of power for essential loads. Lopes *et al.* (2006).

Since the equivalent physical inertia of a microgrid is quite smaller than that of the main grid Nikkhajoei and Lasseter (2009), the control and management of an islanded microgrid is often more challenging than a grid-connected microgrid. Medium or even small interruptions may result in power quality and stability issues. Specifically, the frequency and voltage quality would decline, and system stability would deteriorate. Integrated energy storage can help maintain microgrid instantaneous power balance and improve its dynamic performance through proper energy management strategies Lee and Wang (2008). It can mitigate negative impacts of distributed generation power fluctuations and other interruptions on system stability and power quality.

2.1.1 The Role of Energy Management System

The energy management system maintains the power quality, provides ancillary services to the grid, helps microgrid to participate in energy markets, and generally optimizes the microgrid operation Katiraei *et al.* (2008). It performs these functions by considering requirements of the distribution network operator. The information and communication infrastructure plays an important role in the operation of the energy management system. Microgrids increasing role in the grid poses new challenges for their energy management systems De Brabandere *et al.* (2007). They should be able to smoothly transition between islanded and grid-connected modes under intentional or unintentional conditions, integrate demand side strategies, and handle increasing penetration of renewable energy by developing advanced scheduling and dispatching strategies.

2.1.2 Hierarchical Control

The overall microgrid management system is a complex multi-objective control system that deals with issues from different technical areas, time scales, and physical levels. Some areas of interest include load power sharing, voltage/frequency and power quality regulation, market participation, and short/long-term scheduling. A hierarchical control scheme has been proposed and widely accepted as a standardized solution for efficient microgrids management, as depicted in Fig. 2.1. These three-level hierarchical control is organized as follows Guerrero *et al.* (2013). The primary control layer deals with the inner control of the distributed units by adding virtual inertias and controlling their output impedances. The primary control also regulates the local power, voltage, and current. It normally follows the set-points given by the secondary level controller.

In the hierarchy, a secondary control appears on top of the primary control. Its task is regulating the frequency and voltage amplitude deviations caused by the virtual inertias and output virtual impedances and reducing harmonics. In addition, this layer is responsible for frequency synchronization and power exchange with the main grid or other microgrids.

The tertiary control regulates the power flows between the grid and the microgrid at the point of common coupling. Furthermore, the aim of tertiary control is to introduce intelligence in the whole system. The tertiary control would attempt to optimize the microgrid operation based on economical and efficiency-related metrics. To this end, it relies on information from various sources to make high-level decisions with respect to the operation of the microgrid.

It should be noted this is a hierarchical control scheme for a single microgrid connected to the grid. In the case of multi-microgrid, it can be envisioned that there is another control layer on top of this inner-microgrid hierarchy that regulates power flow among the microgrids and utility grid in a coordinated way. Another configuration that is suited more for the present study is a two-level hierarchy structure in which high-level control makes the power flow decision and low-level control at the inverters regulates the frequency and voltage amplitude to follow the reference powers as depicted in 1.2.

2.2 Microgrid Control Strategies

This section reviews decentralized and centralized schemes in control of a microgrid.

2.2.1 Decentralized Control

In the primary layer of the hierarchical control, power electronic convertors interface distributed energy resources to the microgrids. These converters are parallel-connected throughout the microgrid. The droop control method is often applied to

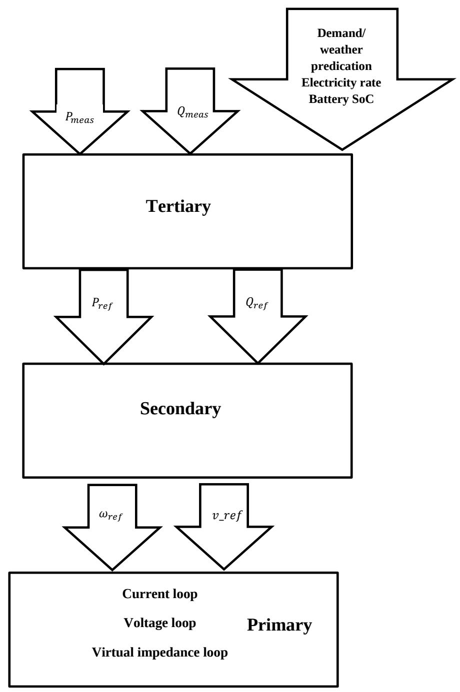

Figure 2.1: hierarchy in control of a microgrid

avoid circulating currents among the converters without the use of any critical communication Katiraei and Iravani (2006). For parallel inverters, the droop method consists of subtracting proportional parts of the output average real/reactive powers to the frequency/amplitude of each module to emulate virtual inertia (i.e., the average real power of each module is linearly dependent on its frequency and the average reactive power of each module is linearly dependent on voltage amplitude). These control loops are also called P—f and Q—E droop Guerrero *et al.* (2006). While highly reliable and flexible, the method has several drawbacks. For instance, the conventional droop method is not suitable when the paralleled system must share nonlinear loads, because the control units should take into account harmonic currents. Thus, harmonic-current-sharing techniques have been proposed to avoid circulating distortion current when sharing nonlinear loads such as adding output virtual reactors Guerrero *et al.* (2005). Furthermore, the power sharing in the droop control method is affected by the units output and line impedances. The virtual output impedance control loop can be utilized to solve this problem Yao *et al.* (2011). Other notable disadvantages of the droop method are its load-dependent frequency and voltage amplitude deviations. To solve these problems, a secondary controller can be implemented to regulate the frequency and voltage amplitude in the microgrid Shafiee *et al.* (2014a).

Decentralized microgrid controllers can be classified into three groups based on the interconnecting line impedances. In highly dispersed networks, the impedances are predominantly inductive and the voltage magnitudes and phase angles at different sources can be very different. Chandorkar *et al.* (1993) showed that in such cases, the distributed system could be operated without the use of phase-locked loops and that real and reactive powers could be shared based on the converter ratings. When the microgrid is spread out over a smaller area, the impedances are still inductive but also have a significant resistive component. While the voltage magnitudes of the sources are almost the same, their phases could be significantly different.

In very small networks, the line impedance is small and predominantly resistive. Neither magnitude nor phase angle differences are significant at any point. The voltage-droop control has limitations when used in microgrids with significant resistive line impedance. In such cases, the usual real power-frequency droop and reactive power-voltage droop adopted from conventional power system control practice, no longer hold. Instead, the real power is affected primarily by the voltage magnitude, whereas the reactive power is mostly influenced by the phase angle difference Guerrero *et al.* (2007). In all cases, the main common quantity is the steady-state frequency which must be the same for all sources. In the grid-connected mode, the microgrid frequency is determined by the grid. In the islanded mode, the frequency is decided upon and enforced by the microgrid local controller. Decentralized control of inverters requires set-points for real and reactive power. These references are usually produced by the energy management system of the microgrid.

2.2.2 Centralized Control

In a centralized controller, the microgrid components are considered as one integrated system. The overall system dynamics are derived and control signals are generated using a proper control strategy. These control commands are then sent to the inverters and other units controllers in the microgrid via a communication network. Kim *et al.* (2011) presented a general structure for centralized control of a microgrid in involving two control layers: Microgrid Management System (MMS) and Local Controller (LC). The MMS is a centralized controller that deals with management functions such as disconnection and re-synchronization of the microgrid and the load shedding process. In addition to this function, the MMS is responsible for supervisory control of distributed generations and the energy storage system. The MMS generates power output set-points for LCs. The LC is located at each microsource and controls the power output according to the reference set by the MMS.

Tan *et al.* (2012) presented a centralized control system that coordinates parallel operations of distributed generation inverters within a microgrid. Their approach employs a model predictive control strategy that allows faster computational times for large power microgrids by optimizing the steady-state and the transient models separately.

2.3 Energy Management System in Microgrid

The problem of energy management of a microgrid has been extensively investigated in the literature from the following perspectives:

- Mode of operation
  - Grid-connected mode
  - Island mode (stand-alone)
- Type of optimization
  - Centralized
  - Decentralized
- Optimal control
  - Optimal power flow
  - Economic dispatch
  - Demand side management
  - Carbon dioxide emission reduction

- Structure of network
  - Single microgrid
  - Network of microgrids

Next, recent papers in each of these categories are briefly reviewed.

2.3.1 Mode of Operation

A microgrid should be capable of operating in grid-connected and islanded modes. Microgrids should regulate their voltage and frequency in order to protect the grid and the loads during transition between these operation modes. Islanded microgrids can supply the electricity needs of remote communities with underdeveloped transmission infrastructure. Grid-connected microgrids can deliberately disconnect themselves from the utility grid and continue to operate in islanded mode in the event of a grid disruption or planned maintenance. The rest of this section reviews the existing energy management strategies in islanded and grid-connected modes.

Islanded Mode

Dursun and Kilic (2012) examined the performance of three power management strategies for a standalone microgrid. The strategies were initially designed to increase the operation time of a fuel-cell unit and to ensure continuous flow of power in the system. The authors devised a control algorithm to manage the power flow and the fuel cell operation time in the network considering the battery state of charge and load demand. To this end, three possible scenarios leading to their control strategies were considered. Their most efficient strategy turned out to be: charge the battery if there is a surplus power in the microgrid and the battery is not fully charged, and run the fuel-cell if the net demand is positive or battery is fully discharged. Liao and Ruan (2009) proposed a power management control strategy for a standalone microgrid equipped with energy storage and solar generation. In their approach, the solar generation system provides the base load, whereas, the battery compensates for fluctuations in demand. They control uni-directional and bi−directional DC-DC converters to operate in a desired mode based on the battery state of charge and weather conditions. The proposed power management strategy coordinates the two sources to ensure that the power system operates at high efficiency with good dynamic performance.

Dahmane *et al.* (2013) developed an algorithm for optimal power management of a standalone hybrid system that contains solar, wind and diesel generators, as well as battery energy storage. In their strategy, the solar unit operates at maximum power using a maximum power point tracking algorithm to supply the load and the wind generator only supplements the solar generation if a power shortage occurs. A diesel generator is also available to meet the load demand and to charge the battery in the absence of sufficient solar and wind powers, and when the battery is fully discharged. Nfah *et al.* (2007) modelled and performed an energy analysis for a microgrid system in a remote location in North Cameroon. The system aimed to supply rural households and schools. They give priority to utilizing the wind energy and store any excess energy in the battery. The diesel generator starts operating when the batteries are fully discharged.

Sachs and Sawodny (2016) presented an advanced control strategy for optimal microgrid operation using a two−layer model predictive method. The first layer computes optimal power dispatch commands, based on real−time predictions of future power profiles. To improve the robustness of the control strategy to prediction errors, a boundary value problem is solved to adjust the diesel generator power in the second stage. The model predictive control framework is further used to adapt the weights of the forecast algorithm. They focused on microgrids in remote rural areas with no connection to the grid.

Grid-Connected Mode

Rani *et al.* (2013) proposed a photovoltaic system to supply DC loads from a grid-connected system without any interruption. They developed a linear programming−based energy flow management scheme to achieve this goal. Battistelli *et al.* (2012) assessed the contribution of vehicle-to-grid systems to support energy management of small electric power systems by providing a practical model for the microgrid. The assessment was conducted by determining the power output of various generating units and the input/output power from grid. Mohamed and Mohammed (2013) proposed an algorithm to optimize the operation of a distribution system by considering the cost and stability. Their energy management system controls the available power from existing energy sources to meet the demand. Energy generated from renewable sources is given the highest priority. The batteries primarily act for large loads to enhance the stability of the system and decrease voltage dips. They employed a fuzzy system to determine the amount of energy required from the battery when renewable energy sources are unable to satisfy the load.

Khodabakhsh and Sirouspour (2016) presented two methods for online optimal control of an energy storage unit in a grid−connected microgrid. In their model, load demand, solar generation, and electricity rate are uncertain. Their primary optimization model is a scenario-based stochastic conditional value at risk. They used a multivariate Gaussian distribution for modelling of the uncertainty. Worst-case scenario-based stochastic conditional value at risk stochastic optimization approach was then employed to obtain a second optimization model. This led to a set of robust constraints with respect to price variations that guarantees reducing the computation time. Sirouspour (2016) presented an off-line control strategy for an energy storage in a grid-connected microgrid. He assumed that uncertainty in the microgrid electricity cost and net demand with a priori known distributions. The energy management system was formulated as a stochastic chance constraint optimization problem. The equivalent deterministic convex nonlinear optimization formulation of the original optimization model was then derived and solved with standard optimization algorithms.

2.3.2 Type of Optimization

Based on the hierarchy introduced at the beginning of this chapter, the functions of energy management system can be implemented in a centralized or decentralized way. The level of decentralization depends on the amount of autonomy of the local controllers. They can simply execute commands from the upper-level centralized controller or make decisions locally based on information received from the other units. Each approach has its own advantages and disadvantages, and one may be more suitable than the other depending on the type of microgrid (e.g., residential, commercial, industrial), ownership of microgrids, network size and topology. Generally speaking, computational and communication infrastructure costs are lower in a decentralized system. These systems are also more flexible and easier to expand, and are more robust with respect to single-point failures. Centralized realizations have tighter control and supervision over the entire system, and their control algorithms are usually easier to develop and implement.

Centralized Control

A centralized energy management system usually needs substantial computing power and resources to process considerable amount of data in making decisions. It requires reliable real-time communication in order to exchange information with the individual units. According to the literature, centralized control is more suitable in the following situations Tsikalakis and Hatziargyriou (2011); Olivares *et al.* (2011); Vaccaro *et al.* (2011); Tsikalakis and Hatziargyriou (2008):

- small-scale microgrids where centralized information gathering and decision making can be carried out with low communication and computation cost.
- when all the microgrids in the network have a common goal so that the central energy management system can operate the network as one unit.
- military microgrids with strict security requirements.
- networks with a fixed configuration.

Yue *et al.* (2017) examined optimization-based scheduling of resources in a centralized energy management system. In addition, they proposed a method for the control of the voltages of various DC buses in a DC residential distribution system. Almada *et al.* (2016) studied control and management of a microgrid with distributed energy resources connected to a single bus. Their microgrid management system uses a centralized heuristic approach that considers a stochastic model for photovoltaic output power, a fuel cell, the state of charge of batteries, a variable load profile, and the electricity tariff. Their goal was to integrate local energy resources into grid to reduce cost and enhance reliability and quality of the power supply. They also evaluated the responses of the power converters of the distributed energy resources in the microgrid during grid connection, standalone operation, and transition between these operating modes. Prodan and Zio (2014) proposed a framework for microgrid energy management based on the concept of rolling horizon control. The microgrid considered in their work is connected to the grid via a transformer and contains a local load, a wind turbine, and a battery unit. Optimal scheduling of the battery was sought for minimizing cost. To this end, a predictive control framework was proposed that considers cost, power consumption, and power generation profiles.

Decentralized Control

Decentralized controllers have been proposed as an alternative to centralized methods to increase operation flexibility. Recent progress in communication technology and information exchange algorithms have enabled the use of decentralized control and management in practical applications Qiu *et al.* (2011).

An emerging research trend in distributed energy management is based on concepts in multi-agent systems. The control hierarchy and functions in such schemes are similar to those in centralized methods. However, the decision making authority is transferred to the local controllers by increasing their autonomy. Local decisions are made based on information on demand, power generation and electricity price forecasts, and neighbouring controllers states. Decentralized control and energy management can eliminate the need for large central computing infrastructure since the decisions are made mostly at the local level. They can continue to operate in the event of failure at a single unit. It is also easier to implement plug-and-play functionality in a distributed system, which considerably enhances microgrid flexibility/expandability. On the other hand, decentralized control requires good synchronization among the units for safe and stable operation. Decentralized control and energy management is preferable when Xu and Liu (2011); Liu *et al.* (2014); Colson *et al.* (2014):

- microgrid is large or its units are widely dispersed which makes centralized data acquisition difficult.
- resources are owned by different entities who have their own operation goals and require local decision making.
- microgrid system is expected to grow by installation of new units over time.

Mao *et al.* (2014) presented a multiagent-based hybrid energy management system with both centralized and decentralized energy control functionalities. Within this framework, three-level hierarchical energy management strategies were presented. A coordinated energy management framework was realized by combining autonomous control of local distributed energy resources at the local level with coordinated energy control at the central level. Kuznetsova *et al.* (2015) presented a microgrid energy management method using robust optimization. Uncertainties in wind power generation and loads were described in the form of prediction intervals. Their benchmark system was a microgrid comprising a middle-size train station with integrated photovoltaic power production system, an urban wind power plant and a residential district. They modelled each stakeholder was modelled as an agent, with the goal of decreasing its cost/increasing its revenue. They showed how the probabilities of occurrence of certain events, e.g., failure of power lines, electricity demand, and price peaks, highly condition reliability and performance indicators of the microgrid.

2.3.3 Optimal Control Techniques

Optimal control techniques for controlling microgrids can be classified according to the objective function they minimize or maximize. The objective function can quantify costumers satisfaction, reliability of the network, environmental impacts, etc.

Optimal Power Flow

Optimal power flow in a microgrid is challenging due to uncertainty in the loads, generation units, state of charge of the batteries, and electricity rates models. Li *et al.* (2012) studied power flow in a microgrid under variable load and generation conditions. They considered typical properties of inverter-interfaced microsources, including P-Q inverter, P-V inverter, and the converters rated current and linear modulation constraints. They also investigated voltage enhancement and active power losses. Conti *et al.* (2012) presented a weighted-sum objective function for solving a multi-objective optimization problem within an optimal power flow framework in a microgrid with multiple distributed generation units and battery storage systems, using a niching evolutionary algorithm. Levron *et al.* (2013) presented a method for optimal control of energy storage devices in a microgrid. Stored energy was controlled to balance renewable. They also proposed an optimal power flow solution that considers limits on the storage capacity, voltages, currents, and powers.

Morstyn *et al.* (2016) proposed a multi-agent dynamic optimal power flow strategy for microgrids with distributed energy storage systems. This control strategy uses a convex formulation of the AC dynamic optimal power flow problem developed from a d-q reference frame voltage-current model and linear power flow approximations. The resulting convex dynamic optimal power flow problem is divided between autonomous agents and solved based on local information and neighbour-to-neighbour communication over a communication network, by using a distributed primal subgradient algorithm. Ravichandran *et al.* (2016) proposed an online control scheme for power flow energy management of a microgrid equipped with renewable generation, battery, and integrated electric vehicles. They formulated the problem as a chance constraint optimization in the form of mixed integer linear program. They showed that in the presence of uncertainties in the prediction of demand, electric vehicles state of charge and their connection time, the proposed energy management system can significantly reduce cost and the probability of not meeting the electric vehicles charging requirements, compared to a non-stochastic optimization formulation.

Economic Dispatch

Jin *et al.* (2017) proposed a dynamic economic dispatch method. They considered a microgrid as a discrete time system, and defined dynamic economic dispatch as finding the optimal control strategy for the system in a finite time period. They established a dynamic economic dispatch model for microgrids and developed a dynamic programming algorithm for solving the problem. Liang *et al.* (2012) introduced a decentralized economic dispatch approach in which optimal decisions on power generation are made by each generation unit locally without a central controller. They presented a heterogeneous wireless network architecture for microgrids to improve the convergence speed of the general nonlinear multi-agent problem. Nutkani *et al.* (2017) presented a comprehensive economic dispatch scheme that considers distributed generation costs, their power ratings, distributed generation dispatch priorities, and droop characteristics. The proposed scheme also allows for on-line power reserve to be set and regulated within the microgrid.

Demand Side Management

Wu *et al.* (2011) proposed a demand side management strategy considering uncertainty in wind power generation. Their focus was on an isolated microgrid with one wind turbine, one fast-responding conventional generator, and several users. In their model, the users act as independent decision makers in shaping their own load profiles. Using the dynamic potential game theory, they analyzed and coordinated the interactions among the users to efficiently utilize the available renewable and conventional energy resources and minimize the total energy cost. They derived closed-form expressions for the best responses for the users that participate in demand side management. Then, they investigated the efficiency of the constructed game model at its equilibrium.

An energy management system for a renewable-based microgrid was proposed by Palma-Behnke *et al.* (2011). It provided on-line set-points for each generation unit, operation modes for a water supply system, and signals for consumers based on a demand side management mechanism. The energy management system minimizes the operational costs while supplying water and electric load demands. Logenthiran *et al.* (2012) presented a demand side management strategy for a smart grid based on a load shifting technique. A heuristic-based evolutionary algorithm that adapts the heuristics in the problem was developed for solving the proposed optimization problem. A stochastic programming model was proposed by Aghajani *et al.* (2017) to minimize operating costs and emissions from non-renewable sources in a microgrid. They used a probability density function to predict the wind speed and solar irradiance. They also suggested the use of incentive-based payments as price offer packages for implementing demand response programs.

Yaghmaee *et al.* (2017) proposed a two-tier cloud-based demand side management to control residential load of customers equipped with local power generation and storage facilities. They considered a power system consisting of multiple regions. In each region, an edge cloud was utilized to find the optimal power consumption schedule for customer appliances in that region. They proposed a two-level optimization algorithm with a linear multilevel cost function. At the edge cloud, power consumption, level of local storage, and power demand from local storage facilities and power grid are scheduled. The core cloud gathers data on the total demand from consumers in different regions and finds the optimal power consumption schedule for each region.

Carbon Dioxide Emission Reduction

Reducing carbon dioxide emissions has been a principal goal of many energy management systems. To this end, variables directly linked to carbon dioxide emission have been incorporated in energy management optimization models. Kanchev *et al.* (2012) presented a microgrid energy management optimization model with local solar generators. Using predictions of available energy, state of charge of storage devices, and load, the microgrid energy management system solves a 24-hour ahead operational planning problem using the unit commitment approach. The objective function is either the CO_2 equivalent emissions, the fuel consumption or a trade-off between these two. Elsied *et al.* (2016) proposed an energy management system in order to optimize microgrid performance in a real-time operation. A binary particle swarm optimization algorithm is used to minimize energy cost and carbon dioxide and pollutant emissions, while maximizing power from renewable energy resources.

2.3.4 Structure of Network

Two possible structures can be envisioned for a network of microgrids. Either all microgrids are able to exchange energy with each other and the grid, or only individual microgrid transactions are permitted. For individual microgrids optimal control strategy can be described as: seeking the cheapest source of energy, that could be off-peak utility energy or an internal renewable energy for example, purchasing it to meet the demand and storing the surplus in the energy storage unit. It would minimize the purchase of grid energy during peak hours. However, in multi-microgrid scenarios, due to the complexity of the system and competing objectives of the microgrids, the optimal solution strategy can be much more complicated. In energy management in a network of microgrids that is the main concern of this thesis, solutions are found from multi-objective optimization problems, solved either centrally or in a distributed fashion. In this section, recent studies in the literature are reviewed.

Single Grid-connected Microgrid

The problem of energy management has been studied extensively in the literature for single grid-connected microgrids , e.g., see Kanchev *et al.* (2011); Zhang *et al.* (2013); Arboleya *et al.* (2015). Malysz *et al.* (2014) presented an optimization-based control method for a storage unit in a grid-connected microgrid. They considered the electricity cost, battery related operation costs, and utility oriented goals such as peak reduction and load smoothing in their objective function. They also proposed a robust counterpart of their nominal optimization problem to deal with uncertainty in the prediction of demand and renewable energy. Shi *et al.* (2017) presented an online energy management system for real-time operation of microgrids that takes into account the power flow and underlying power distribution network and the associated constraints. They modelled online energy management as a stochastic optimal power flow problem and employed Lyapunov optimization to devise an online algorithm to solve it in real time. Oriti *et al.* (2016) demonstrated a power electronics-based energy management system. Their method controls a single-phase voltage source battery inverter as a current source or a voltage source depending on the status of the AC grid and the user preference. It also guarantees power for critical loads in the event of grid failure and reduces the peak power by supplying some of the peak demand through the battery. Liu *et al.* (2016) proposed an optimal bidding strategy in the day-ahead market of a microgrid using a hybrid stochastic/robust optimization model. The microgrid coordinates the energy consumption or production of its components, and trades electricity both in day-ahead and real-time markets to minimize its operating cost.

A number of papers have focused on energy efficiency and demand profile improvement in a single-microgrid, e.g., see Ferruzzi *et al.* (2015); Wang *et al.* (2014); Baharlouei and Hashemi (2014). Pascual *et al.* (2015) proposed an energy management strategy for a residential microgrid consisting of photovoltaic panels and a small wind turbine. Their proposed control strategy uses information on the battery state of charge, the power at each microgrid node as well as the load and renewable generation forecasts to improve the microgrid power profile at the point of connection to the grid. Wu *et al.* (2011) developed a mixed-integer-linear-program optimization over a rolling horizon window for robust optimal control of a battery-based storage system in a grid-connected electricity microgrid. The user electricity cost and utility-oriented goals related to peak demand and load smoothing are included in the objective function of the optimization problem. Utility and cost optimization have been considered in a number of other papers as well, e.g., see Ahmadi *et al.* (2015); Liu *et al.* (2015); Elsied *et al.* (2015). Jiang and Fei (2015) proposed a cost-effective energy ecosystem in a community microgrid with distributed energy resources. The energy ecosystem is to achieve high-quality energy service and low cost for all the households. Ross *et al.* (2015) formulated a multi-objective optimization to optimize different benefits that can be gained with a microgrid. The multi-objective optimization was implemented through scalarization functions that are determined a priori based on valuation functions applicable to specific microgrids and jurisdictions.

Multiple Microgrids

Potential economical and environmental benefits that could arise from coordinated energy management of a group of microgrids have led to research in multi-microgrid energy management. The problem of energy management in a network of microgrids is a relatively new topic Fathi and Bevrani (2013); Asimakopoulou *et al.* (2013); Nguyen and Le (2013); Rahbar *et al.* (2014). Coordinated energy management in such settings can yield increased economic and environmental benefits for the consumers and utility operators. Ouammi *et al.* (2015) presented a centralized model predictive control for optimal exchange of power in a network of microgrids. They assumed power transmission lines exist between each pair of local microgrids. In their model, a microgrid sells power when its net demand is negative, without taking into account the energy level of the storage devices; consequently, the storage devices have no role in power trading. Wang *et al.* (2015b) proposed a control strategy for coordinated operation of networked microgrids in a distribution system. They formulated the problem as a stochastic bi-level optimization with the distribution network operator at the upper level, and the microgrids at the lower level. The resulting nonlinear optimization model was approximated by a mixed integer linear program. However, mixed integer linear problems are non-convex optimizations with computation times that could grow very rapidly with the size of the problem; this behaviour renders mixed integer linear program-based optimization impractical for real-time energy management in large networks of microgrids.

Wang *et al.* (2015a) introduced a hierarchical power scheduling approach to optimally manage power trading, storage and distribution in a smart power grid with a macrogrid and cooperative microgrids. They formulated the problem as a convex optimization problem and then decomposed it into a two-tier formulation, where the first stage is an offline optimization. This was then approximated for online implementation. They also proposed three algorithms to solve the problem hierarchically that are nonlinear with computational complexity in the order of N^6. Song *et al.* (2015) proposed an optimal electric energy management of a cooperative multi-microgrid community with sequentially coordinated operations. Their goal was to distribute the computations in order to make optimal 24-hour energy management of multi-microgrids possible. They assume a combined heat and power generator exists in each microgrid. However, this work does not resolve the redundancy of the solution in a multi-microgrid energy management problem. The work of Chakraborty *et al.* (2015) presented an optimal coalition formation mechanism in multi-microgrid energy trading and analyzed the characteristics of an optimal response from a coalitional game theoretical perspective. The proposed method does not consider energy storage devices and line capacity constraints. Moreover, it may yield solutions in which a microgrid can simultaneously buy power from the grid and sell it to other local microgrids.

Energy management in a multi-microgrid community can be decentralized Lv and Ai (2016); Shafiee *et al.* (2014b); Hossain *et al.* (2016) or centralized Dagdougui *et al.* (2016); Nikmehr and Najafi Ravadanegh (2016) frameworks. Olivares *et al.* (2014) presented a mathematical formulation of the microgrid energy management problem and its implementation in a centralized system for isolated microgrids. Using a model predictive control framework, the optimal operation of the microgrid is determined over an extended horizon of evaluation and recourse. The energy management problem is decomposed into unit commitment and optimal power flow problems in order to avoid a mixed-integer non-linear formulation. The microgrid is modelled as a three-phase unbalanced system with both dispatchable and non-dispatchable distributed generation.

Arefifar *et al.* (2017) presented optimized and coordinated strategies for performing and assessing energy management in multiple microgrid systems. The energy management process was formulated for multi-microgrid systems that simultaneously incorporate several energy generation/consumption units, including different types of distributed generators, energy storage units, electric vehicles, and demand response.

Due to the probabilistic nature of some loads and generators, a novel probabilistic index was defined to measure the success of energy management scenarios in terms of cost minimization. Moreover, by using the new index, common types of energy controllers, such as distributed generations, storage units, electric vehicles and demand side management were implemented simultaneously and individually, and the impact of each addition on the performance index and operational costs is investigated.

Kou *et al.* (2017) presented a distributed economic model predictive control scheme for coordinated stochastic energy management of multiple microgrids. Based on probabilistic forecasts of renewable power generation and microgrid load, this scheme effectively handles uncertainties in both supply and demand. The proposed method was evaluated on a system with ten interconnected microgrids. Fang *et al.* (2016) presented a collective energy dispatch solution to optimally coordinate distributed generation, distributed storage units and critical demands across multiple microgrids based on a tree stem-leaves approach. The energy distribution network consisting of multiple microgrids was modelled mathematically as a weighted matrix simultaneously considering power loss and reliability statistics. The revised minimum spanning tree algorithm was adopted to identify the optimal distributed generation-critical loads and storage unit-critical loads mappings for energy supply; an algorithm using linear matrix inequalities determined the non-critical loads to be supplied and added them to the stems as tree leaves. Such energy network structure formed by stem and leaves can vary over time in case that significant changes are identified during microgrid operation and the functionalities can be implemented through intelligent system management tools.

2.4 Summary

A review of the state of the art in energy management of microgrids was presented in this chapter. The review covered the literature from a number of different angles, including the microgrid mode of operation (Section 2.3.1), type of optimization problem (Section 2.3.2), optimal control approaches (Section 2.3.3), and structure of network (Section 2.3.4).

Chapter 3

Multi-Objective Optimization

This chapter briefly reviews some fundamental concepts in multi-objective optimization problems, that are used later in the thesis. The review is not comprehensive and simply focuses on materials relevant to the future chapters. These include the concept of Pareto optimality, and various scalarization and non-scalarization techniques for seeking Pareto optimal solutions of a multi-objective optimization problem.

A typical multi-objective optimization problem is stated as

$$\begin{aligned} \min_{\boldsymbol{x}} \quad & \mathbf{F}(\boldsymbol{x}) = \Big[F_1(\boldsymbol{x}), \cdots, F_k(\boldsymbol{x})\Big]^T \\ \text{subject to} \quad & g_i(\boldsymbol{x}) \leq 0, \quad i = 1, \cdots, n \\ & h_j(\boldsymbol{x}) = 0, \quad j = 1, \cdots, m \end{aligned} \tag{3.1}$$

Here the goal is to *minimize* the objective vector $\mathbf{F}(\boldsymbol{x})$, which contains k scalar objectives, subject to n inequality and m equality constraints. The decision vector is $\boldsymbol{x} \in \mathbb{R}^q$, where q is the number of independent decision variables. The feasible solution space is defined as $\boldsymbol{X} = \{\boldsymbol{x} | g_i(\boldsymbol{x}) \leq 0, i = 1, \cdots, n; \& h_j(\boldsymbol{x}) = 0, j = 1, \cdots, m\}$, that is the set of all decision vectors that satisfy the constraints of the problem, and the attainable space is $\{\mathbf{F}(\boldsymbol{x}) | \boldsymbol{x} \in \boldsymbol{X}\}$, the set of objective vector values of feasible points.

Unlike in their single-objective counterparts, the concept of optimality in multi-objective optimization problems is not evident. In fact, there is typically no single global optimal solution for such problems, but rather there exists a family of solutions that satisfy some notion of optimality. The concept of Pareto optimality has been widely used to characterize optimal solutions in vector optimization problems, and is defined as follows Marler and Arora (2004)

Definition 1: A feasible solution $\hat{\boldsymbol{x}} \in \boldsymbol{X}$ for the problem in (3.1) is *Pareto* optimal (efficient), if there is no other $\boldsymbol{x} \in \boldsymbol{X}$ such that $\mathbf{F}(\boldsymbol{x}) \preceq \mathbf{F}(\hat{\boldsymbol{x}})$, with inequality relation holding element-wise. If $\hat{\boldsymbol{x}}$ is Pareto optimal, $\mathbf{F}(\hat{\boldsymbol{x}})$ is called a nondominated point. The set of all Pareto optimal points $\hat{\boldsymbol{x}} \in \boldsymbol{X}$ is denoted $\boldsymbol{X_E}$ and called the efficient set.

There are numerous methods for finding Pareto optimal points of a multi-objective optimization problem by converting it to ordinary single-objective optimization problems Ehrgott (2006). These methods are often categorized based on whether they yield necessary or sufficient conditions for Pareto optimality Ehrgott (2006). They can be classified as scalarizing and non-scalarizing methods. These methods incorporate parameters such as coefficients, exponents, and constraint limits. By varying these parameters they can generate the efficient set of the optimization problem. The compromise programming and sum of the costs are two scalarization methods, and the lexicographic programming is a non-scalarization method, that will be used in this thesis for seeking Pareto optimal points of a multi-objective optimization problem.

They will be briefly discussed next.

3.1 Compromise Programming

The *utopia point* for a multi-objective optimization is defined as follows.

Definition 2: The point $\mathbf{F}^u = \left[F_1^u, \cdots, F_k^u\right]^T$ given by

$$F_i^u := \min_{\boldsymbol{x}} \quad \{F_i(\boldsymbol{x}) | \boldsymbol{x} \in \boldsymbol{X}\} \tag{3.2}$$

is called the utopia point of the multi-objective optimization problem (3.1). The best outcome of a multi-objective optimization problem is the utopia point. However, in general, the utopia point is not attainable. Instead, a *compromise solution* may be sought that is as close as possible to the utopia point, based on a conventional vector norm. The following single-objective optimization may then be formulated on this basis.

$$\begin{aligned} \min_{\boldsymbol{x}} \qquad & \left\{ \sum_{i=1}^{k} \left| F_i(\boldsymbol{x}) - F_i^u \right|^p \right\}^{\frac{1}{p}} \\ \text{subject to} \quad & g_i(\boldsymbol{x}) \leq 0, \quad i = 1, \cdots, n \\ & h_j(\boldsymbol{x}) = 0, \quad j = 1, \cdots, m \end{aligned} \tag{3.3}$$

The objective function is l_p-norm of the distance to the utopia point, and is strictly monotone for $1 \leq p \leq \infty$ Therefore, the solution to this optimization problem is efficient (Pareto optimal) for the original multi-objective problem Ehrgott (2006).

3.2 Weighted Sum of the Costs

One common scalarization method is the so-called weighted sum of the costs method, which converts a multi-objective optimization to the following conventional single-objective problem:

$$\begin{aligned} \min_{\boldsymbol{x}} \quad & \sum_{l=1}^{k} w_l F_l(\boldsymbol{x}) \\ \text{subject to} \quad & g_i(\boldsymbol{x}) \leq 0, \quad i = 1, \cdots, n \\ & h_j(\boldsymbol{x}) = 0, \quad j = 1, \cdots, m \end{aligned} \tag{3.4}$$

Here the scalarized objective function is the weighted summation of all individual costs of the multi-objective optimization problem (3.1). In Zadeh (1963), it has been shown that if all of the weights are positive, the solution to (3.4) is Pareto optimal for the original multi-objective optimization in (3.1).

3.3 Lexicographic Programming

A lexicographic optimization problem arises when the objectives of multi-objective optimization problem have to be considered in a hierarchical manner. Lexicographic order is defined as Migdalas *et al.* (2013):

Definition 3: Let $\mathbf{y}^1, \mathbf{y}^2 \in \mathbb{R}^z$, and if $\mathbf{y}^1 \neq \mathbf{y}^2$ let $w^\star := min\ \{w \mid \mathbf{y}^1_w \neq \mathbf{y}^2_w\}$, $\leq_{lex}$ denotes the lexicographic order and is defined as $\mathbf{y}^1 \leq_{lex} \mathbf{y}^2 := \mathbf{y}^1_{w^\star} \leq \mathbf{y}^2_{w^\star}\ \ or\ \ \mathbf{y}^1 = \mathbf{y}^2$(Here $\mathbf{y}^1_w$ denotes wth element of vector $\mathbf{y}^1$.)

In this approach, the objectives are compared according to the lexicographic order in the attainable space. An optimal solution to such a problem is called lexicographically optimal as defined below.

Definition 4: A feasible solution $\hat{\mathbf{x}} \in \mathbf{X}$ is lexicographically optimal if there is no $\mathbf{x} \in \mathbf{X}$ such that $\mathbf{F}(\mathbf{x}) \leq_{lex} \mathbf{F}(\hat{\mathbf{x}})$.

It can be shown a lexicographic optimal point is also Pareto optimal Ehrgott (2006). In the lexicographic formulation, first the components of the objective vector are arranged in the order of their importance. Then, the following optimization problems are solved one at a time:

for $\quad s = 1, \cdots, k.$

$$\begin{aligned} \min_{\boldsymbol{x}} \quad & F_s(\boldsymbol{x}) \\ \text{subject to} \quad & g_i(\boldsymbol{x}) \leq 0, \quad i = 1, \cdots, n \\ & h_j(\boldsymbol{x}) = 0, \quad j = 1, \cdots, m \\ & F_l(\boldsymbol{x}) = F_l(\boldsymbol{x_l^\star}), \quad l = 1, \cdots, s-1, s > 1 \end{aligned} \tag{3.5}$$

where s is the objective function position in the priority sequence and $F_l(\boldsymbol{x_l^\star})$ is the optimum of the lth function, found in the lth iteration.

Chapter 4

Energy Management in a Network of Grid-Connected Microgrids Using Compromise Programming

In Chapter 2, the crucial role of energy management for efficient operation of a network of microgrids was underlined. Moreover, the general form of a multi-objective optimization problem for energy management and different approaches to solve this problem were briefly reviewed. In this chapter, a multi-objective optimization model for energy management in a network of microgrids with local storage and renewable energy and with connection to the utility grid is proposed. The microgrids in the network can exchange power locally with each other and with the utility grid. A pricing regime is introduced in which favourable local buy/sell rates encourage local exchange of power. The energy management, i.e. the control of storage devices and computation of local and grid components energy transactions, is formulated as an optimization problem on a rolling horizon basis. The net cost of electricity, including peak charge, is the objective to be minimized for each microgrid. The resulting problem is essentially a constrained multi-objective optimization which will be converted to a single-objective problem using the concept of compromise programming. A utopia point is defined as a vector of best achievable costs for individual microgrids, when they can take advantage of the favourable local buy/sell prices at all times. Norm l_1 and l_2 of the distance of the actual cost from the utopia cost are used as the objective function to be minimized. Linear/quadratic programming counterparts of the original problem are then developed that avoid binary/integer variables and can be solved in substantially shorter times, making them suitable for real-time implementation.

4.1 General Nonlinear Optimization Model

Elements of the vector $\mathbf{F}(\boldsymbol{x})$ in (3.1), i.e. local objectives, are defined as the net cost of electricity for the corresponding microgrids. Using the electricity rate scheme introduced in Section 1.2, the corresponding single-objective optimization can be stated as

$$\min\left\{\sum_{i=1}^{NoG}\left|\mathbf{c}^{bl^T}\left[\mathbf{P}_i^l\right]^+ + \mathbf{c}^{sl^T}\left[\mathbf{P}_i^l\right]^- + \mathbf{c}^{bg^T}\left[\mathbf{P}_i^g\right]^+ + \mathbf{c}^{sg^T}\left[\mathbf{P}_i^g\right]^- + c_i^{pk}P_i^{pk} - F_i^u\right|^p\right\}^{\frac{1}{p}} \quad (4.1a)$$

subject to, for $k = 1, \cdots, N_h \quad and \quad i = 1, \cdots, NoG$

Power Exchange constraints:

$$\mathbf{P}_i^{l,min} \preceq \mathbf{P}_i^l + \mathbf{P}_i^g \preceq \mathbf{P}_i^{l,max} \tag{4.1b}$$

$$\mathbf{P}^{mg,min} \preceq \mathbf{P}^g \preceq \mathbf{P}^{mg,max} \tag{4.1c}$$

$$-P_i^{rcl,max}\mathbf{h} \preceq \mathbf{P}_i^l(k) - \mathbf{P}_i^l(k-1) + \mathbf{P}_i^g(k) - \mathbf{P}_i^g(k-1) \preceq P_i^{rcl,max}\mathbf{h} \tag{4.1d}$$

$$\sum_{j=1}^{NoG} \mathbf{P}_j^l = 0 \tag{4.1e}$$

$$\sum_{j=1}^{NoG} \mathbf{P}_j^g = \mathbf{P}^g \tag{4.1f}$$

$$\mathbf{P}_i^l + \mathbf{P}_i^g = \mathbf{P}_i^{bat} + \mathbf{P}_i^n \tag{4.1g}$$

Battery Constraints:

$$E_i(k+1) = E_i(k) + \eta_i^c \mathbf{h}(k) \left[\mathbf{P}_i^{bat}(k)\right]^+ + \eta_i^{d^{-1}} \mathbf{h}(k) \left[\mathbf{P}_i^{bat}(k)\right]^- - P_i^{lossb}\mathbf{h}(k) \tag{4.1h}$$

$$\mathbf{P}_i^{bat,min} \preceq \mathbf{P}_i^{bat} \preceq \mathbf{P}_i^{bat,max} \tag{4.1i}$$

$$E_i^{min} \leq E_i(k+1) \leq E_i^{max} \tag{4.1j}$$

$$\eta_i^c \mathbf{h}^T \left[\mathbf{P}_i^{bat}\right]^+ + \eta_i^{d^{-1}} \mathbf{h}^T \left[\mathbf{P}_i^{bat}\right]^- - P_i^{lossb}\mathbf{h}^T\mathbf{1} = E_i^{final} - E_i^0 \tag{4.1k}$$

$$-P_i^{rcb,max}\mathbf{h} \preceq \mathbf{P}_i^{bat}(k) - \mathbf{P}_i^{bat}(k-1) \preceq P_i^{rcb,max}\mathbf{h} \tag{4.1l}$$

Peak Shaving Constraints:

$$
\begin{aligned}
& P_i^{pk} \geq 0 \\
& \sum_{j=1}^{NoG} P_j^{pk} \geq \mathbf{P}^g(k) - P^b \\
& -\Delta_1\left(\sum_{j=1}^{NoG} P_j^{pk} - \mathbf{P}^g(k) + P^b\right) \leq P_i^{pk} - \mathbf{P}_i^{bg}(k) \leq \Delta_1\left(\sum_{j=1}^{NoG} P_j^{pk} - \mathbf{P}^g(k) + P^b\right)
\end{aligned} \tag{4.1m}
$$

Island Mode Constraint:

$$
\sum_{i=1}^{NoG} E_i(k+1) \geq \sum_{t=1}^{NoH} \sum_{i=1}^{NoG} \mathbf{h}(t+k)\mathbf{P}_i^n(t+k) \tag{4.1n}
$$

In this formulation, $[\bullet]^+$ and $[\bullet]^-$ denote non-negative part, i.e. $[\bullet]^+ = \max(\bullet, 0)$, and non-positive part, i.e. $[\bullet]^- = \min(\bullet, 0)$ of a variable respectively. Indices i and k refer to the microgrid and time step in the control horizon, respectively. The optimization model is formulated over the control horizon $\mathbf{h}$. A bold variable is a decision vector over the control horizon containing values of control decisions at all time steps. An explanation of the optimization constraints follows next.

4.1.1 Single-Objective Cost

As stated earlier, local objectives are defined as the net cost of electricity for the corresponding microgrids. Here the single objective cost (4.1a) is the Euclidean distance between the vector of local costs and their corresponding utopia point, the lowest possible electricity costs for the individual microgrids, with an exclusive use of the preferred local buy/sell rates F_i^u. In other words, the utopia point for each individual microgrid is calculated by assuming that they can purchase all required power locally and also sell their surplus power locally as well to gain the highest possible cost saving. Here only $p = 1$ *or* 2 , i.e., l_1-norm and l_2-norms, are considered.

4.1.2 Power Exchange Constraints

The constraints in (4.1b) ensure that net power of each microgrid remains within the line capacity limits. Similarly, the aggregated net power of the microgrids, $\mathbf{P}^g$, is within the line limits defined in (4.1c). Changes in the microgrids net power over consecutive sample times are limited by (4.1d) to avoid large power fluctuations.

The constraint (4.1e) simply states that local exchanges of power add up to zero, i.e., the power bought locally is equal to power sold locally. The total power exchanged with the utility grid is determined through (4.1f). The power balance constraint for each microgrid is given in (4.1g), where $\mathbf{P}_i^{bat}$ is the battery power, $\mathbf{P}_i^g$ is power from/to the utility grid, $\mathbf{P}_i^l$ is locally exchanged power, and $\mathbf{P}_i^n$ is net demand power. The net demand vector, defined as the difference between local generation and the electricity usage of the load, is given by

$$\mathbf{P}_i^n = \mathbf{P}_i^{Loads} - \mathbf{P}_i^{Solar} - \mathbf{P}_i^{Wind}, i = 1, \cdots, NoG \tag{4.2}$$

4.1.3 Battery Constraints

For the ith microgrid, the evolution of the stored energy can be expressed by a discrete-time dynamic model in (4.1h). In this equation, $E_i(k)$ is stored energy in ith microgrid at time step k, that is usually in kWh unit, η_i^c and η_i^d are charging and discharging efficiency of ith microgrid, $\mathbf{h}(k)$ is the length of each time step on the prediction horizon measured in hours, P_i^{lossb} is self discharging loss in kW. Constraints (4.1i) and (4.1j) impose limits on the battery power and energy. The end of horizon battery energy level is set by the constraint (4.1k). Large changes in battery charging or discharging powers are prevented by (4.1l). Reducing the value of $P_i^{rcb,max}$ in this constraint would yield a smoother battery charging/discharging profile, at the expense of possibly not being able to fully utilize the battery capacity for electricity cost reduction. Other forms of battery operation related costs and constraints similar to those in our group's earlier work in Malysz *et al.* (2014) could be easily incorporated into the optimization formulation.

4.1.4 Peak Shaving Constraints

Utilities usually charge their larger consumers for their peak power in a billing cycle if it is in excess of a base power P^b. Here, the peak power is $\max(\mathbf{P}^g(k) - P^b)$, where the max is computed over time. The variable P_i^{pk} represents the contribution of the i'th microgrid to the peak power and therefore the term $c_i^{pk} P_i^{pk}$in the cost function is the share of peak cost for the corresponding microgrid. The term $c_i^{pk} P_i^{pk}$ in the cost function along with the peak shaving inequality constraints guarantee that at the time of peak power when $\sum_{j=1}^{NoG} P_j^p = \max(\mathbf{P}^g(k) - P^b)$, the contribution of individual microgrids to the peak power is correctly computed as $P_i^p = \mathbf{P}_i^{bg}(k)$. Note that Δ_1 is a large positive number.

4.1.5 Island Mode Constraint

It is desirable to guarantee continued operation of the microgrids in the event of an emergency grid blackout for a certain amount of time. The linear inequality constraint in (4.1n) imposes an adaptive lower bound on the combined stored energy in the network at any given time to ensure that the system can operate for at least NoH time steps in the event of a blackout. Note that the predicted net demands of the microgrids are used to compute the total required energy for continuous operation during the blackout. Errors in these predictions could impact the actual minimum operation time in the event of a black-out. For example, over-estimating the renewable generation and under-estimating the demand would shorten this time. Choosing a more conservative number for NoH would force the network to store a larger amount of back-up energy for potential black-outs to account for such prediction uncertainty. The downside to this approach is that a smaller portion of the network storage capacity could be utilized for reducing electricity costs during normal operation.

4.2 Counterpart Linear/Quadratic Optimization Model

It is straightforward to show that the proposed energy management optimization formulation is convex. However, the nonlinear terms min($\bullet$) and max($\bullet$) in the objective and constraints render the problem rather difficult to solve. An equivalent problem formulation is presented next that avoids min($\bullet$) and max($\bullet$). To this end, let $\mathbf{P}_i^l = \mathbf{P}_i^{bl} + \mathbf{P}_i^{sl}$ by introducing two new variables $\mathbf{P}_i^{bl}$ and $\mathbf{P}_i^{sl}$. The following constraints are also added to the formulation

$$\begin{aligned}
&\mathbf{P}_i^{bl} \succeq \mathbf{P}_i^{l} \\
&\mathbf{P}_i^{bl} \succeq \mathbf{0}
\end{aligned} \tag{4.3}$$

The terms in the cost function for the local buying and selling are replaced with

$$\mathbf{c}^{bl^T}\mathbf{P}_i^{bl} + \mathbf{c}^{sl^T}\mathbf{P}_i^{sl} = (\mathbf{c}^{bl} - \mathbf{c}^{sl})^T\mathbf{P}_i^{bl} + \mathbf{c}^{sl^T}\mathbf{P}_i^{l} \tag{4.4}$$

Here it is assumed $\mathbf{c}^{bl} \succ \mathbf{c}^{sl}$. This assumption is reasonable as a positive difference between the buy and sell prices represents the cost of operating the local infrastructure. With this assumption and the presence of the terms in (4.4) in the cost, it is straightforward to show that indeed

$$\begin{aligned}
\mathbf{P}_i^{bl} &= \left[\mathbf{P}_i^{l}\right]^+ = \max(\mathbf{P}_i^{l}, 0) \\
\mathbf{P}_i^{sl} &= \left[\mathbf{P}_i^{l}\right]^- = \min(\mathbf{P}_i^{l}, 0) = \mathbf{P}_i^{l} - \mathbf{P}_i^{bl}
\end{aligned} \tag{4.5}$$

This eliminates $\min(\bullet)$ and $\max(\bullet)$ from the problem formulation, leading to an equivalent but an easier problem to solve.

The max and min involving $\mathbf{P}_i^{g}$ can be similarly eliminated. Two new variables $\mathbf{P}_i^{bg}$ and $\mathbf{P}_i^{sg}$ are defined and $\mathbf{P}_i^{g} = \mathbf{P}_i^{bg} + \mathbf{P}_i^{sg}$. The terms associated with the grid buy/sell in the cost function are replaced with $(\mathbf{c}^{bg} - \mathbf{c}^{sg})^T\mathbf{P}_i^{bg} + \mathbf{c}^{sg^T}\mathbf{P}_i^{g}$. The following constraints are also added

$$\begin{aligned}
&\mathbf{P}_i^{bg} \succeq \mathbf{P}_i^{g} \\
&\mathbf{P}_i^{bg} \succeq \mathbf{0} \\
&\mathbf{P}_i^{sg} = \mathbf{P}_i^{g} - \mathbf{P}_i^{bg}
\end{aligned} \tag{4.6}$$

The battery power variable can be manipulated similarly. However, since this variable does not appear in the cost function, a small term $\boldsymbol{\alpha}^T \mathbf{P}_i^c$ is added to the cost, where $\boldsymbol{\alpha}^T$ is a vector with positive small elements. Now, by defining $\mathbf{P}_i^{bat} = \mathbf{P}_i^c + \mathbf{P}_i^d$, and following similar steps as those in the previous case, the nonlinear max($\bullet$) and min($\bullet$) terms involving the battery signals are removed.

Using the above results, the following equivalent convex optimization problem is proposed

$$\min\left\{ \sum_{i=1}^{NoG} \left| (\mathbf{c}^{bl} - \mathbf{c}^{sl})^T \mathbf{P}_i^{bl} + \mathbf{c}^{sl^T} \mathbf{P}_i^l + (\mathbf{c}^{bg} - \mathbf{c}^{sg})^T \mathbf{P}_i^{bg} + \mathbf{c}^{sg^T} \mathbf{P}_i^g + \boldsymbol{\alpha}^T \mathbf{P}_i^c + c_i^{pk} P_i^{pk} - F_i^u \right|^p + \boldsymbol{\alpha}^T \mathbf{P}^{bg} \right\}^{\frac{1}{p}} \tag{4.7a}$$

subject to, for $k = 1, \cdots, N_h \quad and \quad i = 1, \cdots, NoG$

Power Exchange Constraints:

$$\mathbf{P}_i^{l,min} \preceq \mathbf{P}_i^l + \mathbf{P}_i^g \preceq \mathbf{P}_i^{l,max} \tag{4.7b}$$

$$\mathbf{P}^{mg,min} \preceq \mathbf{P}^g \preceq \mathbf{P}^{mg,max} \tag{4.7c}$$

$$-P_i^{rcl,max}\mathbf{h} \preceq \mathbf{P}_i^l(k) - \mathbf{P}_i^l(k-1) + \mathbf{P}_i^g(k) - \mathbf{P}_i^g(k-1) \preceq P_i^{rcl,max}\mathbf{h} \tag{4.7d}$$

$$\sum_{j=1}^{NoG} \mathbf{P}_j^l = 0 \tag{4.7e}$$

$$\sum_{j=1}^{NoG} \mathbf{P}_j^g = \mathbf{P}^g \tag{4.7f}$$

$$\mathbf{P}_i^l + \mathbf{P}_i^g = \mathbf{P}_i^{bat} + \mathbf{P}_i^n \tag{4.7g}$$

$$\begin{aligned}
&\mathbf{P}^{bg} \succeq \sum_{j=1}^{NoG} \mathbf{P}_j^g \\
&\mathbf{P}^{bg} \succeq \mathbf{0} \\
&\mathbf{P}^{sg} = \sum_{j=1}^{NoG} \mathbf{P}_j^g - \mathbf{P}^{bg}
\end{aligned} \tag{4.7h}$$

$$\begin{aligned}
&\mathbf{P}_i^{bl} \succeq \mathbf{P}_i^l \\
&\mathbf{P}_i^{bl} \succeq \mathbf{0} \\
&\mathbf{P}_i^{sl} = \mathbf{P}_i^l - \mathbf{P}_i^{bl}
\end{aligned} \tag{4.7i}$$

$$\begin{aligned}
&\mathbf{P}_i^{bg} \succeq \mathbf{P}_i^g \\
&\mathbf{P}_i^{bg} \succeq \mathbf{0} \\
&\mathbf{P}_i^{sg} = \mathbf{P}_i^g - \mathbf{P}_i^{bg}
\end{aligned} \tag{4.7j}$$

Battery Constraints:

$$E_i(k+1) = E_i(k) + \eta_i^c \mathbf{h}(k)\mathbf{P}_i^c(k) + \eta_i^{d^{-1}} \mathbf{h}(k)(\mathbf{P}_i^{bat} - \mathbf{P}_i^c) - P_i^{lossb}\mathbf{h}(k) \tag{4.7k}$$

$$\mathbf{P}_i^{bat,min} \preceq \mathbf{P}_i^{bat} \preceq \mathbf{P}_i^{bat,max} \tag{4.7l}$$

$$E_i^{min} \leq E_i(k+1) \leq E_i^{max} \tag{4.7m}$$

$$\eta_i^c \mathbf{h}^T \mathbf{P}_i^c + \eta_i^{d^{-1}} \mathbf{h}^T(\mathbf{P}_i^{bat} - \mathbf{P}_i^c) - P_i^{lossb}\mathbf{h}^T\mathbf{1} = E_i^{final} - E_i^0 \tag{4.7n}$$

$$-P_i^{rcb,max}\mathbf{h} \preceq \mathbf{P}_i^{bat}(k) - \mathbf{P}_i^{bat}(k-1) \preceq P_i^{rcb,max}\mathbf{h} \tag{4.7o}$$

$$\mathbf{P}_i^c \succeq \mathbf{P}_i^{bat}, \quad \mathbf{P}_i^c \succeq \mathbf{0} \tag{4.7p}$$

Peak Shaving Constraints:

$$
\begin{aligned}
& P_i^{pk} \geq 0 \\
& \sum_{j=1}^{NoG} P_j^{pk} \geq \mathbf{P}^g(k) - P^b \\
& -\Delta_1 \Bigg(\sum_{j=1}^{NoG} P_j^{pk} - \mathbf{P}^g(k) + P^b \Bigg) \leq P_i^{pk} - \mathbf{P}_i^{bg}(k) \leq \Delta_1 \Bigg(\sum_{j=1}^{NoG} P_j^{pk} - \mathbf{P}^g(k) + P^b \Bigg)
\end{aligned} \tag{4.7q}
$$

Island Mode Constraint:

$$
\sum_{i=1}^{NoG} E_i(k+1) \geq \sum_{t=1}^{NoH} \sum_{i=1}^{NoG} \mathbf{h}(t+k)\mathbf{P}_i^n(t+k) \tag{4.7r}
$$

It must be noted that in this work, only the cases with $p = 1, 2$ are considered. For $p = 1$, by defining new decision variables $t_i, i = 1, \cdots, NoG$, the optimization problem (4.7) can be reformulated as a standard linear program,

$$
\min \Bigg\{ \sum_{i=1}^{NoG} \Bigg(t_i + \boldsymbol{\alpha}^T (\mathbf{P}_i^{bl} + \mathbf{P}_i^{bg} + \mathbf{P}_i^c) + \zeta P_i^p \Bigg) + \boldsymbol{\alpha}^T \mathbf{P}^{bg} \Bigg\} \tag{4.8a}
$$

subject to all constraints from (4.7b) to (4.7r) and for $i = 1, \cdots, NoG$

$$
-t_i \leq (\mathbf{c}^{bl} - \mathbf{c}^{sl})^T \mathbf{P}_i^{bl} + \mathbf{c}^{sl^T} \mathbf{P}_i^l + (\mathbf{c}^{bg} - \mathbf{c}^{sg})^T \mathbf{P}_i^{bg} + \mathbf{c}^{sg^T} \mathbf{P}_i^g + \boldsymbol{\alpha}^T \mathbf{P}_i^c + c_i^{pk} P_i^{pk} - F_i^u + \boldsymbol{\alpha}^T \mathbf{P}^{bg} \leq t_i \tag{4.8b}
$$

where ζ is a small positive number.

For $p = 2$, the objective function is quadratic and all constraints are linear so the optimization model using l_2-norm is a standard quadratic program. Effective algorithms are available for solving linear and quadratic programming problems. Finally, it is worth noting that the total number of decision variables of the optimization model is $N_h \cdot Nolv \cdot NoG + Nogv \cdot Nh + 2 \cdot NoG$ for l_1-norm formulation, and $N_h \cdot Nolv \cdot NoG + Nogv \cdot Nh + NoG$ for l_2-norm formulation, respectively. Here $Nolv$ is the number of local decision variables that is 6, and $Nogv$ is the number of global decision variables that is 3 for this optimization problem.

No conventional generation unit has been considered in local microgrids in the current formulation. However, conventional generation can be easily included in the optimization formulation by adding a linear term to the cost function component for each microgrid, representing the cost of such power, linear inequality constraints for upper and lower bounds of conventional generation, and the corresponding power term to the power balance equations, wherever applicable. This would not alter the form of the resulting optimization problem.

4.2.1 Island Mode Operation

In the event of a blackout in the utility grid, the microgrids network can continue its operation using the stored and available renewable energy. The energy constraints related to island mode operation ensure that there is sufficient energy stored in system for continued operation for at least NoH time steps during the blackout. The original optimization formulation requires some adjustments so it can be used for energy management in island mode. First at each step of rolling horizon control, the largest possible control horizon is determined based on the current level of stored energy and predicted net energy demand. This ensures longest possible operation if the blackout persists. Moreover, since exchange of power with the grid is no longer feasible, the following constraints need to be imposed

$$\mathbf{P}_j^g = 0 \tag{4.9}$$

island mode inequality constraints are also no longer needed. The revised optimization formulation can be used to determine optimal battery charge/discharge decisions.

4.3 Simulation Results

In this section, different operation scenarios are considered to analyze the response of the proposed multi-microgrid energy management optimization models. The simulations are carried out in the MATLAB environment using the IBM ILOG CPLEX LP solver on an Intel Core 2 Duo 3.00 GHz running Windows 7. The electricity usage and solar generation data used in the simulations have been provided by Burlington Hydro Inc. (Burlington, ON, CANADA). The electricity usage data is from the utility operator customers with peak usage over 50 kW and the solar energy generation units are capable of up to 30 kW output power.

4.3.1 System Response

A multi-microgrid system with one hundred microgrids is considered. Summer electricity pricing in place in the province of Ontario, Canada are used, i.e., 6.2 ¢/kWh (7*p.m.*-7*a.m.*), 9.2 ¢/kWh (7*a.m.*-11*a.m.*, and 5*p.m.*-7*p.m*), 10.8 ¢/kWh (11*a.m.*-5*p.m.*). Denoting these prices by the vector $\mathbf{c}^{buy}$, the other buy and sell prices are set to $\mathbf{c}^{bl} = 0.57\mathbf{c}^{buy}$, $\mathbf{c}^{bg} = \mathbf{c}^{buy}$, $\mathbf{c}^{sl} = 0.5\mathbf{c}^{buy}$, $\mathbf{c}^{sg} = 0.07\mathbf{c}^{buy}$. The battery characteristics are $E_i^{min} = 0$kWh, $E_i^{max} = 50$kWh, $\mathbf{P}_i^{bat,max} = -\mathbf{P}_i^{bat,min} = 12$kW, $\mathbf{P}_i^{rcb,max} =$

$-\mathbf{P}_i^{rcb,min} = 10$kW/h, $\eta_i^d = \eta_i^c = 0.95$, $P_i^{lossb} = 139$W, and the end of horizon battery energy level is set as $E_i^{final} = E_i^0$. The time-step averaged microgrid power/differential power limits are chosen as $\mathbf{P}_i^{l,max} = -\mathbf{P}_i^{l,min} = 25$kW/h, $\mathbf{P}_i^{rcl,max} = 20$kW/h and $\mathbf{P}^{mg,max} = -\mathbf{P}^{mg,min} = 2500$kW. The control prediction horizon is set to one day with a variable time step vector $h = \begin{bmatrix} 0.25\ 0.25\ 0.5\ 0.5\ 0.5\ 1\ 1\ 2\ 2\ 2\ 2\ 3\ 3\ 3\ 3 \end{bmatrix}^T$ so, $N_h = 15$ and rolling horizon controller runs every 15 minutes. The peak price is set to $c_p = 11¢/kW$ for a 24hour optimization prediction window, which translates to an effective 3.3$/kW peak price on a monthly basis.

The results of a 24-hour simulation with rolling horizon controller using the l_1-norm in the compromise programming method are plotted in Figs. 4.1 and 4.2. The time of use electricity pricing divides the 24-hour window into five distinct time intervals, separated by the dotted vertical lines. The first (0-7hours) and fifth (19-24hours) intervals are the off-peak period with the lowest electricity cost, the second (7-11hours) and fourth (17-19hours) intervals are mid-peak, and the third interval (11-17hours) is peak, with the highest electricity cost. It is notable that the exchange of power with the utility grid occurs primarily during the off-peak hours in the form of purchasing electricity at a low rate. During the on-peak and mid-peak hours, the microgrids exchange power amongst themselves locally to take advantage of the favourable local buy/sell prices. This clearly demonstrates the effectiveness of cooperative energy management in scenarios where microgrids can participate in a local energy market to minimize their cost or maximize their profit. The benefit of this scheme to the grid operator is also evident from a shift of the demand to off-peak hours, as seen in Fig. 4.2.d.

In summary, the coordinated control scheme enables the units in the partnership

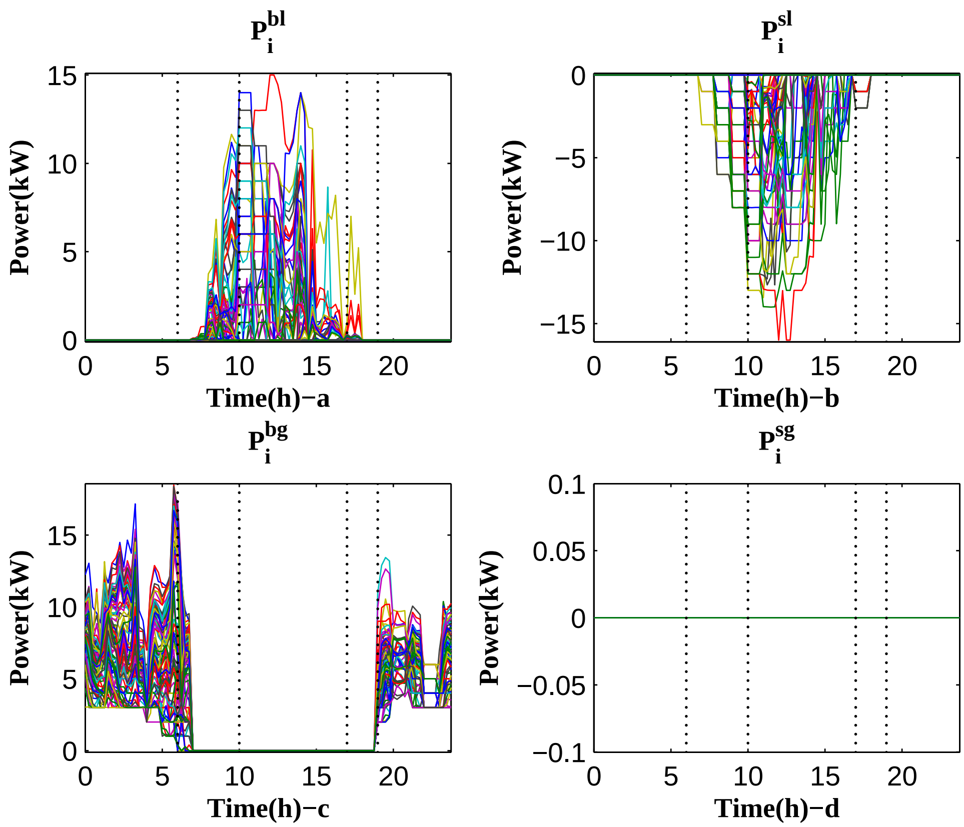

Figure 4.1: Exchange of powers in the compromise programming method using l_1-norm in grid-connected mode operation: (a) locally purchased powers, (b) locally sold powers, (c) powers purchased from the utility grid, and (d) powers sold to the utility grid.

to share their resources to substantially reduce their electricity cost. As a result, the utility operator may collect smaller revenue but would have much greater control over the demand side (via time of use price incentives) and can benefit from the load shifting enabled by coordinated control of large groups of customers. This is a practical way to transition to a more distributed model of grid operation, where there would be less reliance on large centralized power generation.

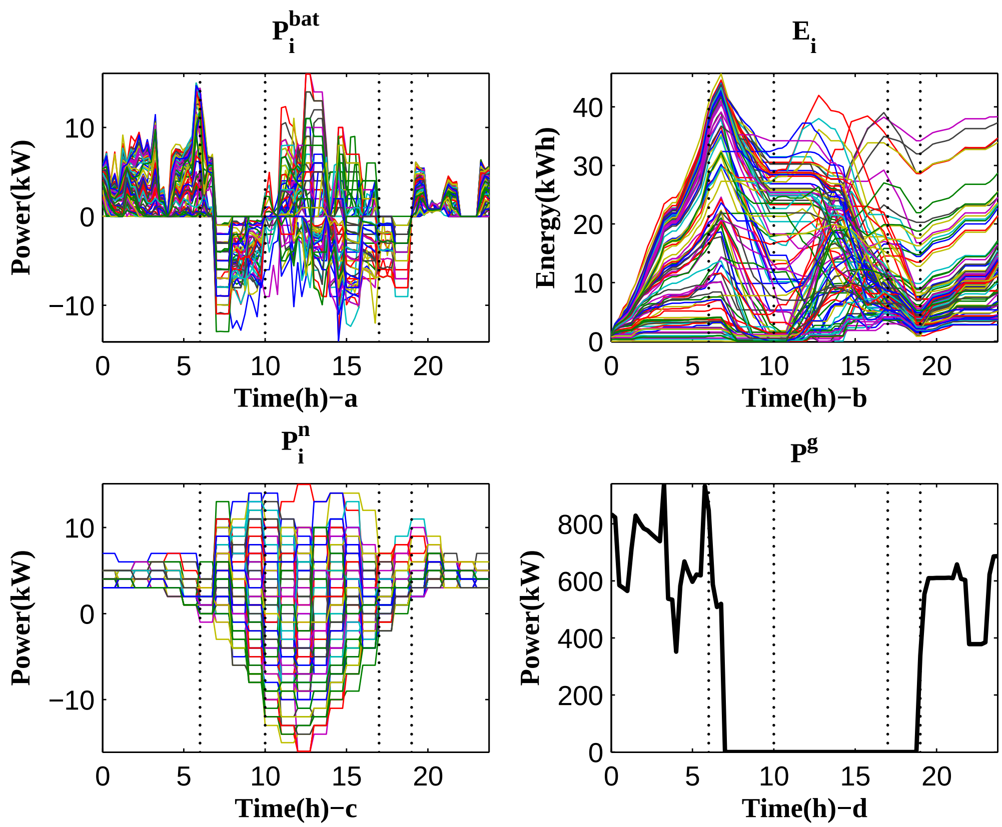

Figure 4.2: Power/energy signals in the compromise programming method using l_1-norm optimization in grid-connected mode operation: (a) battery charging/discharging powers, (b) battery energy levels, (c) microgrids net demand powers, and (d) the aggregate power exchanged with the utility grid.

The results of simulations with the compromise programming using l_2-norm formulation of the optimization problem are depicted in Figs. 4.3 and 4.4. It is noted that the different colors in Figs. 4.1-4.4 represent data from different microgrids. As it can be seen from these figures, the optimization model results are similar to the previous case. A notable point here is that generally the power and energy profiles resulting from the l_2-norm formulation are smoother than those obtained from the l_1-norm optimization model; this is most likely due to the fact that the cost function

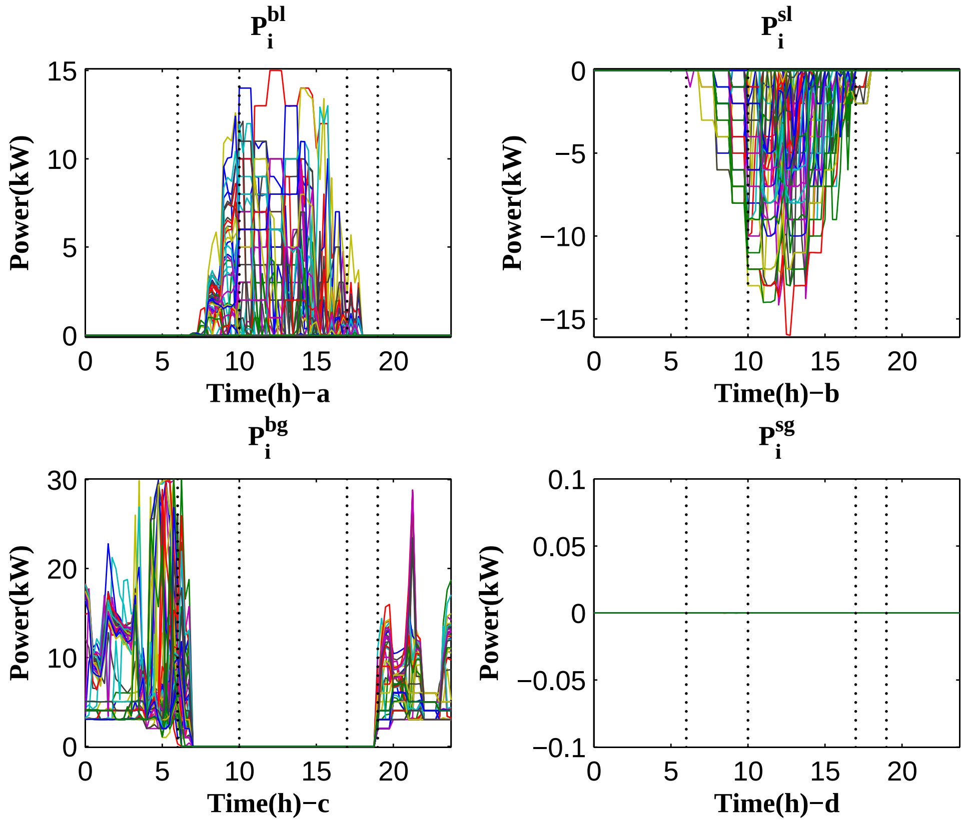

Figure 4.3: Exchange of powers in the compromise programming method using l_2-norm in grid-connected mode operation: (a) locally purchased powers, (b) locally sold powers, (c) powers purchased from the utility grid, and (d) powers sold to the utility grid.

is differentiable in the former case. It is also noted that since the optimization models employ a rolling horizon control strategy with the predicted demand, microgrids start buying power from the utility grid and charging their batteries towards the end of the day.

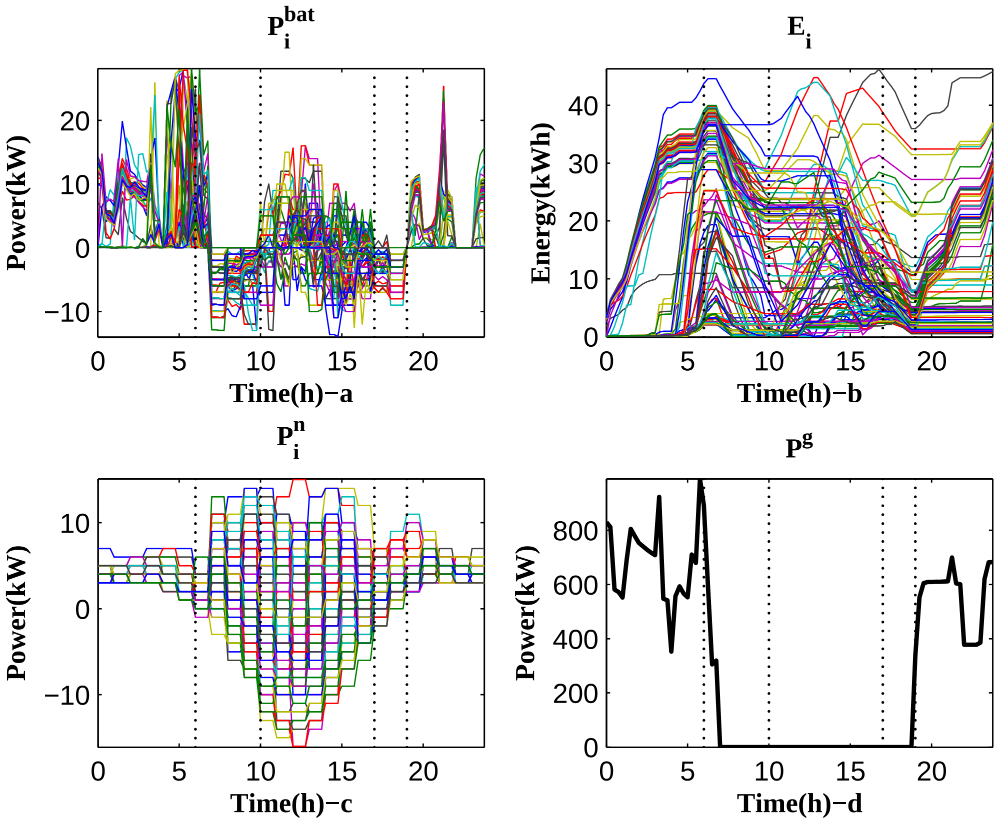

Figure 4.4: Power/energy signals in the compromise programming using l_2-norm in grid-connected mode operation: (a) battery charging/discharging powers, (b) battery energy levels, (c) microgrids net demand powers, and (d) the aggregate power exchanged with the utility grid.

4.3.2 Island Mode Operation

A blackout scenario during the normal operation of the system is considered here. A network of ten microgrids is simulated. The batteries are assumed to be initially charged at $50kWh$, with $E_i^{max} = 100kWh$; moreover, $NoH = 32$ in the island mode constraint. The results of simulations using l_1-norm are presented in Figs. 4.5. and 4.6. The blackout occurs at $66h$, i.e., the $18th$ hour of the third day, as denoted by a dotted vertical line in all figures and continues for the rest of simulation time.

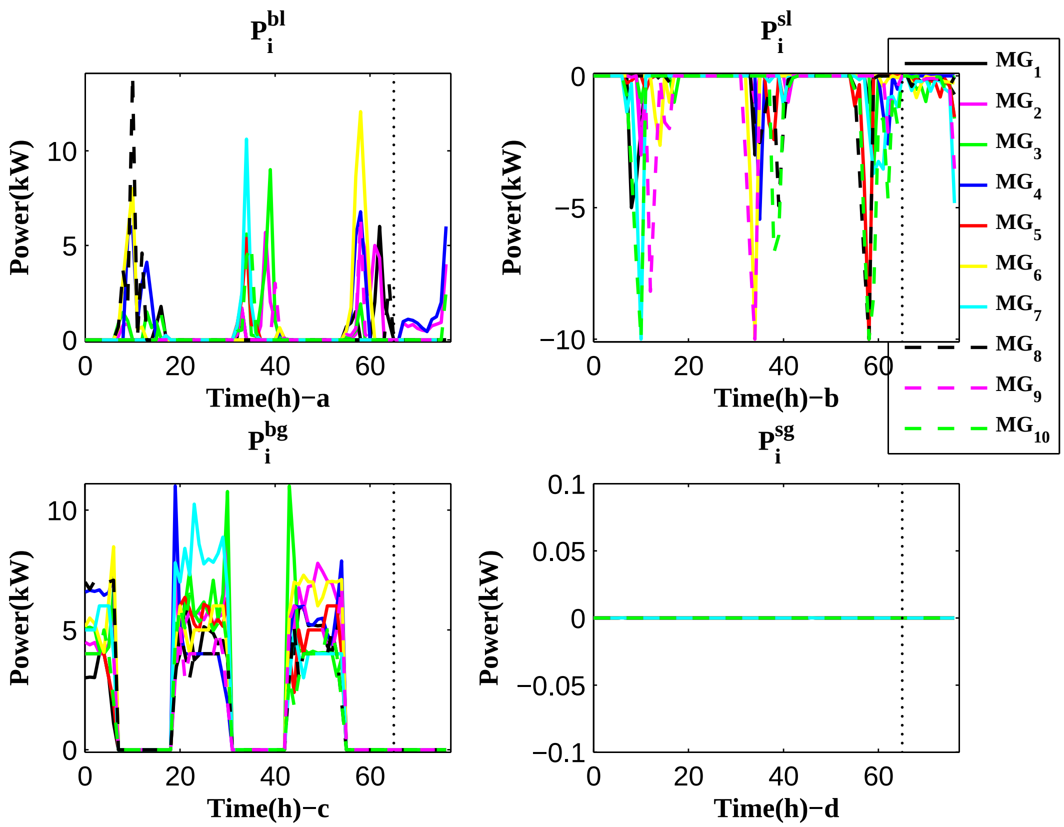

Figure 4.5: Exchange of powers in a network of ten microgrids in the compromise programming method using $l_1$norm in island mode operation-blackout start time denoted by the dotted vertical line: (a) locally purchased powers, (b) locally sold powers, (c) powers purchased from the utility grid, and (d) powers sold to the utility grid.

As this marks the beginning of the night, solar power is no longer available and the system has to rely solely on the stored energy for blackout operation. The grid-related buy/sell powers are all zero during the blackout; as a result, the aggregate exchanged power with the utility grid is also zero in Fig. 4.6.d. It is noted that the system keeps operating beyond $74h$ which is the guaranteed operation time based on $NoH = 32$ in the island mode constraint, until the batteries are fully discharged.

Table 4.1: Optimization runtime for one control time step using l_1-norm formulation

NoG	Max. CPU Time(s)	Avg. CPU Time(s)	Number of Dec. Vars
5	1.1	0.3	505
10	2.7	0.8	965
25	11.5	7.9	2345
50	40.4	31.9	4645
100	228.9	180.8	9245
200	890.3	810.3	18445

4.3.3 Computational Complexity

A great feature of the proposed optimization models is that they are convex linear programs free of binary decision variables, for which effective fast solvers exist. The scalability of the computations of the algorithms with the number of microgrids is investigated. Simulations have been carried out by varying the number of microgrids and recording the average and maximum computation times of solving the optimization problems, per time step of rolling horizon control. The results are reported in Tables 5.2 and 4.2 using l_1-norm and l_2-norm, respectively. These results are presented in the form of bar graphs in Fig. 4.7. Given that control time steps are 15 minutes each, it is evident that even in for the case of 200 microgrids, an optimal solution to the energy management problem can be found in real-time. Note that the computation times of the two optimization formulations are similar. For comparison, the solution time for a formulation of the optimization problem involving binary variables, which is not reported in this thesis, was in order of days running on the same computer. Therefore, the absence of binary/integer variables in the proposed optimization models is critical for achieving a real-time solution.

Table 4.2: Optimization runtime for one control time step using l_2-norm formulation

NoG	Max. CPU Time(s)	Avg. CPU Time(s)	Number of Dec. Vars
5	1.3	0.3	500
10	3.7	1.4	955
25	13.1	9.1	2320
50	48.6	38.5	4595
100	250.3	201.2	9145
200	903.2	844.6	18245

4.3.4 System Performance

The performance of the proposed multi-microgrid energy management (EMS-MG) optimization strategies is compared to two other cases. The basic case is when the microgrids are connected directly to the utility without energy management control (No-EMS). In the second case, the microgrids would still be directly connected to the utility grid but perform their own individual optimal energy management (EMS-DG). In this case as well as in the basic case, only grid buy and sell prices are applicable since no local exchange of power is permitted. The formulation of the linear program optimization problem for the single-microgrid system is not presented here due to space constraints. Simulations have been carried out for a period of one month.

The results of the simulations are reported in Tables 4.3 and 5.3, using l_1-norm formulation and l_2-norm formulations, respectively. It is noted that the EMS-MG yields substantially lower total electricity cost than the other two strategies. Note that since the microgrids exchange power locally, resources such as energy storage units and solar power could be shared among them to achieve large savings, without the need for installation of these capacities across all microgrids; this is an attractive feature of the proposed multi-microgrid energy management strategies. Another interesting observation is that larger networks of microgrids have larger pool of resources to share,

Table 4.3: Comparison of electricity costs under three different configurations using l_1-norm

NoG	EMS-MG	EMS-DG	Imp.(%)	No-EMS	Imp.(%)
5	481	916	47.05	1053	54.32
10	931	1833	49.20	2111	55.90
25	2331	5342	56.36	5596	58.34
50	5167	13654	62.15	14316	63.90
100	10431	33347	68.72	33670	69.02

Table 4.4: Comparison of electricity costs under three different configurations using l_2-norm

NoG	EMS-MG	EMS-DG	Imp.(%)	No-EMS	Imp.(%)
5	477	916	47.93	1053	54.70
10	921	1833	49.75	2111	56.37
25	2301	5342	56.93	5596	58.88
50	5139	13654	62.36	14316	64.10
100	10409	33347	68.79	33670	69.08

generally achieving higher cost savings than small networks under the proposed multi-microgrid energy management approach. For instance, a network of 100 microgrids sees about 69.02% reduction in its total electricity bill at the end of the month, compared to 54.32% for network of five(5).

4.4 Summary

In this chapter, a multi-objective optimization model for energy management in a network of microgrids with local storage and renewable energy and with connection to an external utility grid was presented. The microgrids can exchange power locally with each other and with the utility grid. A pricing regime was introduced in which favourable local buy/sell prices incentivize local exchange of power. Energy management, i.e. the control of storage devices, was formulated as an optimization problem on a rolling horizon basis. The net cost of electricity, including peak charge, was defined as the objective to be minimized for each microgrid. The resulting problem is essentially a constrained multi-objective optimization which was converted to a single-objective problem using the concept of compromise programming. A utopia point was defined as a vector of best achievable costs for individual microgrids, when they can take advantage of the favourable local buy/sell prices at all times. Norm l_1 and l_2 of the distance of the actual cost from the utopia cost were used as the objective function to be minimized.

In Section 4.2, a reformulation of the optimization problem was presented that eliminates nonlinear min and max functions without the use of binary or integer variables. This yielded convex linear and quadratic optimization problems for l_1 and l_2 norms, respectively, that can be effectively solved with existing optimization routines. In Section 4.3, numerical simulations were carried out with actual electricity and solar generation data. A comparison of the proposed multi-microgrid energy management strategy with the cases with no energy management, and with independent microgrid energy management showed a very substantial reduction in overall electricity cost using the proposed approach. The computation times for solving the optimization problem at each time step were also within the constraints of real-time implementation for a network as large of 200 microgrids using a conventional desktop computer.

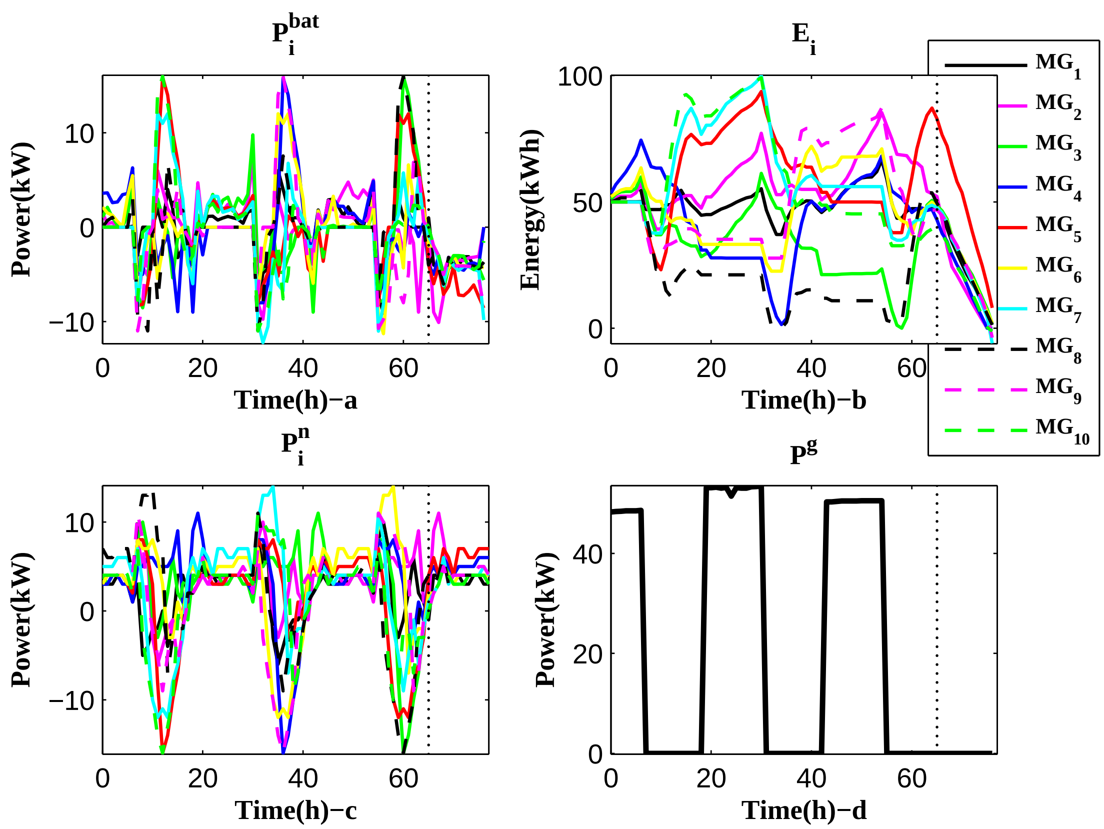

Figure 4.6: Power/energy signals in a network of ten microgrids in the compromise programming method using l_1-norm optimization in island mode operation-blackout start time denoted by the dotted vertical line: (a) battery charging/discharging powers, (b) battery energy levels, (c) microgrids net demand powers, and (d) the aggregate power exchanged with the utility grid.

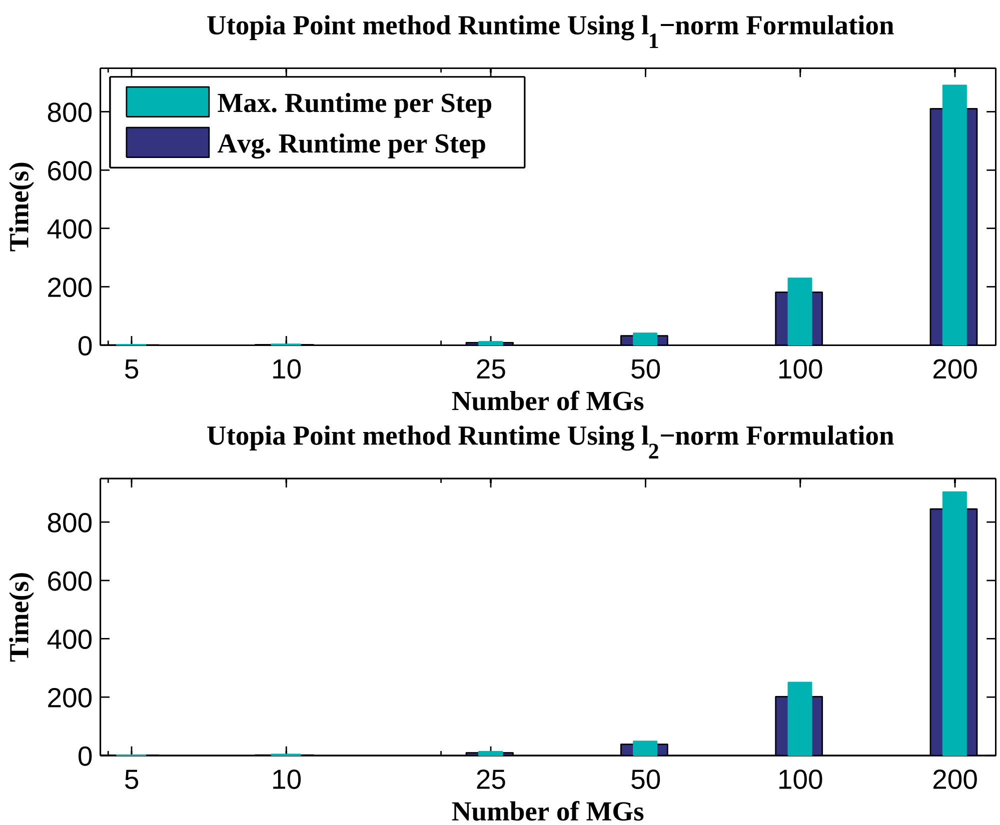

Figure 4.7: Average and maximum computation times per time step of the rolling horizon control.

Chapter 5

Coordinated Optimal Dispatch of Energy Storage in a Network of Grid-connected Microgrids by Minimizing Sum of Costs

5.1 Optimization Model

In the previous chapter, the compromise programming was used to find a Pareto optimal point of the general multi-objective optimization problem of energy management in a network of grid-connected microgrids. The solutions minimized the norm-1 and norm-2 distances between an ideal cost, i.e., the utopia point in the objective space, and the actual cost. In this chapter, the sum of the electricity costs of the microgrids is used as the performance objective to convert the multi-objective optimization problem to a conventional single-objective optimization problem. Moreover, new fairness constraints are introduced that would ensure all microgrids would fairly benefit from participating in the network scheme. This concept will be discussed in details later in this chapter.

Using the method proposed in Chapter 4, the nonlinear multi-objective optimization model of optimal power dispatch for a multi-microgrid network can be converted to a linear programming optimization problem. The steps taken for this conversion are similar to those in the previous chapter and are omitted for brevity. The resulting optimization model is given below.

$$\min \sum_{i=1}^{NoG} \left((\mathbf{c}^{bl} - \mathbf{c}^{sl})^T \mathbf{P}_i^{bl} + \mathbf{c}^{sl^T} \mathbf{P}_i^{l} + (\mathbf{c}^{bg} - \mathbf{c}^{sg})^T \mathbf{P}_i^{bg} + \mathbf{c}^{sg^T} \mathbf{P}_i^{g} + \boldsymbol{\alpha}^T \mathbf{P}_i^{c} \right) + c^p P^p + \boldsymbol{\beta}^T \mathbf{P}^{bg} \tag{5.1a}$$

subject to, for $k = 1, \cdots, N_h \quad and \quad i = 1, \cdots, NoG$

Power Exchange constraints:

$$\mathbf{P}^{mg,min} \leq \mathbf{P}^{g} \leq \mathbf{P}^{mg,max} \tag{5.1b}$$

$$\sum_{j=1}^{NoG} \mathbf{P}_j^{l} = 0 \tag{5.1c}$$

$$\begin{aligned} &\mathbf{P}^{bg} \geq \sum_{j=1}^{NoG} \mathbf{P}_j^{g} \\ &\mathbf{P}^{bg} \geq 0 \end{aligned} \tag{5.1d}$$

$$\mathbf{P}^{g} = \sum_{j=1}^{NoG} \mathbf{P}_j^{g} \tag{5.1e}$$

$$\mathbf{P}_i^{l,min} \leq \mathbf{P}_i^l + \mathbf{P}_i^g \leq \mathbf{P}_i^{l,max} \tag{5.1f}$$

$$-P_i^{rcl,max}\mathbf{h} \leq \mathbf{P}_i^l(k) - \mathbf{P}_i^l(k-1) + \mathbf{P}_i^g(k) - \mathbf{P}_i^g(k-1) \leq P_i^{rcl,max}\mathbf{h} \tag{5.1g}$$

$$\mathbf{P}_i^l + \mathbf{P}_i^g = \mathbf{P}_i^{bat} + \mathbf{P}_i^n \tag{5.1h}$$

$$\begin{aligned} &\mathbf{P}_i^{bl} \geq \mathbf{P}_i^l \\ &\mathbf{P}_i^{bl} \geq \mathbf{0} \\ &\mathbf{P}_i^{sl} = \mathbf{P}_i^l - \mathbf{P}_i^{bl} \end{aligned} \tag{5.1i}$$

$$\begin{aligned} &\mathbf{P}_i^{bg} \geq \mathbf{P}_i^g \\ &\mathbf{P}_i^{bg} \geq \mathbf{0} \end{aligned} \tag{5.1j}$$

Battery Constraints:

$$E_i(k+1) = E_i(k) + \eta_i^c \mathbf{h}(k)\mathbf{P}_i^c(k) + \eta_i^{d^{-1}}\mathbf{h}(k)(\mathbf{P}_i^{bat} - \mathbf{P}_i^c) - P_i^{lossb}\mathbf{h}(k) \tag{5.1k}$$

$$\mathbf{P}_i^{bat,min} \leq \mathbf{P}_i^{bat} \leq \mathbf{P}_i^{bat,max} \tag{5.1l}$$

$$E_i^{min} \leq E_i(k+1) \leq E_i^{max} \tag{5.1m}$$

$$\eta_i^c \mathbf{h}^T \mathbf{P}_i^c + \eta_i^{d^{-1}}\mathbf{h}^T(\mathbf{P}_i^{bat} - \mathbf{P}_i^c) - P_i^{lossb}\mathbf{h}^T\mathbf{1} = E_i^{final} - E_i^0 \tag{5.1n}$$

$$-P_i^{rcb,max}\mathbf{h} \leq \mathbf{P}_i^{bat}(k) - \mathbf{P}_i^{bat}(k-1) \leq P_i^{rcb,max}\mathbf{h} \tag{5.1o}$$

$$\begin{aligned} &\mathbf{P}_i^c \geq \mathbf{P}_i^{bat} \\ &\mathbf{P}_i^c \geq \mathbf{0} \end{aligned} \tag{5.1p}$$

Island Mode Constraint:

$$\sum_{i=1}^{NoG} E_i(k+1) \geq \sum_{t=1}^{NoH} \sum_{i=1}^{NoG} \mathbf{h}(t+k)\mathbf{P}_i^n(t+k) \tag{5.1q}$$

Peak Shaving Constraint:

$$\begin{aligned} &P^p \geq 0 \\ &P^p \geq \mathbf{P}^g(k) - P^b \end{aligned} \tag{5.1r}$$

Fair Power Exchange Constraints:

$$\mathbf{P}_i^{bg} = \mathbf{x}_i \mathbf{P}^{bg} \tag{5.1s}$$

$$\mathbf{P}_i^{sl} = \mathbf{y}_i \mathbf{P}^{sl} \tag{5.1t}$$

$$\mathbf{P}^{sl} = \sum_{j=1}^{NoG} \mathbf{P}_j^{sl} \tag{5.1u}$$

where

$$\mathbf{x}_i = \frac{\mathbf{P}_i^{share,b}}{\max\left(\sum_{i=1}^{NoG} \mathbf{P}_i^{share,b}, \epsilon\right)} \tag{5.2}$$

$$\mathbf{y}_i = \frac{\mathbf{P}_i^{share,s}}{\max\left(\sum_{i=1}^{NoG} \mathbf{P}_i^{share,s}, \epsilon\right)} \tag{5.3}$$

and

$$\mathbf{P}_i^{share,b} = \begin{cases} 0, & \text{if } \mathbf{P}_i^n - \min\left(\frac{E_i^0}{\mathbf{h}(1)}, \mathbf{P}_i^{bat,max}\right) \leq 0 \\ \mathbf{P}_i^n - \min\left(\frac{E_i^0}{\mathbf{h}(1)}, \mathbf{P}_i^{bat,max}\right), & \text{otherwise} \end{cases} \tag{5.4}$$

$$\mathbf{P}_i^{share,s} = \begin{cases} 0, & \text{if } \mathbf{P}_i^n - \min\left(\frac{E_i^0}{\mathbf{h}(1)}, \mathbf{P}_i^{bat,max}\right) \geq 0 \\ \min\left(\frac{E_i^0}{\mathbf{h}(1)}, \mathbf{P}_i^{bat,max}\right) - \mathbf{P}_i^n, & \text{otherwise} \end{cases} \tag{5.5}$$

An explanation of the optimization objective function and constraints follow next.

5.1.1 Scalarized Objective Function

First, it is noted that in the single-value aggregated cost function (5.1a), the weights of local costs are all set to one. This simply implies that the optimal solution, which is one of the Pareto optimal points, minimizes the total cost incurred by the microgrids over the control horizon. Obviously, non-equal positive weights could also be used to obtain other Pareto optimal solutions, but this is not considered in this thesis.

5.1.2 Power Exchange Constraints

All power exchange constraints were explained in Section 4.1.2.

5.1.3 Battery Constraints

All battery constraints were explained in Section 4.1.3.

5.1.4 Island Mode Constraint

Microgrids should be able to operate in island mode in the case of a power outage in the main grid. A minimum energy level for the total storage in the network is computed adaptively to ensure sufficient energy reserve in the case of a blackout event. This is enforced by adding constraint (5.1q) to the optimization model, which essentially requires sufficient stored energy for a minimum operation time during a blackout. In this constraint, NoH is the minimum number of time steps that the multi-microgrid system should be able to continue its operation in island mode. Note that the predicted net demand is used in the calculation of the required energy.

5.1.5 Peak Shaving Constraints

The term $c^p P^p$ in objective function represents a peak power cost, associated with the total peak power demand over a base demand P^b at the point of coupling to the utility grid. The inequality constraints in (5.1r) together with the positiveness of c^p guarantee that $P^p = \max\left(\mathbf{P}^g(k) - P^b, 0\right)$, where the maximum is computed over the elements of vector.

5.1.6 Fair Power Exchange Constraints

As stated earlier, the local buy price is set to less than the grid buy price, and the local sell price is higher than the grid sell price to incentivize local exchange of power. Given this rate scheme, it is important to give fair opportunities for buying and selling local power fairly among all microgrids as an incentive for their participation in the network-based resource sharing. The proposed fairness constraints are given in (5.1s) and (5.1u). The constraint (5.1s) simply requires that the purchased power from the utility grid to be a portion, $\mathbf{x}_i$, of total buying from the utility grid, $[\mathbf{P}_i^g]^+$. The buying factor $\mathbf{x}_i$ is defined in (5.2) as a function of $\mathbf{P}_i^{share,b}$ in (5.4); here ϵ is a small positive number. Note that $\mathbf{P}_i^{share,b}$ is defined for individual microgrids based on their current net demand and battery energy level. The idea is to allocate microgrids with higher net demand and lower stored energy a larger share of expensive grid power. Similarly, fairness in selling is ensured by (5.1u), where $\mathbf{P}^{sl}$ is total local sell power defined in (5.1u). The selling factor is defined in (5.3) and (5.5). Here a microgrid with larger solar power and stored energy would have a larger allocation of preferred local sell power.

It should be noted that the term $\boldsymbol{\alpha}^T \mathbf{P}_i^c$ can also be interpreted as the cost of battery operation in the corresponding microgrid. In such case, elements of this vector, $\boldsymbol{\alpha}$, are the cost associated with battery activities and can be determined based on the battery useful lifetime as a function of number of charge/discharge cycles, battery capacity, and its capital cost as follows:

$$\boldsymbol{\alpha}(i) = C\frac{T}{E_t}\text{in \$h/kWh} \tag{5.6}$$

Here C is the initial capital cost of the battery, E_t is the total charged/discharged energy over the lifetime of the battery, and T is the length of the control step in hours. The value of E_t can be estimated as

$$E_t = \sum_{k=0}^{N_{cd}-1}(1-\delta)^k E_{bat}^{max} = \frac{1-(1-\delta)^{N_{cd}}}{\delta}E_{bat}^{max}, \tag{5.7}$$

where N_{cd} is the rated lifetime of the battery in number of charge cycles, and δ is the rate of decline in battery capacity per charge cycle.

Optimal battery charge/discharge activities and partitioning of power variables to local/grid components are obtained by solving the optimization problem in (5.1), with the decision variables listed in Table 5.1. Finally, it is worth noting that the total number of decision variables of the optimization model is $N_h \cdot Nolv \cdot NoG + Nogv \cdot Nh + 1$. Here N_h is the number of time steps in rolling horizon window, $Nolv$ is the number of local decision variables that is 6, and $Nogv$ is the number of global

Table 5.1: Decision variables in the optimization model

Local Decision Variables	
$\mathbf{P}_i^l$	Local exchange power of ith microgrid.
$\mathbf{P}_i^{bl}$	Local imported power to the ith microgrid.
$\mathbf{P}_i^{sl}$	Local exported power from the ith microgrid.
$\mathbf{P}_i^g$	Exchange power of the utility grid with ith microgrid.
$\mathbf{P}_i^{bg}$	Purchased power from the utility grid by ith microgrid.
$\mathbf{P}_i^{sg}$	Sold power to the utility grid by ith microgrid.
$\mathbf{P}_i^{bat}$	Charging/discharging power of ith microgrid.
$\mathbf{P}_i^c$	Charging power of ith microgrid.
E_i	Battery energy level of ith microgrid.
$\mathbf{P}^{sl}$	Total local imported power
Global Decision Variables	
$\mathbf{P}^g$	Exchange power of the utility grid.
P^p	Auxiliary peak shaving variable.

decision variables that is 3 for this optimization problem.

5.2 Simulation Results

In this section, different operation scenarios are considered to analyze the performance of the proposed multi-microgrid energy management optimization model. The simulations are carried out in the MATLAB environment using the IBM ILOG CPLEX LP solver on an Intel Core 2 Duo 3.00 GHz running Windows 7. The electricity usage and solar generation data in the simulations have been provided by Burlington Hydro Inc. (Burlington, ON, CANADA). The electricity usage data is from the utility operator customers with peak usage over 50 kW and the solar energy generation units are capable of up to 30 kW output power.

5.2.1 System Response

A network with one hundred microgrids is considered. The electricity rates in the province of Ontario, Canada at the time of data collection were off-peak (6.2 ¢/kWh $7p.m.$-$7a.m.$), mid-peak (9.2 ¢/kWh $7a.m.$-$11a.m.$), and on-peak ($5p.m.$-$7p.m$, 10.8 ¢/kWh $11a.m.$-$5p.m.$). Denoting these rates by the vector $\mathbf{c}^{buy}$, the other buy and sell prices are set to $\mathbf{c}^{bl} = 0.57\mathbf{c}^{buy}$, $\mathbf{c}^{bg} = \mathbf{c}^{buy}$, $\mathbf{c}^{sl} = 0.5\mathbf{c}^{buy}$, $\mathbf{c}^{sg} = 0.07\mathbf{c}^{buy}$. The battery characteristics are $E_i^{min} = 0$kWh, $E_i^{max} = 30$kWh, $\mathbf{P}_i^{bat,max} = -\mathbf{P}_i^{bat,min} = 7.5$kW, $\mathbf{P}_i^{rcb,max} = -\mathbf{P}_i^{rcb,min} = 5$kW/h, $\eta_i^d = \eta_i^c = 0.95$, $P_i^{lossb} = 139$W, and the end of horizon battery energy level is set as $E_i^{final} = E_i^0$. The time-step averaged microgrid power/differential power limits are chosen as $\mathbf{P}_i^{l,max} = -\mathbf{P}_i^{l,min} = 20$kW/h, $\mathbf{P}_i^{rcl,max} = 15$kW/h and $\mathbf{P}^{mg,max} = -\mathbf{P}^{mg,min} = 2000$kW. The control prediction horizon is set to one day with a variable time step vector $h = \begin{bmatrix} 0.25\ 0.25\ 0.5\ 0.5\ 0.5\ 1\ 1\ 2\ 2\ 2\ 2\ 3\ 3\ 3\ 3 \end{bmatrix}^T$ so, $N_h = 15$ and rolling horizon controller runs every 15 minutes. The peak price is set to $c_p = 11¢/kW$ for a 24hour optimization prediction window, which translates to an effective 3.3\$/kW peak price on a monthly basis.

The results of a 24-hour simulation with rolling horizon controller are plotted in Figs. 5.1 and 5.2. The time of use electricity pricing divides the 24-hour window into five distinct time intervals, separated by the dotted vertical lines. The first (0-7hours) and fifth (19-24hours) intervals are the off-peak period with the lowest electricity cost, during which microgrids purchase power from the grid to meet their load demand and charge their batteries. During the mid-peak time (7-11hours and 17-19hours) microgrids exchange power mostly locally to take advantage of the favourable local buy/sell prices. Local transactions are even more prevalent during the on-peak period (11-17hours) when the grid electricity rate is the highest. It is also noteworthy that during the peak some microgrids are forced to sell some of their excess power to the grid. This is due to the fairness constraint for selling. The charging of the batteries at the end of the day is due to the rolling horizon nature of the controller; the batteries are charged using inexpensive off-peak grid power to prepare for the next day operation. The results in this section demonstrate, qualitatively, that the proposed energy management scheme enables the microgrids in the network to share their storage and renewable energy resources to reduce their electricity cost. The benefit of this energy management scheme to the grid operator is also evident from a shift of the demand to off-peak hours, as seen in Fig. 5.2.d.

5.2.2 Computational Complexity

As it was shown in the previous section, the proposed optimization model is a convex linear program free of binary decision variables, for which effective fast solvers exist. The scalability of the computations of the algorithms with the number of microgrids is investigated. Simulations have been carried out by varying the number of microgrids and the average and maximum computation times for solving the optimization problems, per time step of rolling horizon control have been recorded. The results are reported in Table 5.2. Given that the control time steps are 15 minutes long, real-time computation of the solution is possible even for a network as large as 200 microgrids. This is a great advantage of such binary-free optimization model. For comparison, a counterpart mixed-binary optimization model registered a computation time in the order of days to converge to a solution for one time step on the same computer.

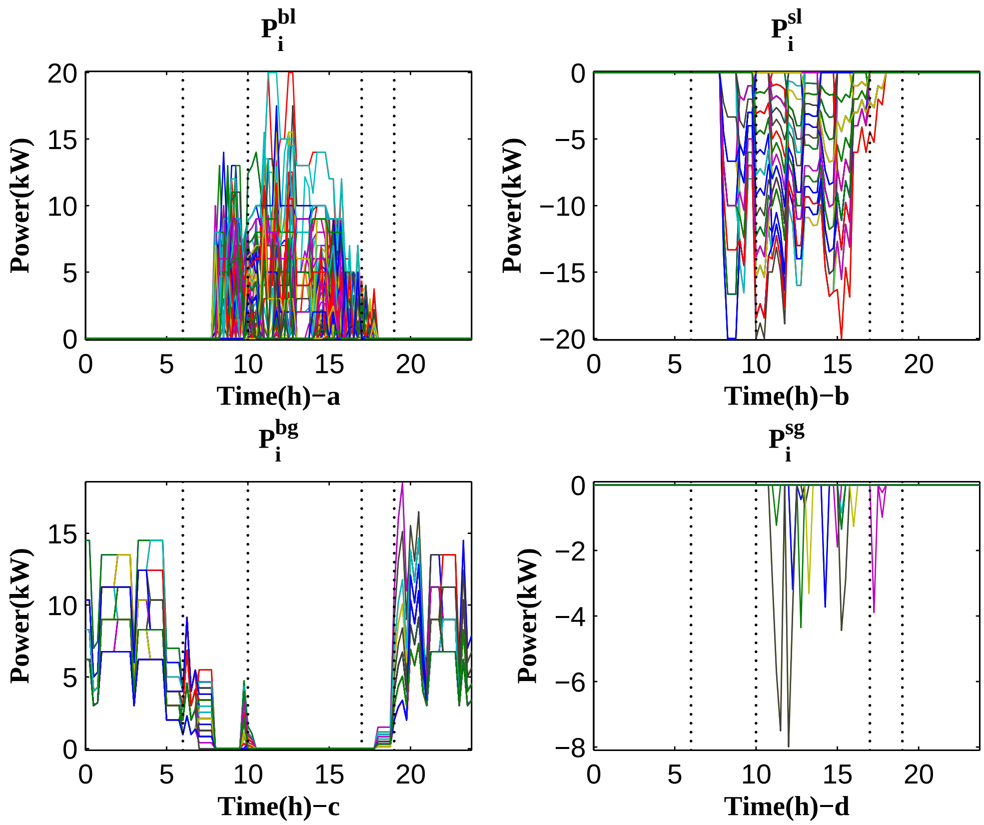

Figure 5.1: Exchange of powers in the sum of costs optimization for a network of 100 microgrids: (a) locally purchased powers, (b) locally sold powers, (c) powers purchased from the utility grid, and (d) powers sold to the utility grid.

5.2.3 System Performance

The electricity costs of the microgrids in the network are compared under four different energy management strategies. The basic case, No-EMS, is when the microgrids are connected to the utility grid without energy management control. In the second case, EMS-DG, the microgrids optimally dispatch their storage unit on an individual basis using the grid/buy sell rates. No local energy transaction is permitted among the microgrids in either of these cases. A third case, EMS-MG-NB, is considered

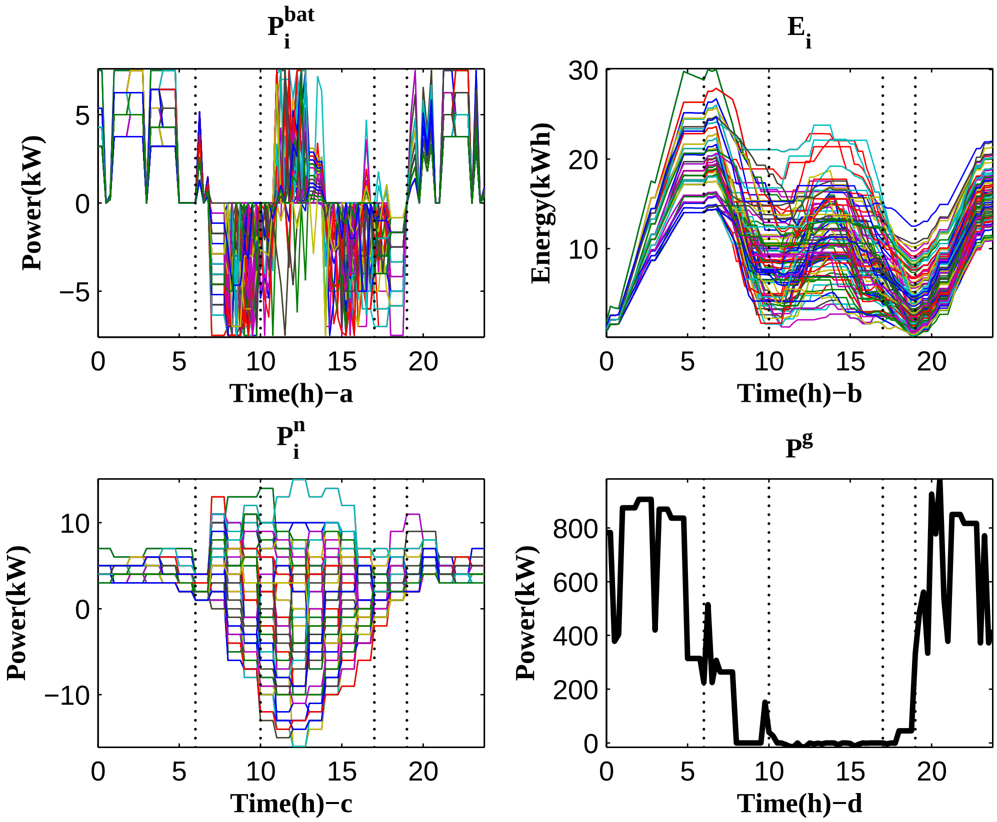

Figure 5.2: Power/energy signals in the sum of costs optimization for a network of 100 microgrids: (a) battery charging/discharging powers, (b) battery energy levels, (c) microgrids net demand powers, and (d) the aggregate power exchanged with the utility grid.

in which microgrids have no storage units but are still able to trade power locally using the proposed optimization-based energy management strategy. While there is no energy storage to dispatch in this case, local power transactions could still reduce the electricity costs of the microgrids. The last scenario, EMS-MG-WB, adds energy storage to the microgrids and implements the full optimization model with local power transactions and coordinated dispatch of energy storage in the network. The simulations are carried out for a period of one month.

Table 5.2: Optimization runtime for one control time step as a function of number of microgrids

NoG	Max. Time (S)	Avg. Time (S)	Number of Dec. Vars
5	0.10	0.03	496
10	0.15	0.09	946
25	0.76	0.59	2296
50	3.31	2.88	4546
100	16.83	15.20	9046
200	92.12	86.72	18046

The results of the simulations are reported in Table 5.3. It is noted that the EMS-MG-WB yields substantially lower total electricity cost than all other strategies, and especially the two that treat microgrids individually. Interestingly, the case EMS-MG-NB which allows for local power transactions but has no energy storage is also performing significantly better than EMS-DG and No-EMS. This clearly underscores the advantage that comes with treating microgrids as a network and allowing for local power transactions, even in the absence of energy storage.

To demonstrate the benefits to each microgrid from participating in the network scheme, individual monthly electricity costs for a network of ten microgrids are presented in Table 5.4 under the above control scenarios. It is evident from this table that the electricity costs for all microgrids have substantially decreased under the proposed coordinated energy management strategy, with or without energy storage.

Note that since the microgrids exchange power locally, resources such as energy storage units and solar power could be shared among them to achieve large savings, without need for installation of these capacities across all microgrids; this is an attractive feature of the proposed multi-microgrid energy management strategy. Another interesting observation is that larger networks of microgrids have larger pool of resources to share, generally achieving higher cost savings than small networks under the proposed approach. For instance, a network of 100 microgrids sees about 74.87% reduction in its total electricity bill at the end of the month, compared to 57.26% for a network of five(5). Also, a comparison of costs for individual microgrids under coordinated (EMS-MG-WB) and non-coordinated (EMS-DG) energy management control shows that all microgrids benefit from participating in the coordinated control scheme in the form of lower electricity bill. This is significant as it provides incentive for every microgrid to take part in the local power transactions. The use of energy storage in the network in the case of EMS-MG-WB yields considerable reduction in electricity cost compared to the case without them EMS-MG-NB. This may very well justify a long-term return on investment on energy storage capacity in the network, although a thorough economic analysis is warranted before any firm conclusion can be made.

Table 5.3: Comparison of monthly electricity costs under four different configurations by varying number of microgrids in the network (Imp. is defined as percentage reduction of total electricity cost for each scenario compared to the basic No-EMS scenario).

NoG	No-EMS ($)	EMS-DG ($)	Imp.(%)	EMS-MG-NB ($)	Imp.(%)	EMS-MG-WB ($)	Imp.(%)
5	1053	875	16.90	685	34.94	450	57.26
10	2111	1743	17.43	1317	37.61	856	59.45
25	5596	4666	16.62	3281	41.36	1978	64.65
50	14316	12445	13.07	8096	43.44	4402	69.25
100	33670	28489	15.39	16713	50.36	8461	74.87

Table 5.4: Comparison of monthly electricity costs of individual microgrids for a network consisting of 10 microgrids under four control strategies.

	MG 1	MG 2	MG 3	MG 4	MG 5	MG 6	MG 7	MG 8	MG 9	MG 10
No-EMS ($)	212	228	225	216	210	212	209	200	198	201
EMS-DG ($)	175	188	182	181	178	174	171	168	164	162
EMS-MG-NB ($)	135	142	139	136	132	135	127	126	123	122
EMS-MG-WB ($)	88	92	91	88	86	86	84	82	79	80

5.2.4 Battery Sizing

To investigate the impact of the storage size on the system performance, a network of 100 microgrids is considered. All microgrids are equipped with the same storage capacity. Simulations have been carried out by varying the storage capacity. The electricity costs for a one-month period are depicted in Fig. 5.3. As expected, increasing the battery size would help reduce the electricity cost, as this would provide greater flexibility for the energy management algorithm. However after certain point, increasing the storage size has very little impact on the electricity costs since the system cannot utilize the extra capacity any further.

5.3 Summary

In this chapter, a multi-objective optimization model was introduced for storage dispatch in a network of grid-connected microgrids with battery and renewable energy assets. The microgrids in the network would be treated and billed as a single customer by the grid operator. The costs of electricity including the peak cost for the microgrids are the components of the objective vector in the optimization model. The problem was then converted to a single-objective optimization by adding up the cost components. In calculating the electricity cost, each microgrid net power was virtually partitioned into local and grid components, with applicable local and grid buy/sell electricity rates. A rate scenario was considered in which favourable local buy/sell rates incentivize local exchange of power. Fairness constraints were introduced to ensure that all microgrids would be able to benefit from the local buy/sell rates in an equitable manner. In Section 5.2, simulations were carried out with real electricity,

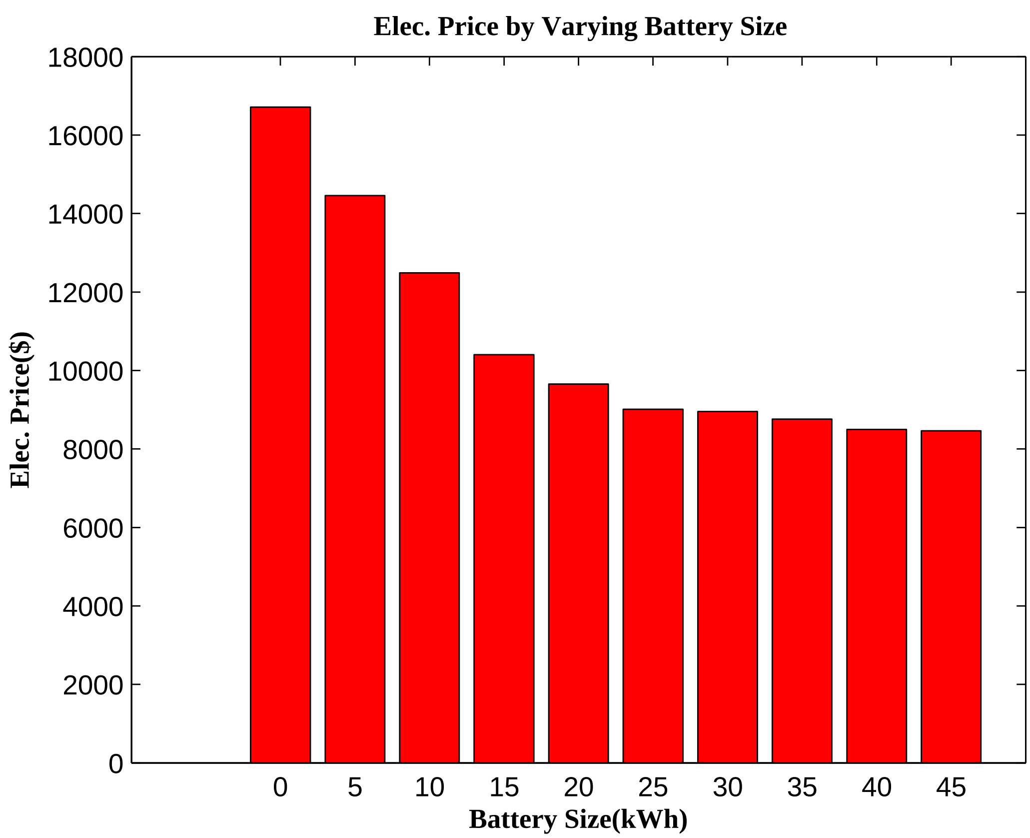

Figure 5.3: Electricity bill of a network of 100 microgrids for one month by varying the batteries size.

and solar generation data on a rolling horizon basis. The proposed multi-microgrid resource sharing strategy was compared with alternative strategies, i.e., individual microgrids with no storage control, and individual microgrids with independent storage control. In both of these cases, no local energy transaction was allowed. The results showed a very substantial reduction in the overall electricity cost using the proposed resource sharing scheme. Another case was also considered in which microgrids had no storage capacity but were still able to carry out local power transactions using the proposed optimization model. The results showed substantial reduction in electricity cost due to local power transactions even in the absence of energy storage. The computation times for solving the optimization problem at each time step were also within the constraints of real-time implementation for a network as large of 200 microgrids using a conventional desktop computer.

Chapter 6

Priority-based Microgrid Energy Management in a Network Environment

6.1 Optimization Model

Since each microgrid has competing goals with other microgrids, network policies for energy transactions among the microgrids plays an important role in encouraging participating in the network. The lexicographic programming model, which will be introduced in this chapter, allows for preferential treatment of the microgrids based on their assigned priority group. This feature can be used to provide a higher incentive to microgrid units with larger renewable and storage capacity for their participation in the network energy management scheme. Here the rationale is that the units with bigger investments in resources should reap higher benefits from their participation. This formulation is essentially a generalization of the methods in Chapters 4 and 5.

When all microgrids are placed at the same priority level, one of the formulations in Chapters 4 and 5 would emerge, depending on the cost objective used.

Let the set of microgrid priority level sets be

$$\mu l = \{\mu l_1, \cdots, \mu l_i, \cdots, \mu l_q\} \tag{6.1}$$

where μl_i is the set of microgrid's objective functions in ith level of priority. Now the corresponding single-objective optimization can be stated as

for $\quad s = 1, \cdots, q$

$$\min \left\{ \S\{\mu l_s\} \right\} \tag{6.2a}$$

for $k = 1, \cdots, N_h \quad and \quad i = 1, \cdots, NoG \qquad .$

Here $\S\{\cdot\}$ is an scalarization operator that can be similar to those defined in Chapters 4 and 5. This operator uses a predefined method of scalarization like sum of the costs or utopia point to transform the objective vector to an ordinary single-objective cost function. In other words, $\S\{\cdot\}$ operator takes the elements of the set μl_s which is a subset of the objective function set and transforms them to a single objective function according to a predefined method of scalarization. For example, if the scalarization method is sum of the costs, this operator adds all elements of set μl_s to generate a single cost function. Also, the auxiliary variables for obtaining a linear/quadratic counterpart optimization model are added to the single-objective cost of each level, which renders the total cost as in 6.2b. The optimization problem is formulated as:

$$\min\left\{\S\{\mu l_s\} + \boldsymbol{\alpha}^T \mathbf{P}^{bg} + \sum_{j\in\mu l-\mu l_s} \big(+ \boldsymbol{\alpha}^T \mathbf{P}_j^{bl} + \boldsymbol{\alpha}^T \mathbf{P}_j^{bg} + \boldsymbol{\alpha}^T \mathbf{P}_j^{c} + \boldsymbol{\alpha}(1) P_j^{pk}\big)\right\} \tag{6.2b}$$

subject to, for $k = 1, \cdots, N_h \quad and \quad i = 1, \cdots, NoG$

Power Exchange constraints:

$$\mathbf{P}_r^{l,min} \preceq \sum_{j\in ML_r} \mathbf{P}_j^l + \mathbf{P}_j^g \preceq \mathbf{P}_r^{l,max} \tag{6.2c}$$

$$\mathbf{P}^{mg,min} \preceq \mathbf{P}^g \preceq \mathbf{P}^{mg,max} \tag{6.2d}$$

$$-P_i^{rcl,max}\mathbf{h} \preceq \mathbf{P}_i^l(k) - \mathbf{P}_i^l(k-1) + \mathbf{P}_i^g(k) - \mathbf{P}_i^g(k-1) \preceq P_i^{rcl,max}\mathbf{h} \tag{6.2e}$$

$$\sum_{j=1}^{NoG} \mathbf{P}_j^l = 0 \tag{6.2f}$$

$$\sum_{j=1}^{NoG} \mathbf{P}_j^g = \mathbf{P}^g \tag{6.2g}$$

$$\mathbf{P}_i^l + \mathbf{P}_i^g = \mathbf{P}_i^{bat} + \mathbf{P}_i^n \tag{6.2h}$$

Battery Constraints:

$$E_i(k+1) = E_i(k) + \eta_i^c \mathbf{h}(k)\mathbf{P}_i^c(k) + {\eta_i^d}^{-1}\mathbf{h}(k)(\mathbf{P}_i^{bat} - \mathbf{P}_i^c) - P_i^{lossb}\mathbf{h}(k) \tag{6.2i}$$

$$\mathbf{P}_i^{bat,min} \preceq \mathbf{P}_i^{bat} \preceq \mathbf{P}_i^{bat,max} \tag{6.2j}$$

$$E_i^{min} \leq E_i(k+1) \leq E_i^{max} \tag{6.2k}$$

$$\eta_i^c \mathbf{h}^T \mathbf{P}_i^c + {\eta_i^d}^{-1}\mathbf{h}^T(\mathbf{P}_i^{bat} - \mathbf{P}_i^c) - P_i^{lossb}\mathbf{h}^T\mathbf{1} = E_i^{final} - E_i^0 \tag{6.2l}$$

$$-P_i^{rcb,max}\mathbf{h} \preceq \mathbf{P}_i^{bat}(k) - \mathbf{P}_i^{bat}(k-1) \preceq P_i^{rcb,max}\mathbf{h} \tag{6.2m}$$

$$\mathbf{P}_i^c \succeq \mathbf{P}_i^{bat}, \quad \mathbf{P}_i^c \succeq \mathbf{0} \tag{6.2n}$$

Peak Shaving Constraints:

$$\begin{aligned}
&P_i^{pk} \geq 0 \\
&\sum_{j=1}^{NoG} P_j^{pk} \geq \mathbf{P}^g(k) - P^b \\
&-\Delta_1\left(\sum_{j=1}^{NoG} P_j^{pk} - \mathbf{P}^g(k) + P^b\right) \leq P_i^{pk} - \mathbf{P}_i^{bg}(k) \leq \Delta_1\left(\sum_{j=1}^{NoG} P_j^{pk} - \mathbf{P}^g(k) + P^b\right)
\end{aligned} \tag{6.2o}$$

Island Mode Constraint:

$$\sum_{i=1}^{NoG} E_i(k+1) \geq \sum_{t=1}^{NoH}\sum_{i=1}^{NoG} \mathbf{h}(t+k)\mathbf{P}_i^n(t+k) \tag{6.2p}$$

Optimality of Higher Order Objective Function Sets Constraint:

$$\S\{\mu l_w(\mathbf{x})\} \leq \S\{\mu l_w(\mathbf{x}^\star)\}, \qquad w = 1, \cdots, s-1, \quad s > 1 \tag{6.2q}$$

Here the indices i, k, and s refer to the microgrid, time step in the control horizon, and the priority level, respectively. The optimization model is formulated over the control horizon with a bold variable denoting a decision vector containing values of the control decisions at all time steps. The vector of decision variables, $\mathbf{x}$, is given by:

$$\mathbf{x} = [\mathbf{P}_i^l, \mathbf{P}^g, \mathbf{P}^{bat}, E_i, P_i^{pk}] \tag{6.3}$$

The optimization constraints are discussed next.

6.1.1 Power Exchange Constraints

The constraints in (6.2c) ensure that net power at each point of the network remains within the line capacity limits. Here, ML_r is defined as r th set of microgrids with power capacity limit which depends on network structure. One plausible configuration can be simply considered by $\mathbf{P}_i^{l,min} \preceq \mathbf{P}_i^l + \mathbf{P}_i^g \preceq \mathbf{P}_i^{l,max}$, that is exchange power limit constraint for each local microgrid. All the other power exchange constraints were explained in Section 4.1.2.

6.1.2 Battery Constraints

All battery constraints were explained in Section 4.1.3.

6.1.3 Peak Shaving Constraints

All peak shaving constraints were explained in Section 4.1.4.

6.1.4 Island Mode Constraint

Island mode constraint has been addressed in Section 4.1.5.

6.1.5 Optimality of higher-Order Objective Function Sets Constraint

This constraint guarantees that the minimum value of the objective sets of higher-order priority microgrids is achieved at each iteration of the solving problem.

Depending on the choice of the scalarization operator, the final optimization problem can be of the linear or quadratic programming form. At each time step, central controller gathers all required the data, i.e., predictions of microgrids demand and local renewable generation, and energy storage charge level, and solves the priority optimization model q times to find power dispatch decisions for each microgrid.

6.2 Simulation Results

In this section, different operation scenarios are considered to analyze the response of the proposed multi-microgrid energy management optimization models. The simulations are carried out in the MATLAB environment using the IBM ILOG CPLEX LP solver on an Intel Core 2 Duo 3.00 GHz running Windows 7. The electricity usage and solar generation data used in the simulations have been provided by Burlington Hydro Inc. (Burlington, ON, CANADA). The electricity usage data is from the utility operator commercial customers with peak usage over 50 kW and the solar energy generation units are capable of up to 30 kW output power.

6.2.1 System Response

A multi-microgrid system with one hundred microgrids is considered. The microgrids are grouped to three levels of priority, high priority consisting of 33 microgrids, medium priority consisting of 33 microgrids, and low priority consisting of 34 microgrids. In all simulations the sum of cost method is employed as the scalarization operator. Summer electricity rates in the province of Ontario, Canada are used, i.e., 6.2 ¢/kWh ($7p.m.$-$7a.m.$), 9.2 ¢/kWh ($7a.m.$-$11a.m.$, and $5p.m.$-$7p.m$), 10.8 ¢/kWh ($11a.m.$-$5p.m.$). Denoting these prices by the vector $\mathbf{c}^{buy}$, the other buy and sell prices

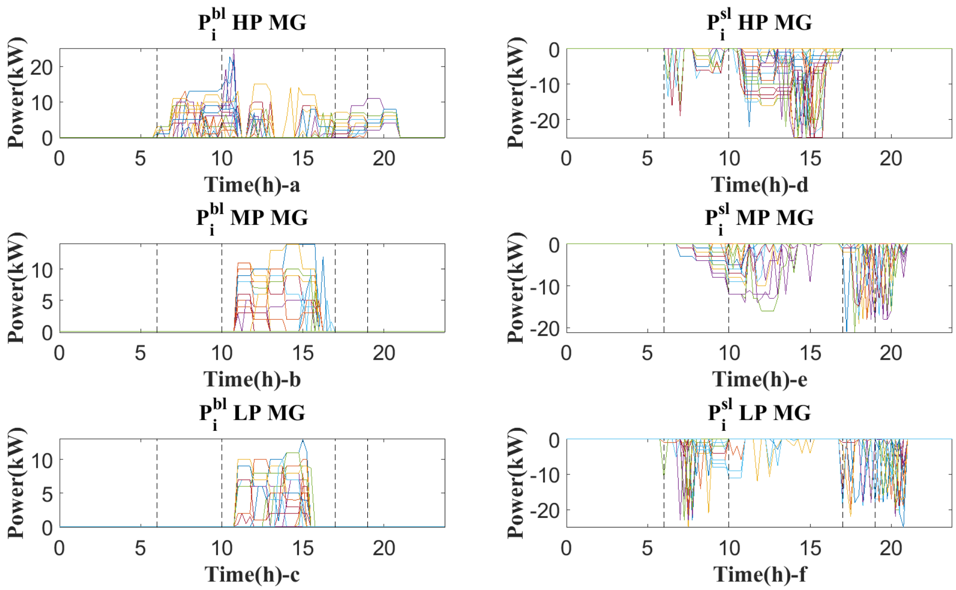

Figure 6.1: Local exchange powers in grid-connected mode operation: (a) purchased powers by high priority microgrids, (b) purchased powers by medium priority microgrids, (c) purchased powers by low priority microgrids, (d) sold powers by high priority microgrids, (e) sold powers by medium priority microgrids, and (f) sold powers by low priority microgrids.

are set to $\mathbf{c}^{bl} = 0.57\mathbf{c}^{buy}$, $\mathbf{c}^{bg} = \mathbf{c}^{buy}$, $\mathbf{c}^{sl} = 0.5\mathbf{c}^{buy}$, $\mathbf{c}^{sg} = 0.07\mathbf{c}^{buy}$. The battery characteristics are $E_i^{min} = 0$kWh, $E_i^{max} = 25$kWh, $\mathbf{P}_i^{bat,max} = -\mathbf{P}_i^{bat,min} = 12$kW, $\mathbf{P}_i^{rcb,max} = -\mathbf{P}_i^{rcb,min} = 10$kW/h, $\eta_i^d = \eta_i^c = 0.95$, $P_i^{lossb} = 139$W, and the end of horizon battery energy level is set as $E_i^{final} = E_i^0$. The time-step averaged microgrid power/differential power limits are chosen as $\mathbf{P}_i^{l,max} = -\mathbf{P}_i^{l,min} = 25$kW/h, $\mathbf{P}_i^{rcl,max} = 20$kW/h and $\mathbf{P}^{mg,max} = -\mathbf{P}^{mg,min} = 2500$kW. The control prediction horizon is set to one day with a variable time step vector $h = \begin{bmatrix} 0.25 \ 0.25 \ 0.5 \ 0.5 \ 0.5 \ 1 \ 1 \ 2 \ 2 \ 2 \ 2 \ 3 \ 3 \ 3 \ 3 \end{bmatrix}^T$ so, $N_h = 15$ and rolling horizon controller runs every 15 minutes. The peak price is set to $c_p = 11¢/kW$ for a 24hour optimization prediction window, which translates to an effective 3.3\$/kW peak price on a monthly basis.

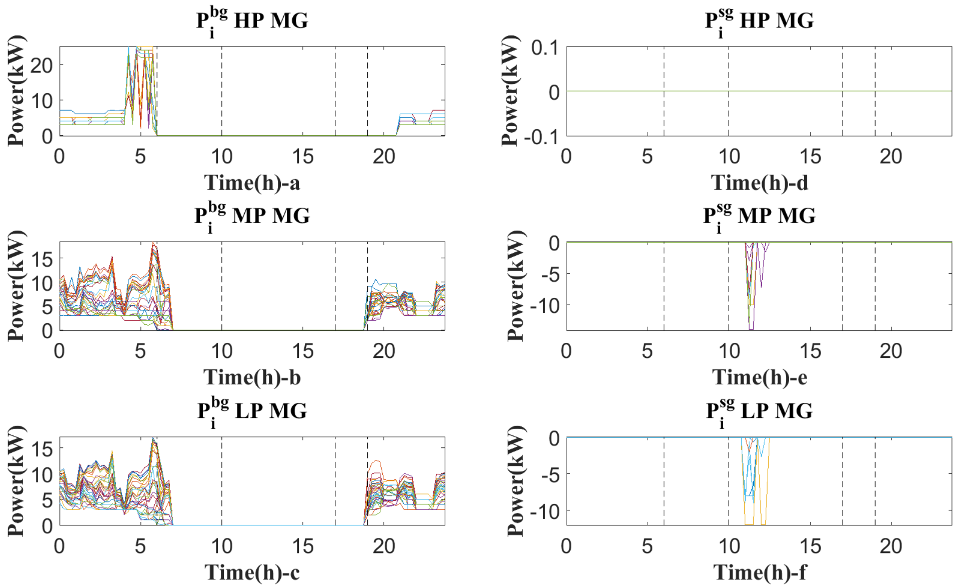

Figure 6.2: Exchange of powers with the utility grid (a) purchased powers by high priority microgrids, (b) purchased powers by medium priority microgrids, (c) purchased powers by low priority microgrids, (d) sold powers by high priority microgrids, (e) sold powers by medium priority microgrids, and (f) sold powers by low priority microgrids.

The results of a 24-hour simulation with the rolling horizon controller are plotted in Figs. 6.1, 6.2 and 6.3. The time of use electricity pricing divides the 24-hour window into five distinct time intervals, separated by the dotted vertical lines. The first (0-7hours) and fifth (19-24hours) intervals are the off-peak period with the lowest electricity cost, the second (7-11hours) and fourth (17-19hours) intervals are mid-peak, and the third interval (11-17hours) is peak, with the highest electricity cost. It is notable the high priority microgrids are mostly trading energy locally with other microgrids, except in the beginning of the day, when there is no local energy in multi-microgrid system. They also utilize other microgrids energy storage. The medium and low priority microgrids purchase energy to first supply their demand, and then

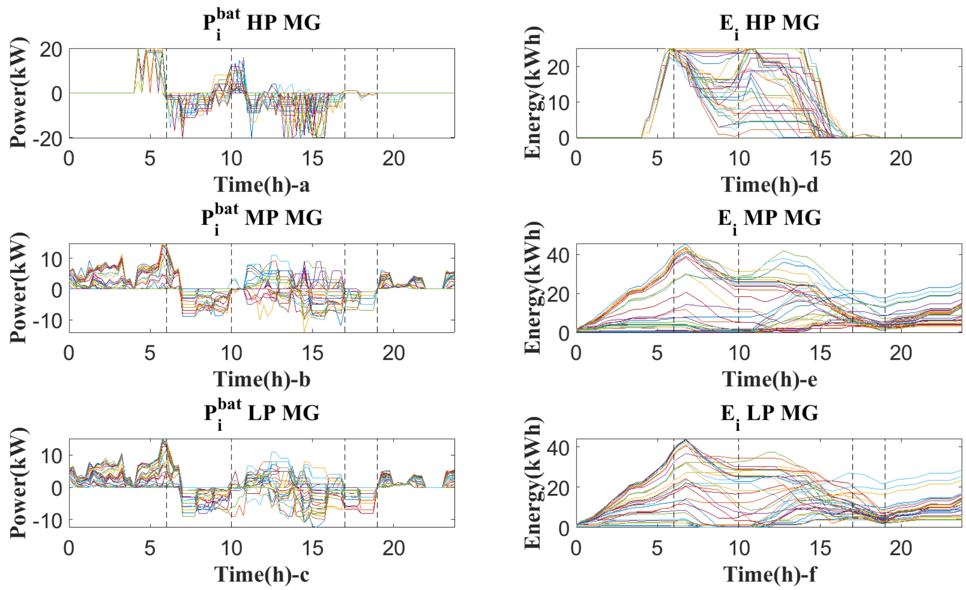

Figure 6.3: Power/energy levels of energy storage devices in grid-connected mode (a) battery charging/discharging powers of high priority microgrids, (b) battery charging/discharging powers of medium priority microgrids, (c) battery charging/discharging powers of low priority microgrids, (d) battery energy levels of high priority microgrids, (e) battery energy levels of medium priority microgrids, and (f) battery energy levels of low priority microgrids.

also serve the high priority microgrids. Furthermore, the high priority microgrids purchase local energy during the on-peak and mid-peak hours, as it is expected because of their prioritization in reducing electricity costs. An interesting feature of the proposed optimization model is that during on-peak hours even medium and low priority microgrids take advantage of local transaction of energy as it can be seen from Figs. 6.2 and 6.3. This locally purchased energy is mostly stored in the storage units of those microgrids that can be later on used internally instead of purchasing expensive energy from the utility grid.

6.2.2 System Performance

The performance of the proposed multi-microgrid energy management system is compared with the sum of the costs method, introduced in previous chapter, No-EMS, when the microgrids are connected to the utility grid without energy management control, and EMS-DG, when microgrids optimally dispatch their storage unit on an individual basis using the grid/buy sell rates without access to the network resources through the local buy/sell transactions for different size multi-microgrid system. In each multi-microgrid configuration we assume that there are $\lfloor \frac{NoG}{3} \rfloor$, where $\lfloor \bullet \rfloor$ is the floor function, microgrids in high and medium priority levels and $NoG - 2 * \lfloor \frac{NoG}{3} \rfloor$ microgrids in low priority level. Total electricity costs for one month billing of each level of priority for three different optimization models are presented in in Table 6.1.

Cost savings in four different comparisons are shown in this table: priority vs No-EMS (Comp. 1), sum of the costs method vs No-EMS (Comp. 2), priority vs sum of the costs method (Comp. 3), and priority vs EMS-DG (Comp.4). From the results, it is clear that high priority microgrids achieve the largest cost saving compared with the other two groups under the proposed lexicographic optimization model. As expected, the sum of the costs method outperforms the lexicographic model on the metric of total electricity cost and distributes the cost savings more uniformly among all microgrids; it would be the method of choice if that is what is desired. Nevertheless, as is evident in the comparison of priority vs EMS-DG, all microgrids including those in the lower priority levels still benefit from significantly lower electricity bills in the priority-based network scheme compared to individual energy management. This demonstrates a clear incentive for all microgrids to share their resources by participating in the network arrangement. The lexicographic model allows for prioritizing groups of microgrids and hence is more versatile than the sum of the costs model. It would simply reduce to the sum of the costs model when only priority group is involved. It is also noteworthy that, generally, the greater the size of the network is the larger the cost savings are due to the availability of more local resources in the network.

Table 6.1: Comparison of electricity costs ($) under thre different optimization model No-EMS, priority and sum of costs (SoC), for different priority levels, high priority (HP), medium priority (MP), and low priority (LP)

NoG	PL	No-EMS	Priority	Comp. 1(%)	SoC	Comp. 2(%)	Comp. 3 (%)	EMS-DG	Comp. 4 (%)
10	HP	665	178	+73.23	271	+59.24	+34.3	540	67.04
	MP	638	331	+48.12	260	+59.24	-27.3	553	40.14
	LP	808	440	+45.54	325	+59.77	-35.4	650	32.08
25	HP	1706	385	+77.43	618	+63.77	+37.7	1352	71.52
	MP	1798	893	+50.33	642	+64.29	-39.1	1423	37.24
	LP	2092	1106	+47.13	718	+65.67	-54.3	1891	41.51
50	HP	4423	852	+80.74	1473	+66.69	+42.2	4074	79.09
	MP	4624	1963	+57.54	1430	+69.07	-37.3	4055	51.59
	LP	5269	2382	+54.79	1499	+71.55	-58.9	4316	44.81
100	HP	10202	1470	+85.59	2806	+72.49	+47.6	8803	83.30
	MP	11071	4165	+62.38	2802	+74.69	-48.6	8770	52.08
	LP	12397	4776	+61.47	2853	+76.98	-67.4	10916	56.25

6.3 Summary

This chapter presented a multi-objective optimization model for energy management in a multi-microgrid community with local storage and renewable energy and with connection to a utility grid. The microgrids can exchange power locally with each other over a common bus, and with the utility grid as well. Priority levels were defined to classify the microgrids according to some importance measures. The lexicographic programming was used to solve the general multi-objective optimization model and prioritize the microgrids. In Section 6.2, numerical simulations were carried out with actual electricity and solar generation data. A comparison of the proposed multi-microgrid energy management strategy with the sum of the cost methods showed the effectiveness of the method for high priority level microgrids (by reduction of the electricity cost upto 47 %).

Chapter 7

Optimal Dispatch of Real and Reactive Power in a Network of Grid-connected Microgrids

So far, the optimization models presented for the problem of energy management in a network of microgrids only considered the optimal dispatch of real power. These models work well as long as the network loads would be purely resistive and the microgrids are closed to each other. In other networks, the power management strategy must also deal with dispatch of reactive power in addition to the real power. The real and reactive power reference commands issued by the high-level energy management system would be then sent to low-level microgrid inverters controllers. These controllers can utilize these references in a droop control technique Lasseter (2002) to also regulate frequency and voltage in the network, if required. In this chapter, a general model for optimal dispatch of real and reactive power in a network of microgrids is presented. The effectiveness of the strategy will be demonstrated through a set of simulations with real demand and solar generation data.

7.1 Optimization Model Formulation

Referring to Chapter 4, a general nonlinear optimization model can be developed for the problem of real-reactive power dispatch in network of microgrids. The model can be then converted to quadratically constrained linear/quadratic program using similar techniques to those employed in Chapter 4. The general optimization model is stated as:

$$\min\left\{ \dagger \left\{ \mathbf{F} \right\} \right\} \tag{7.1a}$$

subject to, for $k = 1, \cdots, N_h \quad and \quad i = 1, \cdots, NoG$

Power Exchange Constraints:

$$\mathbf{S}_r^{l,min^2} \preceq (\sum_{j \in ML_r} \mathbf{P}_j^l + \mathbf{P}_j^g)^2 + (\sum_{j \in ML_r} \mathbf{Q}_j^l + \mathbf{Q}_j^g)^2 \preceq \mathbf{S}_r^{l,max^2} \tag{7.1b}$$

$$\mathbf{S}^{mg,min^2} \preceq (\mathbf{P}^g)^2 + (\mathbf{Q}^g)^2 \preceq \mathbf{S}^{mg,max2} \tag{7.1c}$$

$$-P_i^{rcl,max}\mathbf{h} \preceq \mathbf{P}_i^l(k) - \mathbf{P}_i^l(k-1) + \mathbf{P}_i^g(k) - \mathbf{P}_i^g(k-1) \preceq P_i^{rcl,max}\mathbf{h} \tag{7.1d}$$

$$\sum_{j=1}^{NoG} \mathbf{P}_j^l = 0 \tag{7.1e}$$

$$\sum_{j=1}^{NoG} \mathbf{Q}_j^l = 0 \tag{7.1f}$$

$$\sum_{j=1}^{NoG} \mathbf{P}_j^g = \mathbf{P}^g \tag{7.1g}$$

$$\sum_{j=1}^{NoG} \mathbf{Q}_j^g = \mathbf{Q}^g \tag{7.1h}$$

$$\mathbf{P}_i^l + \mathbf{P}_i^g = \mathbf{P}_i^{bat} + \mathbf{P}_i^n \tag{7.1i}$$

$$\mathbf{Q}_i^l + \mathbf{Q}_i^g = \mathbf{Q}_i^{bat} + \mathbf{Q}_i^n \tag{7.1j}$$

$$\begin{aligned} &\mathbf{P}^{bg} \succeq \sum_{j=1}^{NoG} \mathbf{P}_j^g \\ &\mathbf{P}^{bg} \succeq \mathbf{0} \\ &\mathbf{P}^{sg} = \sum_{j=1}^{NoG} \mathbf{P}_j^g - \mathbf{P}^{bg} \end{aligned} \tag{7.1k}$$

$$\begin{aligned} &\mathbf{Q}^{bg} \succeq \sum_{j=1}^{NoG} \mathbf{Q}_j^g \\ &\mathbf{Q}^{bg} \succeq \mathbf{0} \\ &\mathbf{Q}^{sg} = \sum_{j=1}^{NoG} \mathbf{Q}_j^g - \mathbf{Q}^{bg} \end{aligned} \tag{7.1l}$$

$$\begin{aligned} &\mathbf{P}_i^{bl} \succeq \mathbf{P}_i^l \\ &\mathbf{P}_i^{bl} \succeq \mathbf{0} \\ &\mathbf{P}_i^{sl} = \mathbf{P}_i^l - \mathbf{P}_i^{bl} \end{aligned} \tag{7.1m}$$

$$\begin{aligned} &\mathbf{Q}_i^{bl} \succeq \mathbf{Q}_i^l \\ &\mathbf{Q}_i^{bl} \succeq \mathbf{0} \\ &\mathbf{Q}_i^{sl} = \mathbf{Q}_i^l - \mathbf{Q}_i^{bl} \end{aligned} \tag{7.1n}$$

$$\begin{aligned} &\mathbf{P}_i^{bg} \succeq \mathbf{P}_i^{g} \\ &\mathbf{P}_i^{bg} \succeq \mathbf{0} \\ &\mathbf{P}_i^{sg} = \mathbf{P}_i^{g} - \mathbf{P}_i^{bg} \end{aligned} \tag{7.1o}$$

$$\begin{aligned} &\mathbf{Q}_i^{bg} \succeq \mathbf{Q}_i^{g} \\ &\mathbf{Q}_i^{bg} \succeq \mathbf{0} \\ &\mathbf{Q}_i^{sg} = \mathbf{Q}_i^{g} - \mathbf{Q}_i^{bg} \end{aligned} \tag{7.1p}$$

Battery Constraints:

$$E_i(k+1) = E_i(k) + \eta_i^c \mathbf{h}(k)\mathbf{P}_i^c(k) + {\eta_i^d}^{-1}\mathbf{h}(k)(\mathbf{P}_i^{bat} - \mathbf{P}_i^c) - P_i^{lossb}\mathbf{h}(k) \tag{7.1q}$$

$${\mathbf{S}_i^{bat,min}}^2 \preceq (\mathbf{P}_i^{bat})^2 + (\mathbf{Q}_i^{bat})^2 \preceq {\mathbf{S}_i^{bat,max}}^2 \tag{7.1r}$$

$$E_i^{min} \leq E_i(k+1) \leq E_i^{max} \tag{7.1s}$$

$$\eta_i^c \mathbf{h}^T \mathbf{P}_i^c + {\eta_i^d}^{-1}\mathbf{h}^T(\mathbf{P}_i^{bat} - \mathbf{P}_i^c) - P_i^{lossb}\mathbf{h}^T\mathbf{1} = E_i^{final} - E_i^0 \tag{7.1t}$$

$$-P_i^{rcb,max}\mathbf{h} \preceq \mathbf{P}_i^{bat}(k) - \mathbf{P}_i^{bat}(k-1) \preceq P_i^{rcb,max}\mathbf{h} \tag{7.1u}$$

$$\mathbf{P}_i^c \succeq \mathbf{P}_i^{bat}, \quad \mathbf{P}_i^c \succeq \mathbf{0} \tag{7.1v}$$

Peak Shaving Constraints:

$$
\begin{aligned}
&P_i^{pk} \geq 0\\
&\sum_{j=1}^{NoG} P_j^{pk} \geq \mathbf{P}^g(k) - P^b\\
&-\Delta_1\left(\sum_{j=1}^{NoG} P_j^{pk} - \mathbf{P}^g(k) + P^b\right) \leq P_i^{pk} - \mathbf{P}_i^{bg}(k) \leq \Delta_1\left(\sum_{j=1}^{NoG} P_j^{pk} - \mathbf{P}^g(k) + P^b\right)
\end{aligned}
\tag{7.1w}
$$

Island Mode Constraint:

$$
\sum_{i=1}^{NoG} E_i(k+1) \geq \sum_{t=1}^{NoH}\sum_{i=1}^{NoG} \mathbf{h}(t+k)\mathbf{P}_i^n(t+k) \tag{7.1x}
$$

7.1.1 Scalarized Objective Function

In the single-objective cost of the problem (7.1a), $\dagger\{\bullet\}$ operator is a scalarization or non-scalarization single-objective cost maker for the multi-objective cost $\mathbf{F}$. This operator transforms the multi-objective cost to one of the forms introduced in chapters 4, 5 or 6. Here the local reactive cost of each microgrid is given by

$$
F_{Q_i} = \mathbf{c}_q^{bl^T}\left[\mathbf{Q}_i^l\right]^+ + \mathbf{c}_q^{sl^T}\left[\mathbf{Q}_i^l\right]^- + \mathbf{c}_q^{bg^T}\left[\mathbf{Q}_i^g\right]^+ + \mathbf{c}_q^{sg^T}\left[\mathbf{Q}_i^g\right]^- \tag{7.2}
$$

and the corresponding cost for the real power is

$$
F_{P_i} = \mathbf{c}_p^{bl^T}\left[\mathbf{P}_i^l\right]^+ + \mathbf{c}_p^{sl^T}\left[\mathbf{P}_i^l\right]^- + \mathbf{c}_p^{bg^T}\left[\mathbf{P}_i^g\right]^+ + \mathbf{c}_p^{sg^T}\left[\mathbf{P}_i^g\right]^- \tag{7.3}
$$

The price vectors for the corresponding cost of reactive power can be chosen with a strategy similar to local real power cost. Here decision about whether positive reactive power or negative reactive power would be beneficial to generate in the network relies on the utility grid regulation for reactive power pricing.

7.1.2 Power Exchange Constraints

The constraints in (7.1b) ensure that net apparent power at each point of the network remains within the line capacity limits. Here, ML_r is defined as r th set of microgrids with power capacity limit which depends on network structure. Similarly, the net apparent power of the microgrids at the point of coupling to grid, is within the line limits defined in (7.1c). Changes over consecutive sample times in the net power of the microgrids are also limited by (7.1d) to avoid large fluctuations. The constraints (7.1e) (7.1e) simply state that local exchanges of real and reactive power add up to zero, respectively. The total real power exchanged with the utility grid is determined through (7.1g) and the total reactive power exchanged with the utility grid is determined through (7.1h). The real and reactive power balance constraint for each microgrid is given in (7.1i) and (7.1i), where $\mathbf{P}_i^{bat}$ is the battery real power, $\mathbf{P}_i^{g}$ is real power from/to the utility grid, $\mathbf{P}_i^{l}$ is locally exchanged power, $\mathbf{P}_i^{n}$ is net demand power, $\mathbf{Q}_i^{bat}$ is the battery reactive real power, $\mathbf{Q}_i^{g}$ is reactive power from/to the utility grid, $\mathbf{Q}_i^{l}$ is locally exchanged reactive power, and $\mathbf{Q}_i^{n}$ is net demand reactive power.

It should be noted that there might exist some supplementary techniques in each microgrid to compensate for the reactive power demand such as adding capacitor banks to the network. Here $\mathbf{Q}_i^{bat}$ captures the total reactive power compensation in the network through such means. The decision about share of each subsystem can be made by the low-level controllers in the microgrid. The real net demand vector, defined as the difference between produced real power by generation units and the real power usage of the loads, is given by

$$\mathbf{P}_i^n = \mathbf{P}_i^{Loads} - \mathbf{P}_i^{Solar} - \mathbf{P}_i^{Wind}, i = 1, \cdots, NoG \tag{7.4}$$

Similarly, The reactive net demand vector, defined as

$$\mathbf{Q}_i^n = \mathbf{Q}_i^{Loads} - \mathbf{Q}_i^{Solar} - \mathbf{Q}_i^{Wind}, i = 1, \cdots, NoG \tag{7.5}$$

7.1.3 Battery Constraints

Constraints (7.1r) and (7.1s) impose limits on the battery apparent power and energy. All the other constraints were described in Section 4.1.3.

7.1.4 Peak Shaving Constraints

Peak shaving constraint were fully described in Section 4.1.4.

7.1.5 Island Mode Constraint

Island mode constraint was explained in Section 5.1.4.

7.2 Simulation Results

In this section, different operation scenarios are considered to analyze the response of the proposed multi-microgrid energy management optimization models. The simulations are carried out in the MATLAB environment using the IBM ILOG CPLEX LP

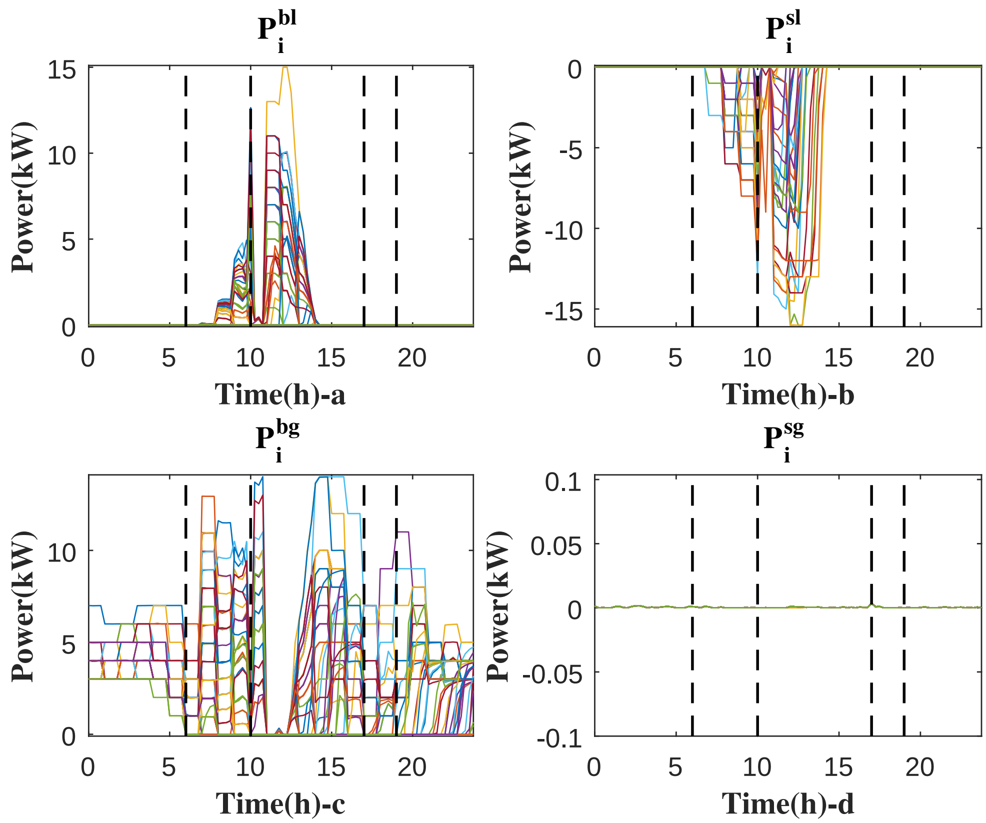

Figure 7.1: Exchange of real powers in a network of 100 microgrids: (a) locally purchased real powers, (b) locally sold real powers, (c) real powers purchased from the utility grid, and (d) real powers sold to the utility grid.

solver on an Intel Core 2 Duo 3.00 GHz running Windows 7. The electricity usage and solar generation data used in the simulations have been provided by Burlington Hydro Inc. (Burlington, ON, CANADA). The electricity usage data is from the utility operator commercial customers with peak usage over 50 kW and the solar energy generation units are capable of up to 30 kW output power.

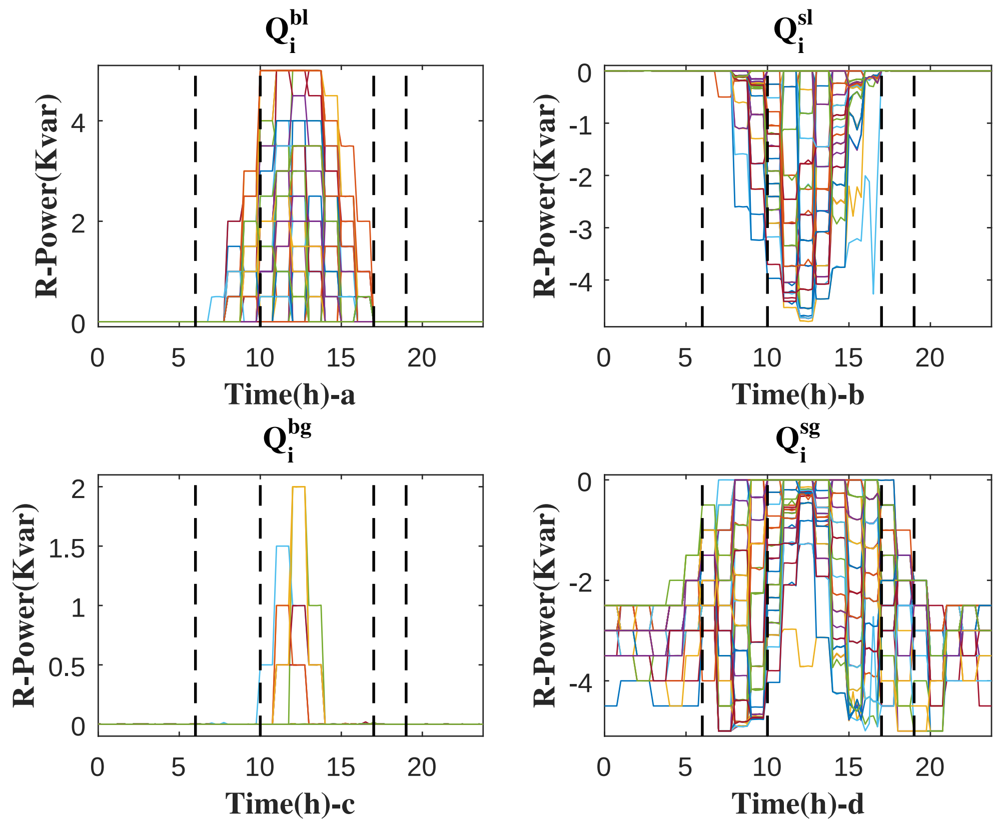

Figure 7.2: Exchange of reactive powers in a network of 100 microgrids: (a) locally purchased reactive powers, (b) locally sold reactive powers, (c) reactive powers purchased from the utility grid, and (d) reactive powers sold to the utility grid.

7.2.1 System Response

A multi-microgrid system with one hundred microgrids is considered. In all simulations the sum of cost method that was used in Chapter 5 is used as the scalarization operator. Summer electricity rates in the province of Ontario, Canada are used, i.e., 6.2 ¢/kWh ($7p.m.$-$7a.m.$), 9.2 ¢/kWh ($7a.m.$-$11a.m.$, and $5p.m.$-$7p.m$), 10.8 ¢/kWh ($11a.m.$-$5p.m.$). Denoting these prices by the vector $\mathbf{c}^{buy}$, the other buy and sell prices are set to $\mathbf{c}_p^{bl} = \mathbf{c}_q^{bl} = 0.57\mathbf{c}^{buy}$, $\mathbf{c}_p^{bg} = \mathbf{c}_q^{bg} = \mathbf{c}^{buy}$, $\mathbf{c}_p^{sl} = \mathbf{c}_q^{sl} = 0.5\mathbf{c}^{buy}$,

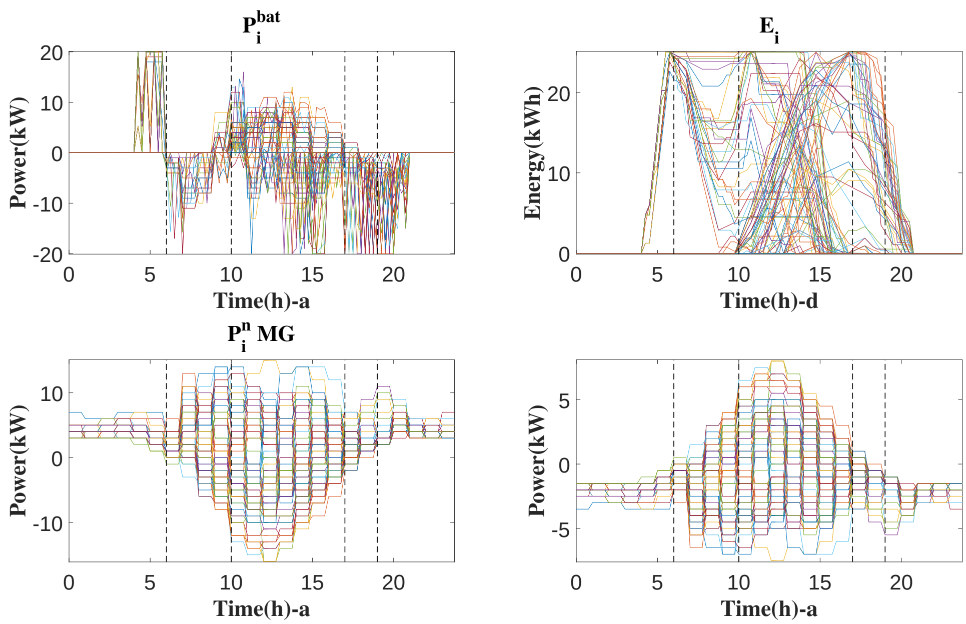

Figure 7.3: Power/energy signals in the general real-reactive energy management system for a network of 100 microgrids: (a) battery charging/discharging powers, (b) battery energy levels, (c) microgrids real net demand powers, and (d) microgrids reactive net demand powers.

$\mathbf{c}_p^{sg} = \mathbf{c}_q^{sg} = 0.07\mathbf{c}^{buy}$. The battery characteristics are $E_i^{min} = 0$kWh, $E_i^{max} = 50$kWh, $\mathbf{S}_i^{bat,max} = -\mathbf{S}_i^{bat,min} = 17$kVA, $\mathbf{P}_i^{rcb,max} = -\mathbf{P}_i^{rcb,min} = 10$kW/h, $\eta_i^d = \eta_i^c = 0.95$, $P_i^{lossb} = 139$W, and the end of horizon battery energy level is set as $E_i^{final} = E_i^0$. The time-step averaged microgrid apparent power/differential power limits are chosen as $\mathbf{S}_i^{l,max} = -\mathbf{S}_i^{l,min} = 35$kVA, $\mathbf{P}_i^{rcl,max} = 20$kW/h, and $\mathbf{S}^{mg,max} = -\mathbf{S}^{mg,min} = 3500$KVA. The control prediction horizon is set to one day with a variable time step vector $h = \begin{bmatrix} 0.25 \; 0.25 \; 0.5 \; 0.5 \; 0.5 \; 1 \; 1 \; 2 \; 2 \; 2 \; 2 \; 3 \; 3 \; 3 \; 3 \end{bmatrix}^T$ so, $N_h = 15$ and rolling horizon controller runs every 15 minutes. The peak price is set to $c_p = 11¢/kW$ for a 24hour optimization prediction window, which translates to an effective 3.3\$/kW peak price on a monthly basis.

The results of a 24-hour simulation with rolling horizon controller are plotted in Figs. 7.1 and 7.2. The time of use electricity pricing divides the 24-hour window into five distinct time intervals, separated by the dotted vertical lines. The first (0-7hours) and fifth (19-24hours) intervals are the off-peak period with the lowest electricity cost. During off-peak and mid-peak hours, microgrids purchase real power from the grid to meet their load demand and charge their batteries. During the on-peak time, microgrids exchange real power mostly locally to take advantage of the favourable local buy/sell prices. As it can be seen, microgrids do not sell their surplus power to utility grid to take advantage of local transaction power among themselves. So, the proposed energy management scheme enables the microgrids in the network to share their storage and renewable energy resources to reduce their electricity cost. Furthermore, The benefit of this energy management scheme to the grid operator is also evident from a shift of the demand to off-peak hours. As it is depicted in Fig. 7.2-d, the net reactive power demand of microgrids are mostly negative, so local microgrids sell the reactive power to the utility grid. The net positive reactive power demand of some microgrids during the on-peak hours is mostly supplied from local sources, as is evident from the results.

7.3 Summary

In this chapter, a general real-reactive energy management system for a network of microgrids was developed. This energy management model considers limits on transaction of apparent power related to various line capacities in the system. These limits translated into a set of quadratic constraints in the multi-objective optimization model. The optimization problem is converted to a convex quadratically constrained linear/quadratic program, which solved with existing optimization solvers to obtain a globally optimal solution in real time. The simulation results in Section 7.2 showed the effectiveness of the approach.

Chapter 8

Conclusion and Future Work

8.1 Conclusion

In this thesis, various strategies for sharing of renewable energy and storage capacity in a network of grid-connected microgrids were proposed. A model of operation and multi-objective optimization formulations were presented for solving the energy management problem in such a network. In the proposed model, the microgrids can exchange power locally with each other and with the utility grid. An electricity rate regime was introduced in which favourable local buy/sell prices incentivize local exchange of power. The energy management problem was formulated as a multi-objective optimization problem on a rolling horizon basis to minimize the cost of electricity for each microgrid. The optimization decision variables were the charge and discharge commands of the batteries, and local and grid shares of power for each microgrid at the point of its coupling to the grid.

In Chapter 4, a reformulation of the optimization problem was presented that eliminates nonlinear min and max functions without the use of binary or integer variables. The compromise programming was used to find a Pareto optimal point of the general multi-objective optimization problem. The objective functions were the norm-1 and norm-2 of the distances between an ideal cost, i.e., the utopia point in the objective space, and the actual cost. These yielded convex linear and quadratic optimization problems for l_1 and l_2 norms, respectively, that can be effectively solved with existing optimization routines.

In Chapter 5, the multi-objective optimization problem was converted to a conventional single-objective optimization by adding the components of the cost vector. Moreover, fairness constraints were introduced to ensure that all microgrids would be benefit from the local buy/sell rates in an equitable manner. The final single-objective optimization formulation was in the form of a linear program.

In Chapter 6, microgrids were classified into different priority groups. The lexicographic programming was used to solve the general multi-objective optimization model and prioritize the microgrids based on their assigned priority. The final optimization formulation was a linear or quadratic program depending on the scalarization method employed in the lexicographic program. In Chapter 7, a general real-reactive energy management system for a network of microgrids was developed. The energy management model considered limits on transactions of apparent power related to various line capacities in the system. These limits then translated into a set of quadratic constraints in the multi-objective optimization model. The optimization problem was converted to a convex quadratically constrained linear/quadratic program, and was solved with standard optimization solvers to obtain a globally optimal solution in real time.

For all proposed energy management models, simulations were carried out with real electricity and solar generation data on a rolling horizon basis. A comparison of the proposed multi-microgrid energy management strategies with the cases with no energy management, and with independent microgrid energy management showed a very substantial reduction in overall electricity cost, in some cases in excess of 70%. The computation times for solving the optimization problem at each time step were also within the constraints of real-time implementation for a network as large of 200 microgrids using a conventional desktop computer.

In summary, the contributions of this work are:

- A model of operation, and methods for control of storage units in a multiple-microgrid system with the goal of sharing renewable energy and storage capacity in the system. Proposed pricing regime in this work would encourage local power transactions and can help substantially reduce the electricity cost of the microgrids, compared to the case where microgrids individually exchange power with the grid. This would end up reducing the need for centralized power generation in the grid.

- Four distinct multi-objective optimization formulations for on-line computation of storage charge/discharge activities and local and grid components of micro-grid power transactions. These are:

  - a formulation that would minimize a measure of distance between the units actual costs and their ideal costs.

  - a formulation that would minimize the total cost of the electricity for the microgrids in the network.

  - a formulation that can prioritize the participating microgrids based on their attribution to predefined priority groups.

  - a generalized formulation for optimal dispatch of real and reactive power that can be used for any network regardless of the type of loads or distance between participants.

  These optimization formulations are convex linear/quadratic program free of binary/integer variables, which guarantee that a globally optimal solution can be obtained in real-time for on-line control for a relatively large network of microgrids.

- The proposed network energy management scheme substantially reduce the individual microgrid electricity costs, in some cases in excess of 70%. This is when the cost is compared to that from optimally managed individual microgrids.
- Utilization of aggregated energy storage in the microgrid network ensure the longest possible uninterrupted operation of the network in the event of islanding.

8.2 Future work

The proposed optimization models make use of a centralized energy management system. As it was discussed in Chapter 2, a centralized energy management system does have some advantages. However, a decentralized method for solving the multi-objective optimization may also be developed. This can help increase robustness with respect to single-component failures, reduce the need for communication of private data over the network, and enable real-time solution for problems involving a greater number of microgrids.

Another possible direction for future work is to consider uncertainty in the prediction of net demand and electricity in the optimization formulation, following a similar line of work by our group in single-microgrid systems in Malysz *et al.* (2014); Sirouspour (2016); Khodabakhsh and Sirouspour (2016); Ravichandran *et al.* (2016). Developing prediction algorithms for power demand, renewable generation, and electric vehicle mobility represent another potential future research direction. In thesis, optimization constraints were introduced to ensure a guaranteed network operation time during a blackout. Other existing tecniques including load curtailment strategies, e.g. see Nguyen *et al.* (2016), and backup generators may also be considered for island mode operation of the network.

As it was explained in Chapter 4, no conventional generator unit has been considered in local microgrids. It was also stated that a simple model can be added to the optimization model to capture the generator activity during steady state operation. This can be extended to a more complicated model of the generator by considering the fuel cost, ramping up constraints, turn on/shut down decisions, etc.

The proposed electricity rate regime exploited the gap between the grid buy/sell rates electricity to encourage local exchange of power. The local electricity rates were fixed and predefined. The impact of these cost reduction can be studied further with the aim of developing dynamic rate selection schemes. Integration of electric vehicles into the proposed control framework and exploring how fleets of electric vehicles and the network of microgrids could be leveraged to provide transportation and energy while using available resources most efficiently are all also promising avenues for future work.

The impact of storage size on system performance was briefly examined in Chapter 5. There exists some work in literature on planning of resources in individual microgrid, e.g, see Yu *et al.* (2014); Bahramirad *et al.* (2012). Optimal sizing of storage and renewable power capacity in microgrid networks is yet another interesting topic for future research.

The high-level energy management schemes proposed in this thesis generate real and reactive power commands for low-level power converters, which are supposed to enforce them. However, it is possible that these commands may not fully be compatible with grid voltage and frequency stabilization requirements, particularly in the case of reactive power control. A possible approach to address this potential issue is to integrate a model of the local distribution network in the optimization framework.

Appendix A

Glossary of Terms and Nomenclature

NoG	Total number of microgrids.
N_h	Number of time steps in control horizon.
$\mathbf{h}$	Vector of time step lengths in hours.
E_i^{min}	Min. energy level of battery in ith microgrid.
E_i^{max}	Max. energy level of battery in ith microgrid.
P_i^{lossb}	Self-discharge power loss of battery in ith microgrid.
η_i^c	Charge efficiency of battery in ith microgrid.
η_i^d	Discharge efficiency of battery in ith microgrid.
$P_i^{rcb,max}$	Max. change in battery charge/discharge power per hour, for ithmicrogrid.
$\mathbf{P}_i^{bat,min}$	Min. charge/discharge real power of battery in ith microgrid.
$\mathbf{P}_i^{bat,max}$	Max. charge/discharge real power of battery in ith microgrid.
$\mathbf{S}_i^{bat,min}$	Min. apparent power of battery in ith microgrid.
$\mathbf{S}_i^{bat,max}$	Max. apparent real power of battery in ith microgrid.

$\mathbf{P}_i^{l,max}$	Max. allowable inflow of real power into ith microgrid.
$\mathbf{P}_i^{l,min}$	Min. allowable inflow of real power from ith microgrid.
$\mathbf{S}_r^{l,max}$	Max. allowable inflow of apparent power into ith microgrid.
$\mathbf{S}_r^{l,min}$	Min. allowable inflow of apparent power into ith microgrid.
$P_i^{rcl,max}$	Max. change in inflow/outflow power per hour, for ith.
$\mathbf{P}^{mg,min}$	Min. allowable outflow of real power at the point of coupling to the utility grid.
$\mathbf{P}^{mg,max}$	Max. allowable outflow of real power at the point of coupling to the utility grid.
$\mathbf{S}^{mg,min}$	Min. allowable outflow of apparent power at the point of coupling to the utility grid.
$\mathbf{S}^{mg,max}$	Max. allowable outflow of apparent power at the point of coupling to the utility grid.
P^b	Power baseline in peak shaving constraint.
Δ_1	An arbitrary large positive number in peak shaving constraint.
E_i^{final}	Desired battery energy at the end of control horizon.
E_i^0	Actual battery energy at the start of control horizon.
$\boldsymbol{\alpha}$	An arbitrary vector with small positive elements.
$\mathbf{c}^{bl}$ or $\mathbf{c}_p^{bl}$	Local electricity buying of real power price.
$\mathbf{c}^{sl}$ or $\mathbf{c}_p^{sl}$	Local electricity selling of real power price.
$\mathbf{c}^{bg}$ or $\mathbf{c}_p^{bg}$	Electricity buying price of real power from the utility grid.
$\mathbf{c}^{sg}$ or $\mathbf{c}_p^{sg}$	Electricity selling price of real power to the utility grid.
$\mathbf{c}_q^{bl}$	Local electricity buying of reactive power price.
$\mathbf{c}_q^{sl}$	Local electricity selling of reactive power price.
$\mathbf{c}_q^{bg}$	Electricity buying price of reactive power from the utility grid.
$\mathbf{c}_q^{sg}$	Electricity selling price of reactive power to the utility grid.
c_i^{pk}	Peak shaving penalty of ith microgrid.
NoH	Minimum island mode operation time in number of time steps.
p_i	Number of microgrids in ith level of priority.

q	Number of priority levels in the network.
μl_i	set of microgrids' objective functions in ith level of priority.
ML_r	rth set of MGs with power capacity limit.
$\mathbf{P}_i^l$	Locally exchanged real power for ith microgrid.
$\mathbf{Q}_i^l$	Locally exchanged reactive power for ith microgrid.
$\mathbf{P}_i^{bl}$	Share of locally imported real power to ith microgrid.
$\mathbf{Q}_i^{bl}$	Share of locally imported reactive power to ith microgrid.
$\mathbf{P}_i^{sl}$	Share of locally exported real power from the ith microgrid.
$\mathbf{Q}_i^{sl}$	Share of locally exported reactive power from the ith microgrid.
$\mathbf{P}_i^g$	Share of real power exchanged with the utility grid by ith microgrid.
$\mathbf{Q}_i^g$	Share of reactive power exchanged with the utility grid by ith microgrid.
$\mathbf{P}_i^{bg}$	Real power purchased from the utility grid by ith microgrid.
$\mathbf{Q}_i^{bg}$	Reactive power purchased from the utility grid by ith microgrid.
$\mathbf{P}_i^{sg}$	Real power sold to the utility grid by ith microgrid.
$\mathbf{Q}_i^{sg}$	Reactive power sold to the utility grid by ith microgrid.
P_i^{pk}	Auxiliary peak shaving variable.
$\mathbf{P}^g$	Total real power exchanged with the utility grid.
$\mathbf{Q}^g$	Total reactive power exchanged with the utility grid.
$\mathbf{P}_i^n$	Real net demand power of ith microgrid.
$\mathbf{Q}_i^n$	Reactive net demand of ith microgrid.
$\mathbf{P}_i^{bat}$	Charging/discharging power of ith microgrid.
$\mathbf{Q}_i^{bat}$	Battery inverter reactive power of ith microgrid.
$\mathbf{P}_i^c$	Charging power of ith microgrid.
E_i	Battery energy level of ith microgrid.

Bibliography

Aghajani, G., Shayanfar, H., and Shayeghi, H. (2017). Demand side management in a smart micro-grid in the presence of renewable generation and demand response. *Energy*, **126**, 622–637.

Ahmadi, M., Rosenberger, J. M., Lee, W.-J., and Kulvanitchaiyanunt, A. (2015). Optimizing load control in a collaborative residential microgrid environment. *Smart Grid, IEEE Transactions on*, **6**(3), 1196–1207.

Almada, J., Leão, R., Sampaio, R., and Barroso, G. (2016). A centralized and heuristic approach for energy management of an ac microgrid. *Renewable and Sustainable Energy Reviews*, **60**, 1396–1404.

Arboleya, P., Gonzalez-Moran, C., Coto, M., Falvo, M. C., Martirano, L., Sbordone, D., Bertini, I., and Di Pietra, B. (2015). Efficient energy management in smart micro-grids: Zero grid impact buildings. *Smart Grid, IEEE Transactions on*, **6**(2), 1055–1063.

Arefifar, S. A., Ordonez, M., and Mohamed, Y. A. R. I. (2017). Energy management in multi-microgrid systems development and assessment. *IEEE Transactions on Power Systems*, **32**(2), 910–922.

Asimakopoulou, G., Dimeas, A., and Hatziargyriou, N. (2013). Leader-follower strategies for energy management of multi-microgrids. *Smart Grid, IEEE Transactions on*, **4**(4), 1909–1916.

Baharlouei, Z. and Hashemi, M. (2014). Efficiency-fairness trade-off in privacy-preserving autonomous demand side management. *Smart Grid, IEEE Transactions on*, **5**(2), 799–808.

Bahramirad, S., Reder, W., and Khodaei, A. (2012). Reliability-constrained optimal sizing of energy storage system in a microgrid. *IEEE Transactions on Smart Grid*, **3**(4), 2056–2062.

Battistelli, C., Baringo, L., and Conejo, A. (2012). Optimal energy management of small electric energy systems including v2g facilities and renewable energy sources. *Electric Power Systems Research*, **92**, 50–59.

Chakraborty, S., Nakamura, S., and Okabe, T. (2015). Real-time energy exchange strategy of optimally cooperative microgrids for scale-flexible distribution system. *Expert Systems with Applications*, **42**(10), 4643–4652.

Chandorkar, M. C., Divan, D. M., and Adapa, R. (1993). Control of parallel connected inverters in standalone ac supply systems. *IEEE Transactions on Industry Applications*, **29**(1), 136–143.

Colson, C. M., Nehrir, M. H., Sharma, R. K., and Asghari, B. (2014). Improving sustainability of hybrid energy systems part ii: Managing multiple objectives with a multiagent system. *IEEE Transactions on Sustainable Energy*, **5**(1), 46–54.

Conti, S., Nicolosi, R., Rizzo, S., and Zeineldin, H. (2012). Optimal dispatching of distributed generators and storage systems for mv islanded microgrids. *IEEE Transactions on Power Delivery*, **27**(3), 1243–1251.

Dagdougui, H., Ouammi, A., Dessaint, L., and Sacile, R. (2016). Global energy management system for cooperative networked residential green buildings. *IET Renewable Power Generation*, **10**(8), 1237–1244.

Dahmane, M., Bosche, J., El-Hajjaji, A., and Dafarivar, M. (2013). Renewable energy management algorithm for stand-alone system. In *Renewable Energy Research and Applications (ICRERA), 2013 International Conference on*, pages 621–626. IEEE.

De Brabandere, K., Vanthournout, K., Driesen, J., Deconinck, G., and Belmans, R. (2007). Control of microgrids. In *Power Engineering Society General Meeting, 2007. IEEE*, pages 1–7. IEEE.

Dursun, E. and Kilic, O. (2012). Comparative evaluation of different power management strategies of a stand-alone pv/wind/pemfc hybrid power system. *International Journal of Electrical Power & Energy Systems*, **34**(1), 81–89.

Ehrgott, M. (2006). *Multicriteria optimization*. Springer Science & Business Media.

Elsied, M., Oukaour, A., Gualous, H., and Hassan, R. (2015). Energy management and optimization in microgrid system based on green energy. *Energy*, **84**, 139–151.

Elsied, M., Oukaour, A., Gualous, H., and Brutto, O. A. L. (2016). Optimal economic and environment operation of micro-grid power systems. *Energy Conversion and Management*, **122**, 182–194.

Fang, X., Ma, S., Yang, Q., and Zhang, J. (2016). Cooperative energy dispatch for multiple autonomous microgrids with distributed renewable sources and storages. *Energy*, **99**, 48–57.

Fathi, M. and Bevrani, H. (2013). Adaptive energy consumption scheduling for connected microgrids under demand uncertainty. *Power Delivery, IEEE Transactions on*, **28**(3), 1576–1583.

Ferruzzi, G., Graditi, G., Rossi, F., and Russo, A. (2015). Optimal operation of a residential microgrid: The role of demand side management. *Intelligent Industrial Systems*, pages 1–22.

Guerrero, J. M., De Vicuna, L. G., Matas, J., Castilla, M., and Miret, J. (2005). Output impedance design of parallel-connected ups inverters with wireless load-sharing control. *IEEE Transactions on industrial electronics*, **52**(4), 1126–1135.

Guerrero, J. M., Matas, J., De Vicuna, L. G. D. V., Castilla, M., and Miret, J. (2006). Wireless-control strategy for parallel operation of distributed-generation inverters. *IEEE Transactions on Industrial Electronics*, **53**(5), 1461–1470.

Guerrero, J. M., Matas, J., de Vicuna, L. G., Castilla, M., and Miret, J. (2007). Decentralized control for parallel operation of distributed generation inverters using resistive output impedance. *IEEE Transactions on industrial electronics*, **54**(2), 994–1004.

Guerrero, J. M., Chandorkar, M., Lee, T.-L., and Loh, P. C. (2013). Advanced control architectures for intelligent microgrids, part i: decentralized and hierarchical control. *IEEE Transactions on Industrial Electronics*, **60**(4), 1254–1262.

Hatziargyriou, N. *et al.* (2014). *Microgrids: architectures and control*. Wiley Online Library.

Hossain, M. J., Mahmud, M. A., Milano, F., Bacha, S., and Hably, A. (2016). Design of robust distributed control for interconnected microgrids. *IEEE Transactions on Smart Grid*, **7**(6), 2724–2735.

Jiang, B. and Fei, Y. (2015). Smart home in smart microgrid: A cost-effective energy ecosystem with intelligent hierarchical agents. *IEEE Transactions on Smart Grid*, **6**(1), 3–13.

Jin, X., Mu, Y., Jia, H., Wu, J., Jiang, T., and Yu, X. (2017). Dynamic economic dispatch of a hybrid energy microgrid considering building based virtual energy storage system. *Applied Energy*, **194**, 386–398.

Kanchev, H., Lu, D., Colas, F., Lazarov, V., and Francois, B. (2011). Energy management and operational planning of a microgrid with a pv-based active generator for smart grid applications. *Industrial Electronics, IEEE Transactions on*, **58**(10), 4583–4592.

Kanchev, H., Lazarov, V., and Francois, B. (2012). Environmental and economical optimization of microgrid long term operational planning including pv-based active generators. In *Power Electronics and Motion Control Conference (EPE/PEMC), 2012 15th International*, pages LS4b–2. IEEE.

Katiraei, F. and Iravani, M. R. (2006). Power management strategies for a microgrid with multiple distributed generation units. *IEEE transactions on power systems*, **21**(4), 1821–1831.

Katiraei, F., Iravani, R., Hatziargyriou, N., and Dimeas, A. (2008). Microgrids management. *IEEE Power and Energy Magazine*, **6**(3), 54–65.

Khodabakhsh, R. and Sirouspour, S. (2016). Optimal control of energy storage in a microgrid by minimizing conditional value-at-risk. *IEEE Transactions on Sustainable Energy*, **7**(3), 1264–1273.

Kim, J.-Y., Park, J. H., and Lee, H.-J. (2011). Coordinated control strategy for microgrid in grid-connected and islanded operation. *IFAC Proceedings Volumes*, **44**(1), 14766–14771.

Koski, J. and Silvennoinen, R. (1987). Norm methods and partial weighting in multicriterion optimization of structures. *International Journal for Numerical Methods in Engineering*, **24**(6), 1101–1121.

Kou, P., Liang, D., and Gao, L. (2017). Distributed empc of multiple microgrids for coordinated stochastic energy management. *Applied Energy*, **185**, 939–952.

Kuznetsova, E., Ruiz, C., Li, Y.-F., and Zio, E. (2015). Analysis of robust optimization for decentralized microgrid energy management under uncertainty. *International Journal of Electrical Power & Energy Systems*, **64**, 815–832.

Lasseter, R. H. (2002). Microgrids. In *Power Engineering Society Winter Meeting, 2002. IEEE*, volume 1, pages 305–308. IEEE.

Lee, D.-J. and Wang, L. (2008). Small-signal stability analysis of an autonomous hybrid renewable energy power generation/energy storage system part i: time-domain simulations. *IEEE Transactions on Energy Conversion*, **23**(1), 311–320.

Levron, Y., Guerrero, J. M., and Beck, Y. (2013). Optimal power flow in microgrids with energy storage. *IEEE Transactions on Power Systems*, **28**(3), 3226–3234.

Li, S., Proano, J., and Zhang, D. (2012). Microgrid power flow study in grid-connected and islanding modes under different converter control strategies. In *Power and Energy Society General Meeting, 2012 IEEE*, pages 1–8. IEEE.

Liang, H., Choi, B. J., Abdrabou, A., Zhuang, W., and Shen, X. S. (2012). Decentralized economic dispatch in microgrids via heterogeneous wireless networks. *IEEE Journal on selected areas in communications*, **30**(6), 1061–1074.

Liao, Z. and Ruan, X. (2009). A novel power management control strategy for stand-alone photovoltaic power system. In *Power Electronics and Motion Control Conference, 2009. IPEMC'09. IEEE 6th International*, pages 445–449. IEEE.

Liu, G., Xu, Y., and Tomsovic, K. (2016). Bidding strategy for microgrid in day-ahead market based on hybrid stochastic/robust optimization. *IEEE Transactions on Smart Grid*, **7**(1), 227–237.

Liu, W., Gu, W., Sheng, W., Meng, X., Wu, Z., and Chen, W. (2014). Decentralized multi-agent system-based cooperative frequency control for autonomous microgrids with communication constraints. *IEEE Transactions on Sustainable Energy*, **5**(2), 446–456.

Liu, Y., Yuen, C., Ul Hassan, N., Huang, S., Yu, R., and Xie, S. (2015). Electricity cost minimization for a microgrid with distributed energy resource under different information availability. *Industrial Electronics, IEEE Transactions on*, **62**(4), 2571–2583.

Logenthiran, T., Srinivasan, D., and Shun, T. Z. (2012). Demand side management in smart grid using heuristic optimization. *IEEE transactions on smart grid*, **3**(3), 1244–1252.

Lopes, J. A. P., Moreira, C. L., and Madureira, A. G. (2006). Defining control strategies for microgrids islanded operation. *IEEE Transactions on Power Systems*, **21**(2), 916–924.

Lv, T. and Ai, Q. (2016). Interactive energy management of networked microgrids-based active distribution system considering large-scale integration of renewable energy resources. *Applied Energy*, **163**, 408 – 422.

Malysz, P., Sirouspour, S., and Emadi, A. (2014). An optimal energy storage control strategy for grid-connected microgrids. *Smart Grid, IEEE Transactions on*, **5**(4), 1785–1796.

Mao, M., Jin, P., Hatziargyriou, N. D., and Chang, L. (2014). Multiagent-based hybrid energy management system for microgrids. *IEEE Transactions on Sustainable Energy*, **5**(3), 938–946.

Marler, R. T. and Arora, J. S. (2004). Survey of multi-objective optimization methods for engineering. *Structural and multidisciplinary optimization*, **26**(6), 369–395.

Marnay, C., Chatzivasileiadis, S., Joos, G., Abbey, C., Lombardi, P., Iravani, R., Mancarella, P., and von Appen, J. (2015). Microgrid evolution roadmap. In *Smart Electric Distribution Systems and Technologies (EDST), 2015 International Symposium on*, pages 139–144. IEEE.

Migdalas, A., Pardalos, P. M., and Värbrand, P. (2013). *Multilevel optimization: algorithms and applications*, volume 20. Springer Science & Business Media.

Mohamed, A. and Mohammed, O. (2013). Real-time energy management scheme for hybrid renewable energy systems in smart grid applications. *Electric Power Systems Research*, **96**, 133–143.

Morstyn, T., Hredzak, B., and Agelidis, V. (2016). Network topology independent multi-agent dynamic optimal power flow for microgrids with distributed energy storage systems. *IEEE Transactions on Smart Grid*.

Nfah, E., Ngundam, J., and Tchinda, R. (2007). Modelling of solar/diesel/battery hybrid power systems for far-north cameroon. *Renewable Energy*, **32**(5), 832–844.

Nguyen, D. T. and Le, L. B. (2013). Optimal energy management for cooperative microgrids with renewable energy resources. In *Smart Grid Communications (SmartGridComm), 2013 IEEE International Conference on*, pages 678–683.

Nguyen, H., Khodaei, A., and Han, Z. (2016). A big data scale algorithm for optimal scheduling of integrated microgrids. *IEEE Transactions on Smart Grid*.

Nikkhajoei, H. and Lasseter, R. H. (2009). Distributed generation interface to the certs microgrid. *IEEE Transactions on Power Delivery*, **24**(3), 1598–1608.

Nikmehr, N. and Najafi Ravadanegh, S. (2016). A study on optimal power sharing in interconnected microgrids under uncertainty. *International Transactions on Electrical Energy Systems*, **26**(1), 208–232.

Nutkani, I. U., Loh, P. C., Wang, P., and Blaabjerg, F. (2017). Decentralized economic dispatch scheme with online power reserve for microgrids. *IEEE Transactions on Smart Grid*, **8**(1), 139–148.

Olivares, D. E., Caizares, C. A., and Kazerani, M. (2011). A centralized optimal energy management system for microgrids. In *2011 IEEE Power and Energy Society General Meeting*, pages 1–6.

Olivares, D. E., Caizares, C. A., and Kazerani, M. (2014). A centralized energy management system for isolated microgrids. *IEEE Transactions on Smart Grid*, **5**(4), 1864–1875.

Oriti, G., Julian, A. L., and Peck, N. J. (2016). Power-electronics-based energy management system with storage. *IEEE Transactions on Power Electronics*, **31**(1), 452–460.

Ouammi, A., Dagdougui, H., Dessaint, L., and Sacile, R. (2015). Coordinated model predictive-based power flows control in a cooperative network of smart microgrids. *Smart Grid, IEEE Transactions on*, **6**(5), 2233–2244.

Palma-Behnke, R., Benavides, C., Aranda, E., Llanos, J., and Sáez, D. (2011). Energy management system for a renewable based microgrid with a demand side management mechanism. In *Computational intelligence applications in smart grid (CIASG), 2011 IEEE symposium on*, pages 1–8. IEEE.

Pascual, J., Barricarte, J., Sanchis, P., and Marroyo, L. (2015). Energy management strategy for a renewable-based residential microgrid with generation and demand forecasting. *Applied Energy*, **158**, 12–25.

Prodan, I. and Zio, E. (2014). A model predictive control framework for reliable microgrid energy management. *International Journal of Electrical Power & Energy Systems*, **61**, 399–409.

Qiu, R. C., Hu, Z., Chen, Z., Guo, N., Ranganathan, R., Hou, S., and Zheng, G. (2011). Cognitive radio network for the smart grid: Experimental system architecture, control algorithms, security, and microgrid testbed. *IEEE Transactions on Smart Grid*, **2**(4), 724–740.

Rahbar, K., Chai, C. C., and Zhang, R. (2014). Real-time energy management for cooperative microgrids with renewable energy integration. In *Smart Grid Communications (SmartGridComm), 2014 IEEE International Conference on*, pages 25–30.

Rani, B. I., Ilango, G. S., and Nagamani, C. (2013). Control strategy for power flow management in a pv system supplying dc loads. *IEEE Transactions on industrial electronics*, **60**(8), 3185–3194.

Ravichandran, A., Sirouspour, S., Malysz, P., and Emadi, A. (2016). A chance-constraints-based control strategy for microgrids with energy storage and integrated electric vehicles. *IEEE Transactions on Smart Grid*.

Ross, M., Abbey, C., Bouffard, F., and Jos, G. (2015). Multiobjective optimization dispatch for microgrids with a high penetration of renewable generation. *IEEE Transactions on Sustainable Energy*, **6**(4), 1306–1314.

Sachs, J. and Sawodny, O. (2016). A two-stage model predictive control strategy for economic diesel-pv-battery island microgrid operation in rural areas. *IEEE Transactions on Sustainable Energy*, **7**(3), 903–913.

Shafiee, Q., Guerrero, J. M., and Vasquez, J. C. (2014a). Distributed secondary control for islanded microgridsa novel approach. *IEEE Transactions on power electronics*, **29**(2), 1018–1031.

Shafiee, Q., Dragičević, T., Vasquez, J. C., and Guerrero, J. M. (2014b). Hierarchical control for multiple dc-microgrids clusters. *IEEE Transactions on Energy Conversion*, **29**(4), 922–933.

Shi, W., Li, N., Chu, C. C., and Gadh, R. (2017). Real-time energy management in microgrids. *IEEE Transactions on Smart Grid*, **8**(1), 228–238.

Sirouspour, S. (2016). Optimal scheduling of a storage device in a grid-connected microgrid using stochastic chance-constraint optimization. In *Industrial Electronics Society, IECON 2016-42nd Annual Conference of the IEEE*, pages 2100–2105. IEEE.

Song, N.-O., Lee, J.-H., Kim, H.-M., Im, Y. H., and Lee, J. Y. (2015). Optimal energy management of multi-microgrids with sequentially coordinated operations. *Energies*, **8**(8), 8371–8390.

Tan, K., Peng, X., So, P., Chu, Y. C., and Chen, M. (2012). Centralized control for parallel operation of distributed generation inverters in microgrids. *IEEE Transactions on Smart Grid*, **3**(4), 1977–1987.

Tsikalakis, A. G. and Hatziargyriou, N. D. (2008). Centralized control for optimizing microgrids operation. *IEEE Transactions on Energy Conversion*, **23**(1), 241–248.

Tsikalakis, A. G. and Hatziargyriou, N. D. (2011). Centralized control for optimizing microgrids operation. In *2011 IEEE Power and Energy Society General Meeting*, pages 1–8.

Vaccaro, A., Popov, M., Villacci, D., and Terzija, V. (2011). An integrated framework for smart microgrids modeling, monitoring, control, communication, and verification. *Proceedings of the IEEE*, **99**(1), 119–132.

Vira, C. and Haimes, Y. Y. (1983). *Multiobjective decision making: theory and methodology*. Number 8. North-Holland.

Wang, D., Ge, S., Jia, H., Wang, C., Zhou, Y., Lu, N., and Kong, X. (2014). A demand response and battery storage coordination algorithm for providing microgrid tie-line smoothing services. *Sustainable Energy, IEEE Transactions on*, **5**(2), 476–486.

Wang, Y., Mao, S., and Nelms, R. (2015a). On hierarchical power scheduling for the macrogrid and cooperative microgrids. *Industrial Informatics, IEEE Transactions on*, **PP**(99), 1–1.

Wang, Z., Chen, B., Wang, J., Begovic, M., and Chen, C. (2015b). Coordinated energy management of networked microgrids in distribution systems. *Smart Grid, IEEE Transactions on*, **6**(1), 45–53.

Wu, C., Mohsenian-Rad, H., Huang, J., and Wang, A. Y. (2011). Demand side management for wind power integration in microgrid using dynamic potential game theory. In *GLOBECOM Workshops (GC Wkshps), 2011 IEEE*, pages 1199–1204. IEEE.

Xu, Y. and Liu, W. (2011). Novel multiagent based load restoration algorithm for microgrids. *IEEE Transactions on Smart Grid*, **2**(1), 152–161.

Yaghmaee, M. H., Moghaddassian, M., and Leon-Garcia, A. (2017). Autonomous two-tier cloud-based demand side management approach with microgrid. *IEEE Transactions on Industrial Informatics*, **13**(3), 1109–1120.

Yao, W., Chen, M., Matas, J., Guerrero, J. M., and Qian, Z.-M. (2011). Design and analysis of the droop control method for parallel inverters considering the impact of the complex impedance on the power sharing. *IEEE Transactions on Industrial Electronics*, **58**(2), 576–588.

Yu, X. E., Malysz, P., Sirouspour, S., and Emadi, A. (2014). Optimal microgrid component sizing using mixed integer linear programming. In *Transportation Electrification Conference and Expo (ITEC), 2014 IEEE*, pages 1–6. IEEE.

Yue, J., Hu, Z., Li, C., Vasquez, J. C., and Guerrero, J. M. (2017). Economic power schedule and transactive energy through an intelligent centralized energy management system for a dc residential distribution system. *Energies*, **10**(7), 916.

Zadeh, L. (1963). Optimality and non-scalar-valued performance criteria. *Automatic Control, IEEE Transactions on*, **8**(1), 59–60.

Zhang, Y., Gatsis, N., and Giannakis, G. (2013). Robust energy management for microgrids with high-penetration renewables. *Sustainable Energy, IEEE Transactions on*, **4**(4), 944–953.